VORONEZHSTATETECHNICAL
UNIVERSITY

*Should be treated as a manuscript*

**Al Tameemi Vasfi Mohammad Kadim**

# PHOTO-ELECTRIC AND GASO-SENSOR PROPERTIES OF $SnO_2$ FILMS

Thesis
for a master of science degree in
physical mathematics

Discipline 01.04.07 – Condensed matter physics

Scientific adviser:
Honoured science worker of
the Russian Federation,
Doctor of Physics and Mathematics,
Professor
RembezaS.I.

Воронеж – 2014

CONTENTS

# INTRODUCTION

The research is relevant due to the fact that the solution of a number of problems which are related to environmental protection, process control, control of human physiological state, food quality etc. demand the establishment of electronic devices which let to register and qualify presence of chemicals and mixes of its in the air, to analyze fumes. Consequently, to develop technology of preparation and research in gas semiconductor films which are sensitive to gas medium is process which gain prominents on Microelectronics and Solid State Electronics.

Solid state semiconductor sensors which are based on metal-oxide SnO2 and ZnO semiconductors is sensitive to broad spectrum atmospheric gases and change electric resistence. Its have a short response time period to change the concentration of gas at a temperature of several hundred °C and high sensitivity, which lets to determine the presence of most organic and inorganic gases at a few propromille concentrations (ppm) in air. Despite a long story of researching and the attemps to release sensors on a thin$SnO_2$ film, the question of reliable implementation of its can't be treated as a solved one. The question is based on: sensitivity, selectivity and stability, which can be realized simultaneously rather difficult and in many cases are optimized empirically, because of the great difficulty of film formation processes and physics of interaction with gases. The question of selectivity and reduction of operating temperatures of sensors can be solved by introducing impurity of additives and catalytic coatings. Another activation method of adsorption processes on surface conditions of a semiconductor sensor is optical impact on sensor elements. It is well known that radiation in a topical range of the powerful UV sourses can significantly improve sensitivity of metal oxide gas sensor by optical activation of surface conditions. Radiation lighting of metal oxide gas sensor compared with the width of a forbidden area of an oxide metal can reduce high operating temperature of the sensor to ambient temperature.Itletstousesensorinareaswhereitisunacceptabletooperateathighertemperatures, in that way expanding the application range and reducing power consumption.

However, sourses of optical radiations in the form of powerful stationary xenon and mercury lamps (used in earlier studies) are not suitable for practical using with portable gas detectors with battery. In such case it is convenient to use LEDs of violet and ultraviolet wareband.

The photoconductivity of polycrystalline wide bandgap semiconductors is characterized by long relaxation time of non-equilibrium charge carriers and a few recombination mechanisms. Identification of the mechanisms of photoconductivity at the moment of exiting in the semiconductor intrinsic and extrinsic optical transitions lets to use of these processes to improve metrological characteristics of thin-film gas sensors.

The object of the study is to determine peculiarities of the mechanisms of photoconductivity SnO2 film in interband transitions of electrons and impurity at the period of activation by light exposure of adsorption processes on surfaces and in the bulk of the film, and as a result of the surface modification of SnO2 impurities catalysts.

To achieve this purpose it is necessary to solve the following tasks:

1. To characterize mechanisms of photoconductivity of SnO2 films illuminated by LEDs with different energies of photons.

2. To study the effect of surface and bulk optical activation of the gas sensitivity of SnO2 films to gas-reducing agents.

3. To investigate the activation process gas sensitivity of SnO2 films of surface modification sensors by salt catalysts of silver and palladium.

4. To study the possibility to improve metrological characteristics of sensors through influence of light and a surface modification of $SnO_2$films by the salts of silver and palladium catalysts which happen at the same time.

Objects of research. For studying we choose crystals of a gas sensor (the size of which is $1\times1\times0,12mm^3$) which contain several elements: a thermal radiator and contacts for a sensitive fibre as a interdigital platinum structure and two gas-sensitive elements

(SE) on the basis of tin dioxide, one of which is alloyed by silver or palladium, and the other one is left unalloyed and is used for comparative characteristic. Thickness of a gas-sensitive film is 250 nm.

Originality of dissertation:

1. It has been shown that the process of relaxation of non-equilibrium charge carriers in polycrystalline $SnO_2$ films, when LEDs light its, is provided by interband and impurity optical transition with deep traps.

2. It was shown for the first time that because of influence of light of purple and green LEDs temperature dependence of gas sensitivity (S) of $SnO_2$ to gases reducers is changed: when the temperature dependence of S = f (T), two peaks of gas sensitivity are observed, but a main peak at 300 - 400 ° C and an additional peak at 100 - 200 ° C.

3. It has been established that the surface modification of $SnO_2$ films by silver and palladium salts leads to an increase of gas response and reduction of operating temperature till room temperature (a silver salt to the ammonia).

Practical significance of the study.

1. The effects of violet LED on the gas response of SnO2 films can be used to improve efficiency and energy saving of gas sensors with sensor SnO2 films.

2. Methods of surface modification of SnO2 films by palladium and silver salts that lets to increase the level of gas response and reduce an operating temperature of gas sensors can be extended to the other impurities catalyst such as platinum and some transition elements.

Propositions to be defended:

1. Influence of LEDs illumination of different energies from purple to red color on the electrical resistance of SnO2 + 1% Si films, and it leads to long-term relaxation of the resistance due to the surface and bulk recombination of nonequilibrium charge carriers with deep traps.

2. Changing of the temperature dependences of gas sensitivity of SnO2 + 1% Si films to the reducing gases in the air when illuminated sensor purple and green layers, and it exhibits in the appearance of two gas sensitivity peaks.

3. The model to increase the gas sensitivity of SnO2 + 1% Si films due to the interaction of photons with the surface states (green LED), as well as due to interband transitions and modulation grain potential barrier (purple LED).

4. Developing process of gas sensitivity of gas sensitivity SnO2 + 1% Si films at room temperature, to the vapors of water (3000 ppm and higher) and ammonia vapors (1000 ppm).

5. The model of increasing of gas sensitivity of SnO2 + 1% Si films to reducing gases in the air as a result of surface modification using palladium and silver, while purple LED lightening.

Work approbation. The results of the study were reported: at annual scientific and technical conferences of professors and teachers, graduate students, undergraduates and students (Voronezh, Voronezh State Technical University, 2012 – 2014); at the All-Russian scientific-practical conference "Problems of safety in the aftermath of emergencies" (Voronezh, Voronezh Institute of the State Fire Service of Russian Emergency Ministry, 2012), at the International scientific conference "Actual problems of solid state physics" (Minsk, 2013); at the VI International Scientific and Technical Conference "Micro - and Nanotechnology in electronics" (Nalchik, Kabardino-Balkarian State University, 2014 г.).

Publishing. On the topic of the dissertation 11 publications, including 4 works in the publications recommended by the RF HAC for scientific degree of candidate of physical and mathematical sciences were published.

The author has been involved in the preparation and the conduct of the experiment and took a part in the discussion of the results and preparation of papers for publication in the joint works.

The structure and scope of the study. The thesis consists of an introduction, four chapters, main results and references which include 94 titles. The study is presented on 158 pages, contains 12 tables and 96 figures.

The work was made on the plan of works GB 2010.34 "Physical fundamentals of the technology and design of semiconductor devices and integrated circuits" and GB 2013.34 "Design and development of manufacturing microelectronic products of technology."

# Chapter 1.

# MODERN IDEAS ABOUTELECTROPHYSICAL PROPERTIES OF METAL-OXID TRANSISTORS AND THE MECHANISMS OF GAS SENSITIVITY IN ITS

## 1.1 Electro physical properties of semiconductor films of tin dioxide

It is known [1,2] that the interaction with the gases of metal oxide semiconductors leads to changes of the surface potential and the electrical resistance is proportional to the concentration of the adsorbed gas. This phenomenon is the basis of semiconductor gas sensors [3]. Nowadays metal oxide semiconductors (tin dioxide and zinc oxide) are used as starting materials for semiconductor gas sensors. Both of these materials in their pure form are n-type conductivity semiconductors with a band gap of 3.2 eV for ZnO, 3.54 eV and for SnO2 [4].

Zinc Oxide – a well-studied wide-gap semiconductor. The centers (which are responsible for the electrical conductivity of zinc oxide (ZnO)) are interstitial zinc atom, or oxygen vacancies, the total concentration of which varies in the range from $10^{16}$ to $10^{19}$ $см^{-3}$. The mobility of electrons in single crystals of zinc oxide at room temperature can reach 200 $см^2/В{\cdot}с$ [5].

Tin dioxide is a wide gap semiconductor that belongs to a group of non-stoichiometric metal oxide semiconductors with O/Sn < 2. Non-stoichiometry of SnO2 may be the result of oxygen vacancies($SnO_{2-x}$), or the presence of interstitial tin atoms ($Sn_{1+y}O_2$).

The formation of neutral positions can be represented by the following reaction:

$$O_O \leftrightarrow V_o^x + 1/2\ O_{2(g)}. \qquad (1.1)$$

Ionization of oxygen vacancies is happening on the scheme

$$V_o^x \leftrightarrow V_o^{\bullet} + e', \quad (1.2)$$

$$V_o^x \leftrightarrow V_o^{\bullet\bullet} + 2e'. \quad (1.3)$$

Basing of electrical conditions of the crystal lattice, we find

$$n = [V_o^{\bullet}] + 2[V_o^{\bullet\bullet}], \quad (1.4)$$

in which n is the concentration of quasi-free electrons.

The deviation of the composition from the stoichiometry *x* for SnO2-x can be represented as the following:

$$x = [V_o^x] + [V_o^{\bullet}] + 2[V_o^{\bullet\bullet}]. \quad (1.5)$$

The explanation non-stoichiometry due to the presence of interstitial tin atoms can be described by the following reactions:

$$Sn_{Sn} + 2O_O \leftrightarrow Sn_i^x + O_{2(g)}, \quad (1.6)$$

$$Sn_i^x \leftrightarrow Sn_i^{4+} + 4e'. \quad (1.7)$$

The condition of electrical neutrality can be written as

$$n = [Sn_i^{4+}]. \quad (1.8)$$

When neutral defects $[Sn_i^x] >> [Sn_i^{4+}]$ are dominated, then the deviation from stoichiometry for $Sn_{1+y}\ O_2$ will be: $y \cong [Sn_i^x]$; but when $[Sn_i^{4+}] >> [Sn_i^x]$ then the deviation will be $y \cong [Sn_i^{4+}]$ [6]. Fig. 1.1 shows the unit cell of the crystal structure of $SnO_2$. Each tin atom in a cell is surrounded by six oxygen atoms and each oxygen atom is surrounded by three tin atoms. The deviation from the shows in the donor or acceptor type conductivity in non-stoichiometric tin dioxide, like zinc oxide, the concentration of donor defects prevails [7].

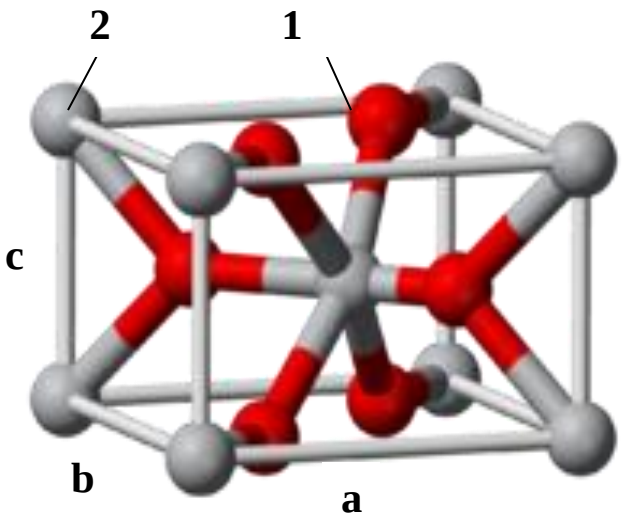


Fig. 1.1. An elementary cell of the crystal structure of tin rutile type dioxide [7] (TiO2): 1 - an oxygen atom; 2 - tin atom

Tin dioxide SnO2 (casseterit) is a colorless crystal with tetrragonal rutile lattice (TiO2) with periods of a = 4,737Å and c = 3,185Å . Zinc oxide ZnO has a hexagonal ZnS-type lattice with periods of a = 0,3249Å and c = 0,5206Å [4].

There are the parameters of the unit cell $MO_2$ with a rutile structure and sphalerite (ZnO) in the table 1.1.

Table 1.1

The parameters of an elementary cell $MO_2$ s

| Oxide | The parameters of a cell, Å | |
|---|---|---|
| | a | C |
| $SnO_2$ | 4,737 | 3,185 |
| $PdO_2$ | 4,946 | 3,379 |
| $GeO_2$ | 4,395 | 2,859 |
| TiO2 | 4,5929 | 2,9591 |
| ZnO | 3,246 | 5,207 |

SnO2 is used in the production of transparent electrically conductive and heat-reflecting material, as well as white pigment in the production of heat-resistant glass, and enamels and glazes. Tin dioxide films which are deposited on glass and plastic substrates are used as deicers on aircraft, automobiles and other types of transport; thermal insulating windows in rooms heated by sunlight, transparent conductive coatings in electronic devices. Cassiterite is the main raw material in the production of tin [6].

Basic physical properties of monocrystalline semiconductor of tin dioxide and zinc oxide polycrystalline are close to the properties which are presented in the Table 1.2 [4].

Physical properties of polycrystalline films of metal oxide semiconductors, depend on the way of production, growth parameters, the presence of dopant, the nature of the substrate, the carrier gas. Additionally, annealing that uses after the production of the films, also has an impact on electrical properties of films.

Table 1.2

Basic physical properties of single-crystal metal oxide semiconductors [4]

| The name of parameter | Symbol | Units of measure | The amount of the parameter | |
|---|---|---|---|---|
| | | | $SnO_2$ | ZnO |
| The temperature of incongruent melting | $T_{melt.}^{incong.}$ | $^oC$ | 1625 | 1975 |
| The density of a solid phase | d | $g/csm^3$ | 6,95 | 5,606 |
| Standard enthalpy (heat) of Formation | $\Delta H^o_f$ | J/kmol | $-581,13 \cdot 10^6$ | $-348,34 \cdot 10^6$ |
| Standard entropy | $S^0$ | J/kmol·gras | $56,52 \cdot 10^3$ | $43,54 \cdot 10^3$ |
| The specific heat at constant Pressure | $C_p$ | J/kmol·deg | 349,598 | 494,042 |
| The energy gasp | $\Delta E$ | eV | 3,54 | 3,2-3,3 |
| The specific resistance | $\rho$ | Ohm·cm | $4 \cdot 10^2$ | $6,7 \cdot 10^{-1}$ |

Dependent on the structure and method of production the thin film structure $SnO_2$ is considered in the study [8]. Tin dioxide films are produced by different methods: chemical vapor deposition, pulverization, spraying. The thickness of the layers was constructed about 100 nm. Tin dioxide films (A-type samples) was obtained by spraying of alcohol (C2H5OH) tin tetrachloride solution SnCl4-5H2O (15 % - water) to the heated (to 450$^o$C) silicon substrate or on an oxidized silicon wafer (A2-type) outdoors.

The films of tin dioxide (B-type samples) were produced by chemical vapor deposition on a hot (350 $^o$C) silicon substrate. The melt $SnCl_2 \cdot 2H_2O$ and humid air as the gas – carrier were used as the reagent. The surface resistance A- and B-type layers changes in a range 0,5 - 2 кОм/□v, it depends on film deposition conditions.

Tin dioxide films (C-type samples) were prepared by reactive sputtering of a target of metallic tin in an oxygen atmosphere at a 0.133 Pa pressure. The substrate temperature was maintained at about 160$^{o}$C . The resistance of films of this type gets over 1 Mohm / □.

All three types of $SnO_2$ layers are polycrystalline and has a cassiterite-type structure. A-type films have a grain size of about 50 nm, and the two-phase structure, it means that, its contain of $SnO_2$ and small amount of SnO. The structure of surface B-type layers which is defined heterogeneity of grain size that varies in the range of 20-50 nm, the layers are non-stoichiometric. C-type films are homogeneous with having size of grains which is less than 20 nm. The data of X-ray diffraction shows only the presence of $SnO_2$ phase. Comparing the methods which we used for the application of tin dioxide films, we can say that C-type films are the most perfect: they are in single-phase mode, have a bit small polycrystalline structure and a smooth surface.

According to the study [9] thin films of tin dioxide (about 1,5·10$^4$ Å thick) are made by spraying an alcohol solution of tin chloride and have a resistance which is about 154 Ом·см for undoped films and 50 Ом·см for the films doped with antimony, and have order light transmittance - 68.2%. In the paper the information that the resistance of tin dioxide 50 microns thick layers at room temperature is (1 - 4) · 10$^6$ Ohm. The temperature dependence of the resistance of tin dioxide layers has a characteristic of the semiconductor exponential form to (150 – 200) °C with an exponent - 0.2 eV. The exponential nature of this dependence can be result of release of electrons from the levels of its own donor defects [11]. It is typical that intrinsic semiconductor exponential decrease in resistance with increasing temperature at T > (150 – 200)°C, is replaced by abnormal areas - increasing resistance by adsorbed oxygen ions.

Studying of the temperature dependence of concentration (n) and the mobility of free charge carriers (μ) by Hall effect shows that at room temperature, initial samples which are relatively high values of these quantities: $n \cong 1 \cdot 10^{15}$ cm$^{-3}$ and

$\mu \cong 100$ $cm^2/(B \cdot c)$. With weakly expressed temperature dependence of the mobility of concentration of free electrons with increasing temperature from 20 °C to (150 - 200) °C firstly it increases as in the case of semiconductors, and then falls.

In the reaction of oxygen and various types of semiconductors, based on metal oxide, at high temperatures the chemisorbed oxygen molecules $O_2^-$ which are on the surface of the semiconductor, firstly move in $O^-$ state and then in $O^{2-}$ state. Chemisorbed oxygen in the form of singly charged ions ($O^-$) and doubly charged ion ($O^{2-}$) creates a new, deeper compared to chemisorbed ion of oxygen molecule $O_2^-$, electron capture centers. Therefore, the observed abnormal increase of resistance, with increasing temperature, is due to the transition from one form of oxygen chemisorption to another one [10 - 13].

There are significances of conductivity ($\sigma$), concentration (n) and mobility ($\mu$) of fundamental carriers for tin dioxide films which are produced in three different ways of electron beam, and applying reactive sputtering of solutions, with subsequent annealing at 400 °C for 2 - 3 hours in the table. 1.3. The parameters of metal oxide films were measured in the range of the temperature 25 - 300 °C.

It is obvious that significances of conductivity, concentration and mobility of fundamental carriers range in a wide temperature range depending on the way of production of films.

Table 1.3

Electrical parameters of tin dioxide films, which are produced in three different ways [8]

| The name of parameter | The way of production of tin dioxide films | | | | | |
|---|---|---|---|---|---|---|
| | Reactive sputtering | | Electron beam spraying | | Application of the solutions | |
| | 25 °C | 300 °C | 25 °C | 300 °C | 25 °C | 300 °C |
| Conductivity $\sigma$, $(Ohm \cdot cm)^{-1}$ | 0,88 | 2,98 | 0,11 | 0,27 | 0,67 | 64,63 |
| Concentration n, $\cdot 10^{17}$ $cm^{-3}$ | 27,1 | 46,8 | 2,0 | 0,8 | 0,43 | 7,34 |
| Mobility $\mu$, $cm^2 \cdot B^{-1} \cdot c^{-1}$ | 2,03 | 3,97 | 3,42 | 20,97 | 96,5 | 549,6 |

Optical properties of SnO2 layers [14] are characterized through rather high transmission coefficients (80 - 90%). Optical K8 colorless glass which is applied as a substrate has a transparency of over 90%. Maximum light absorption is not more than 20%, minimum - about 10%. A slight decrease in the tin dioxide layer thickness leads to a significant increase of the coefficient of optical transmittance. At thickness of 0.07 – 0.09 microns, an average significance of optical transmittance of tin dioxide films is (81 – 83) %.

Research of spectrums of optical transmittance SnO2 films lets to determine the coefficient of light absorption in the films. By the form of spectral dependence of the absorption coefficient we can determine the type of optical transitions (direct or indirect) which lead to the appearance of excess carriers in the condition band, to estimate the size of band gap and the deviation scope of the composition of the films from the stoichiometry.

The principle of operation of semiconductor gas sensors is based on variation of the physical parameters of semiconductor materials that occur in their contact with the gas. The physical parameters, which are changing in the adsorption of gases on the surface of semiconductors, are: electrical conductivity, photoelectric work function, the

mobility of free charge carriers, surface concentration of charge carriers, the lifetime of non-equilibrium charge carriers, optical reflection coefficient, absorption coefficient and others. These characteristics are potential gas sensors output parameters, but not all of them have wide practical application. For metal-oxide semiconductors, such as tin dioxide and zinc oxide, the most informative parameter is the electrical conductivity (resistance) of the material, now that a slight change of the concentration of an analyzed gas causes a significant change in electrical resistance [15].

Gas sensors based on SnO2 have high sensitivity to hydrogen in the air, the interval of which is determining (0.001 - 2) vol%, and to hydrogen in helium - the interval of determining is (0.0001 - 2) vol%. The sensors which are based on tin dioxide also make it possible to define the hydrogen sulfide in the air at the interval (0 - 300) mg / m3, Freon in air - (0 - 10,000) mm / m3, ethanol pairs - (0 - 200) mg / m3 and chlorine pairs - (0 - 200) mg / m3 in the air [16].

The sensors which are based on zinc oxide and tin dioxide can be used to define carbonic oxide (carbon monoxide). In the case of zinc oxide (ZnO) CO concentration measurement range is (20 - 200) ppm, and in the case of tin dioxide the range of measurement of CO concentration (500 - 3000) ppm [15].

## 1.2. Stabilization of the electrical properties of tin dioxide films

Processes of the interaction between gas and SnO2 film surface are strongly depend on the ambient temperature. According to the experimental data [16, 17], the maximum sensitivity of the gas films is noted in the temperature range of 200 - 400 ° C. Because the films are typically produced at lower temperatures, thermal stabilization of their electrical parameters and the structure are very important.

We can partly stabilize electrical parameters of tin dioxide films by doping its with different impurities, particularly antimony (to 3 - 4 atom%), that correspond to the limit of solubility of Sb in tin dioxide [6, 18]. According to the study [6] electrical conductivity of tin dioxide films is significantly increased when doping with antimony, which is a donor impurity in the SnO2 lattice, is happen.

A number of studies [19, 20] indicate that for stabilizing of the physical properties of SnO2 films after their production, it is require a long high-temperature annealing. To understand physical and chemical processes which are responsible for stabilization of properties of tin dioxide films and scientifically based selection of modes of heat treatment, it is necessary to analyze physical and chemical, in particular structural parameters of films and the influence of high-temperature annealing on its.

The authors of the paper [20] provide for SnO2 films which are prepared by solutions and melts of tin salts to carry out annealing at the temperature range (380 - 750 ° C) in the air or in vacuum for 6 hours. For tin dioxide film produced by reactive magnetron spraying into an argon and oxygen atmosphere, it is recommended to carry out heat treatment at the temperature range (300 - 500 ° C) for 4 - 20 hours in the air, in the vacuum or in N2 atmosphere.

For example, SnO2 layers produced by reactive magnetron spraying, were annealed for 30 hours at a temperature of 550 $^{o}$C [21].

The cause of instability of the electrical parameters of tin dioxide can be considered as the deficiency of oxygen in relation to the stoichiometric composition of SnO2 and crystal structure which is not completely formed [21].

This is due to (particularly for a magnetron sputtering method) a significant difference of the synthesis conditions of SnO2 layers from equilibrium. At the initial stage of the annealing, the formation of the structure and stabilization of the electrical resistivity of the layers are happen. Thus in the film formed by the heterophase structure is formed. And this structure contains carbon monoxide and tin dioxide, and monoxide continue oxidize during the further annealing in the air to SnO2. This process determines the particulars of the changing of the resistance of the samples. Accordingly, to stabilize the electrical properties of such samples requires a long time of annealing in the air.

Therefore, for the production of gas-sensitive $SnO_2$ layers of the spraying should be performed in the conditions providing the formation of films with a composition which is the closest to the stoichiometric one. However, in the real conditions the films which are made in such regimes have imperfect crystal structure because of highly non-equilibrium processes which take place during the spraying and the condensation of films through the method of magnetron spraying [22]. This makes it necessary for the stabilizing annealing and the films which are contain only one phase of tin dioxide.

It is noted in the paper [23] that the changing of condensation of nonstoichiometric defects (oxygen vacancies) are formed the donor centers with an ionization energy of not more than 0.15 eV. And it has a great influence on the sensitivity of the sensors based on tin dioxide to reducing gases and on the stability. The stability of the electrical annealed SnO2 samples at the time lets to suggest that as a result of annealing, equilibrium between the intrinsic defects and oxygen in the air is reached.

It is noted in the study [20] that annealing results depend not only on the temperature but also on the composition of the environment. Particularly, when annealing in the air is happen the conduction of the films increases and the resistance decreases. At the same time in a vacuum, on the contrary, it causes an increase in resistivity. The range of annealing

temperatures (400 – 750 $^{o}$C), which is studied in the paper [20], for the analysis of the processes it is convenient to divide into three intervals. In the first temperature interval (400 - 480 $^{o}$C) films conduct electrical parameters is practically independent of the environment in which the annealing is performed. In this temperature interval as in the annealing in the air, and during the annealing in vacuum with increasing annealing temperature the resistance of the films is increased. In the second temperature interval (480 - 550 $^{o}$C) the annealing in the air induces the increase of film conductivity. At higher temperatures (above 550 $^{o}$C) the dependence of the electrical parameters of temperature weakens, and during annealing in vacuum at high temperatures, changing in the electrical properties of the films is practically absent. High-temperature annealing does not change the nature of the crystallite orientation of the film, but has an influence on their size (D). During annealing in the air at temperatures of about 450 ° C crystallite quantity D rises in almost 1.5 times in comparison with the original size and during a further increase of temperature (T> 500 $^{o}$C) stays invariable. Annealing in vacuum in this temperature range has no effect on the crystallite size of the film.

Thus, during the annealing in the air changing of the properties of tin dioxide films can be connected with growth of mid crystallite size.

Impact of the annealing in vacuum on the damage of electro physical properties of the films can be explained by the changes in bulk electro physical characteristics of the crystallites, for example, a decrease of bulk crystallites, caused by generation of the defects in the anion sub lattice of tin dioxide [20].

The effect of high temperature annealing on the optical properties of tin dioxide films is shown in the paper [19]. During the annealing at the temperature range (300 - 500 $^{o}$C) for the first four hours the increase of transparency and the coefficient of optical transmittance of films is happen. Further annealing cycles are not significantly change optical properties of $SnO_2$ films. Increasing of the coefficient of the optical transmission can be based on increasing of crystallite size and additional oxidation of $SnO_2$ phase.

## 1.3. The chemical properties of SnO2

Chemical resistance of SnO2 layers is extremely large. They can not be destroyed by water and water vapors, they are resistant to the influence of solutions of the most salts and acids, but they are destroyed under the influence of hydrofluoric acid or under the boiling with alkalis. For removing of tin dioxide layer from the glass it is necessary to use a long polishing or the treatment with a HCl mixture and a of Zn powder, as a catalyst. In the latter case SnO2 layer is removed quickly enough: the layer is wiped with a cotton swab dipped in this mixture, and then it is washed off with water [14]. Further, in the paper [8] it is marked that the dissolution of tin dioxide takes place in the HCl for 48 hours.

SnO2 has a melting point 1630 ° C; density of 7.0096 g / $cm^3$; specific heat of C ° p =52.2 J / (моль·K); the heat of formation ΔfH = -577,63 kJ / mol; the entropy of S ° 298 = 49.01 kJ / (моль·K). SnO2 evaporates predominantly as SnO, and O2 and $Sn_nO_n$ oxides where n = 2, 3 or 4 are also present in the vapors. Tin dioxide is insoluble in the water and is stable in the aqueous acid solutions, salts, alkalis, of various reducing. Tin dioxide is n-type semiconductor, the band gap of 3.54 eV (300 K); electron mobility 7 cm2 / (V·s); the concentration of free charge carriers 3,5·1014 cm-3; ρ = 3,4·103 Ohm·cm [4]. During the alloying of V-group elements (e.g., antimony Sb) electrical conductivity of tin dioxide is increasing in 103 - 105 times. SnO2 is transparent to visible light and reflects IR-radiation with a wavelength which is more than 2 microns.

In the nature SnO2 is a mineral cassiterite (tin stone). Mono crystals of tin dioxide are by growing produced from vapor phase using oxidation, hydrolysis or pyrolysis of tin compound from solutions of hydrothermal synthesis. Tin dioxide Films produced by oxidation of tin films

Tin dioxide films are produced by the oxidation of tin films using the method of chemical transport reactions of tin chlorides or organotin compounds with following hydrolysis or pyrolysis on substrates and the condensation of tin dioxide in a vacuum from vapor phase containing tin, oxygen and SnO (II).

### 1.4. Various techniques for preparation of SnO2films.

#### 1.4.1. Preparation of tin dioxide films through reactive magnetron sputtering method

Method of reactive magnetron spraying with direct current is spraying of target from metallic tin in the atmosphere of a gas mixture: working - argon and reactive - oxygen. The spraying of a cathode target is due to the bombardment of the surface of the by positive argon ions. An ion generator is plasma of a glow discharge which arises at a low pressure in the atmosphere of a gas mixture when a voltage is applied to the electrodes. Ejected from the target as a result of an ion bombardment the particles form the flow of coating material, which is deposited as a thin film on substrate disposed at a distance from the target. Closed magnetic field locates the glow discharge near the target surface that leads to a significant increase of deposition rate.

According to the existing model of reactive sputtering in the formation of an oxide compound, a chemical reaction may take place generally at surfaces - the sputtering target and the deposited film [26]. There are two phases of the process, depending on the relation velocities of the formation of the chemical compound on the target, and spraying of this compound [27, 28]. At a relatively low content of reactive gas in the spraying formation rate of the compound at the target surface is much less than the spraying rate (the first phase of the process). At increase of content of the reactive gas, the formation rate becomes comparable chemical compound on the target and spraying, and the process proceeds to the second phase. On the surface of the target a thin layer of a chemical compound of a reactive gas with target metal is formed and stored.

Fig. 1.2 shows the diagram of the distribution of the basic streams of oxygen at the reactive spraying on the "Oratorio 5". The oxygen content in the spraying range at a constant amount of incoming and evacuated gas through the a slotted gas gap (the gap between the range of spraying and a common vacuum chamber) is determined by the

amount of oxygen which is adsorbed by the surface of the sputtering target 2 and tin oxide film deposits on the walls of the spray range 3 and on substrates 4.

The main technological regimes during reactive sputtering on the "Oratorio 5" include: voltage and current of discharge the pressure of the gas mixture ($Ar + O_2$) in the range of spraying and $O_2$ condensation in a gas mixture. All these parameters are interrelated and a change in one of them leads to a change in others.

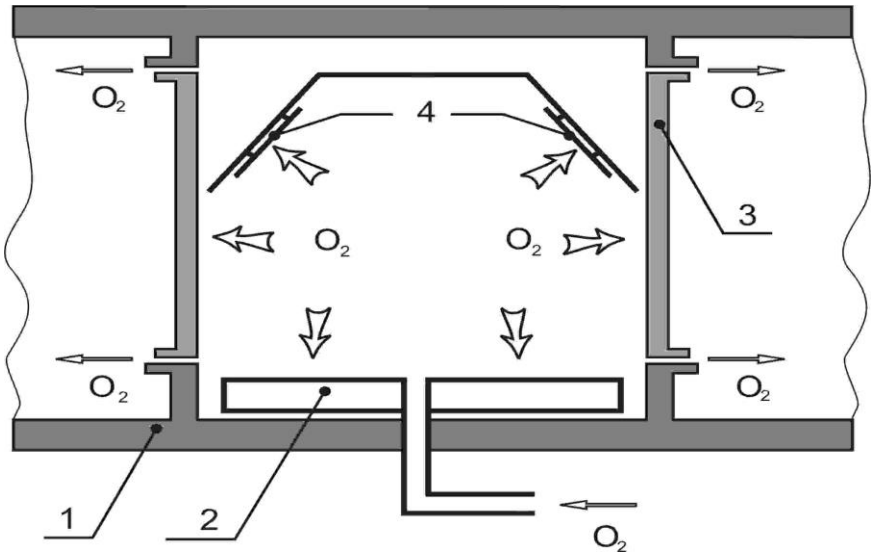


Fig.1.2. Scheme of distribution of basic streams of oxygen at the reactive magnetron spraying on the "Oratorio 5": 1 - vacuum chamber; 2 - the target; 3 – the walls of spraying range; 4 - the substrates [29]

### 1.4.2. Vacuum applications of thin films

During the applying of thin films in a vacuum three main processes are happen at the same time: the generation of directional stream of particles of deposited material; the overflight of particles in vacuum space from their source to the treated surface; the deposition (condensation) of the particles on the surface with the formation of thin film layers. Two methods to generate the stream of particles in a vacuum are used: thermal evaporation of the target and their ion spraying (Figure 1.3.).

At present the most widely used method is ion spraying. This is caused by four basic features of it [30]:

- university of the method which lets to spray metals, dielectrics, semiconductors, alloys and compounds;
- improving of adhesion of films to the substrates because of the greater kinetic energy of sputtered atoms and molecules;
- increased reproducibility film properties because the process is fully controlled and operated;

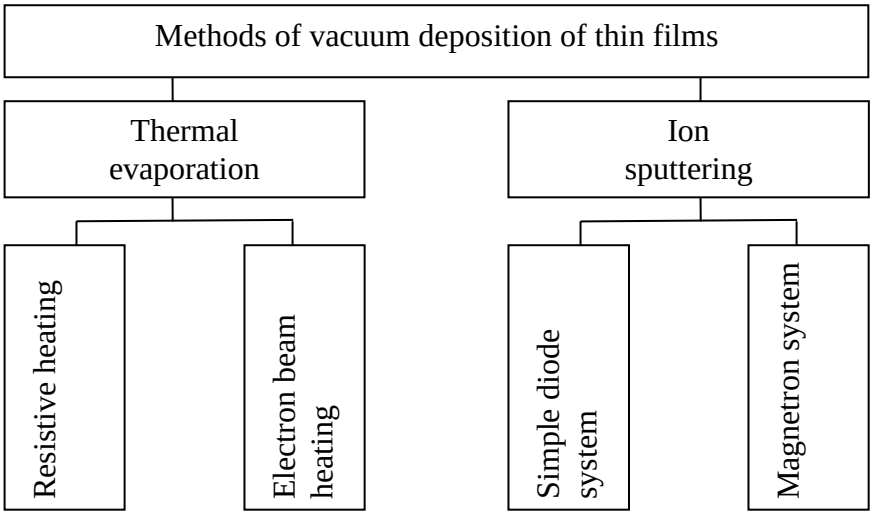


Fig.1.3. Classification of basic methods for vacuum deposition of thin films [29]

- improvement of the composition of formed films as a result of uniform removal of atoms and molecules from the surface of the target of complex composition in the process of an ion bombardment.

Method of ion sputtering is based on the bombardment of the target which is made of deposited material with fast particles (usually positive ions Ar). Ion generator is plasma of glow discharge which occurs in an inert gas atmosphere. Particles ejected from the target form a stream of material which is deposited as a thin film on the substrates disposed at a distance from the target.

Fig. 1.4 demonstrates a scheme of a planar magnetron. The basic elements of magnetron are disc-shaped target 1 cooled with running water 4 and the magnetic system 5. Magnetic force lines are closed between the poles of the magnetic system. Voltage is applied to the cathode, and it is about 300 – 1000 V, and the glow discharge is excited. A closed magnetic field at the surface of the target locates discharge which is near the surface [31].

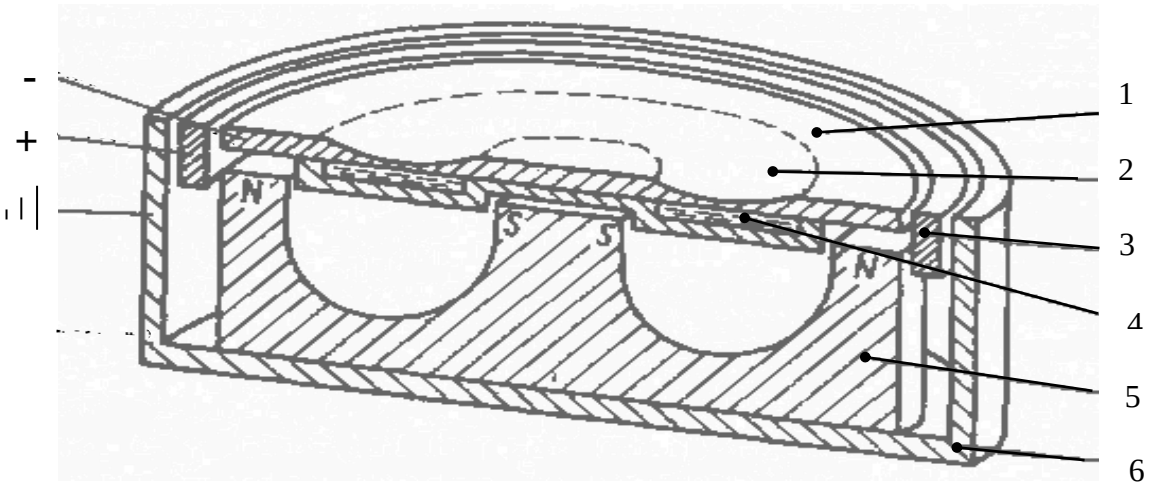


Fig.1.4. Scheme of a planar magnetron [32]: 1 - the target cathode; 2 – a range of erosion on the surface of the target; 3 - the power source; 4 - the cooling system of the cathode; 5 - magnetic system; 6 - grounded outer shield.

Electrons emitted from the cathode by ion bombardment, are in the region of crossed electric and magnetic fields and are trapped. The trajectories of the motion of electrons in a trap are similar to cycloidal. The efficiency of ionization and plasma density in this region is considerably increased. This leads to increasing the concentration of ions at the target surface, to the intensity of ion bombardment, and a significant increase in speed sputtering at relatively low pressures. The plasma density in the discharge rate and maximized the target erosion in the region where the magnetic field lines have the direction close to parallel with respect to the cathode surface.

The basic operating parameters include the magnetrons voltage across the electrodes, the discharge current, the specific power on the target, the gas pressure in the vacuum chamber and the magnetic induction.

The magnetrons belong to the low-voltage sputtering systems; the power supply voltage does not exceed 1000 V. However, typical operating voltages are about of 400 V.

The discharge current can reach several tens of amperes at a current density of to 2000 A / m $^2$ or more.

Specific power is limited to conditions and cooling of the target and the thermal conductivity of the dispensed material and reaches $5\times10^5$ Вт/м$^2$.

The operating pressure of the magnetron is over a wide range $10^{-2}$ – 1 Pa. Ar is used as the main working gas.

The induction of the magnetic field largely determines the nature of the discharge in the magnetron and it is in the range of 0.03 - 0.1 Tesla.

The deposition rate has a significant impact on the properties of the films which with sufficient accuracy can be kept stable due to the the constancy of process parameters such as the discharge current or input power.

An important advantage of sputtering techniques is the possibility of manufacturing the films of the same chemical composition as the sputtering target. This holds true even when the sputtering coefficients of the individual components differ

markedly from one another. This makes it possible to produce complex multi-component materials films by spraying floatable targets [33].

Furthermore, production of films of given complex composition is achieved by sputtering target, which are made from pure individual components in predetermined proportions in area with regard to their spray coefficients. Coefficient of dispersion is defined as the average number of atoms removed from the surface of a solid one incident particle [34]. For the manufacture of semiconductor compounds and dielectrics films using sputtering two kinds: reactive sputtering of metals and dielectrics RF sputtering.

During the spraying on direct current positive of dielectric target ions of the working gas are not neutralized and create on the target surface positive charge. This electric field compensates for the initial charge of the target area located at a negative potential, and it becomes impossible to continue spraying because of the discharge of ions repel target. In order to ensure dielectric sputtering target, it is necessary to neutralize the positive charge on the surface of a high frequency alternating supply potential.

The intensity of the RF sputtering process is determined by the frequency, amplitude RF voltage, the intensity of the external magnetic field, the shape and size of the high-frequency electrode, substrate temperature, the composition of the working gas, the target material and plasma discharge modes.

The films made by high-frequency sputtering, very homogeneous in thickness and composition. They have good adhesion to most surfaces. films depends strongly on the structure of the deposition rate and the substrate temperature [33].

Reactive sputtering is used to deposit of films of chemical compounds (oxides, nitrides). In this method [29] in the working chamber was filled with working gas - argon supplemented with a reactive gas (N2 or O2). The required chemical compound was prepared by selecting a sputtering target material and process gas. These ions bombard a metal cathode gas, knocking out atoms thereof, and on the substrate as a

result of the chemical activity of the reactive gas atoms ionized deposited nitride film or an oxide cathode material.

Because the reaction conditions during the reactive spray substantially depend on the constancy of the concentration of the working gas of the reactive gas, it requires an accurate dose [35].

### 1.5. Mechanisms of gas sensitivity of SnO2 polycrystalline films

According to the model of interaction of gases with the semiconductor surface, proposed by Volkenshtein F. F. [36, 37], we can consider the adsorption of oxygen molecules of the surface of $SnO_2$. Because of film composition deviation of from stoichiometry in the bulk of $SnO_2$ is an excess of oxygen vacancies, which are the centers of adsorption of atmospheric oxygen in the temperature range 200-500 ° C. Figure 1.5 shows a scheme of the band structure of $SnO_2$ in the adsorption of electronegative oxygen molecules from the air. [38]

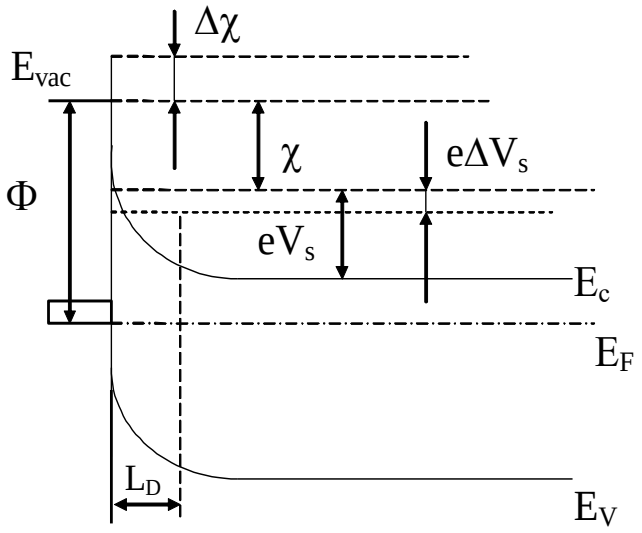


Fig.1.5. The scheme the zone structure of $SnO_2$ during adsorption of electronegative oxygen molecules [38]: $E_c$ - the conduction band; $E_v$ - the valence band; $E_F$ - the Fermi level; F - electron work function from the semiconductor; $eV_S$ - the magnitude of Schottky barrier; $\chi$ - semiconductor electron affinity; $L_D$ - Debye screening length

The oxygen adsorbed on the surface of $SnO_2$ film captures electrons from donor levels, becomes negatively charged and forms the surface of the semiconductor depleted layer or the area of the positive space charge. The degree of oxygen adsorption effect on the electrical properties of tin dioxide can be characterized by the effective

depletion region thickness and height of the Schottky barrier due to the curvature of the bottom of the conduction band.

Depending on the grain size (D) and electrical properties of $SnO_2$ consider three main mechanisms conductivity gas-sensitive metal oxide semiconductor. The manifestation of each mechanism depends on the ratio of the grain size (D) and the thickness of the space charge region $L = 2L_D$, approximately equal to twice the length debaevogo screening. The interaction varies with the gases and the Schottky barrier height changing surface conductivity, i.e. there is the potential barrier height modulation for current flow through the polycrystalline structure.

Different levels of modulation grain boundary potential barriers define three models of electrical conductivity and gas sensitivity (Fig.1.6.):

a) grain-boundary model ($D>>2L_D$) observed in the coarse-grained films with a high concentration of charge carriers, the film resistance is determined by the resistance of grain boundary contacts; the degree of modulation of the Schottky barrier is low;

b) a model of "bottleneck" ($D\geq2L_D$) is observed in films with smaller grains, the conductivity is carried out through the channels between the grains and grain boundaries partially; the average degree of modulation of the Schottky barriers;

c) Model ultrasmall particles ($D<2L_D$) is shown in structures with very small grains, the film resistance is determined by the volume of grain [39, 40]; the greatest degree of modulation of the Schottky barrier

Let us consider some of the features of these models:

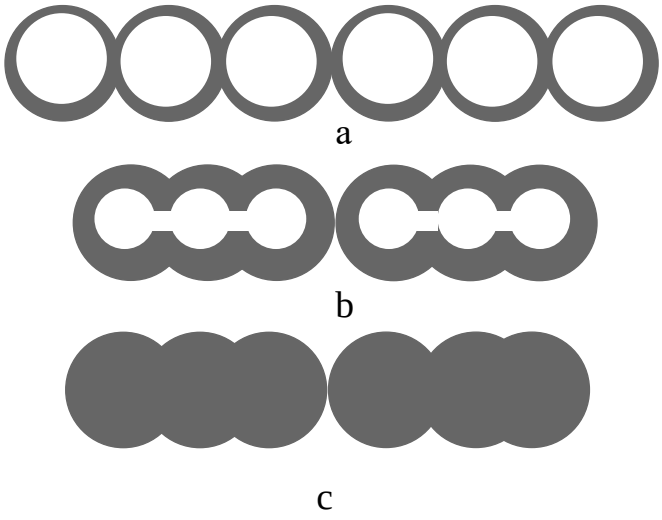


Fig.1.6. Models of change of conductivity of the metal oxide semiconductor, taking into account the grain size [39]: a - grain-boundary model ($D>>2L_D$) ; b - a model of "bottleneck" (D□2LD); c is the model of ultrasmall particles ($D<2L_D$). The shaded region is the space charge.

In the analysis of grain boundary model should take into account that the space charge region occupies a small part of the grain volume, and form a double Schottky barrier (Fig.1.7) on the boundary between two grains. When interacting with the gas poluprovdnika - a reducing agent (e.g., $H_2$ or CO) grain boundary barrier height is reduced and the film resistivity decreases. Thus, when electrons move through the semiconductor in the presence of a gas barrier height that electrons must overcome is reduced. In this case the main current flows through the inner region grains [42] and the degree of change in the electrical resistance is low.

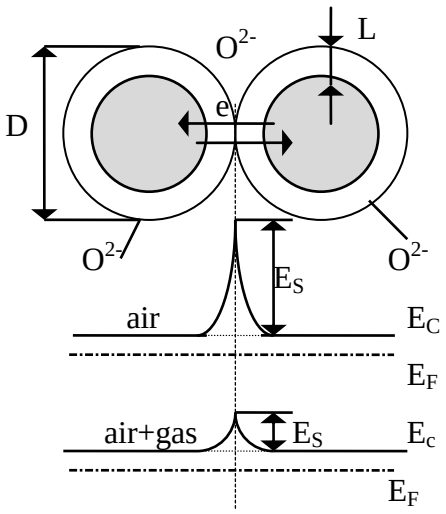


Fig.1.7. A scheme illustrate a grain boundary model (model dual Schottky barrier) and the profile of the conduction band at the grain boundary of [41]: D - diamert grain; L - the width of the space charge region; $E_S$ - the height of the potential barrier; $E_C$ - the bottom of the conduction band; $E_F$ - the Fermi level

The model "bottleneck" [43] it is assumed that the free electrons travel through the channels connecting the individual grains (Fig. 1.8). The thickness of the space charge due to the adsorption of oxygen changes the area of the "bottleneck" and the value of resistance of the film.

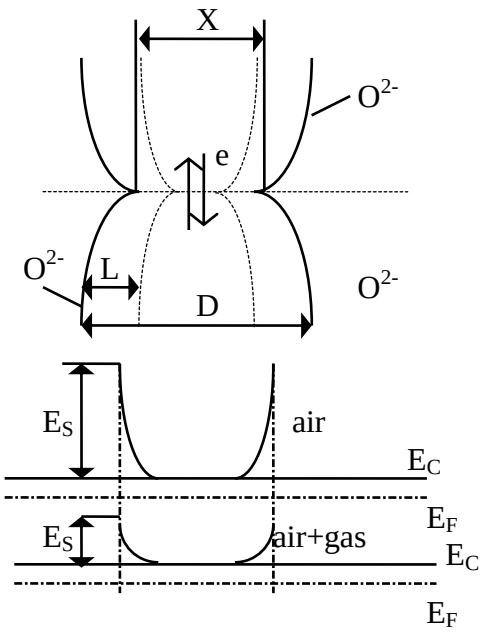


Fig. 1.8. Model "bottleneck" and the profile of the conduction band [41]. Designations are the same as in Fig. 1.7: X - bore diameter.

In [41, 44] that the electrical resistance and a polycrystalline semiconductor gas sensitivity is highly dependent on the grain size. The electrical resistance of the channel is determined by its diameter, the Debye length and the concentration of free charge carriers. According electron microscopy X channel diameter D is proportional to the grain size coefficient of proportionality to: X = kD, where k = (0,8 ± 0,1), if the grain size in the film is in the range D = 4 - 27 nm.

"Bottleneck" model assumes that the electrical resistance of the narrow channel prevails over grain electrical resistance, and the electron concentration within the grain surface and in the space charge of $n_o$ and $n_L$ respectively. Under these conditions, the gas sensitive film (S) can be represented by the ratio of the electric resistance in the air channel ($r_a$) in the gas to the same resistance ($r_g$):

$$S = \frac{r_a}{r_g} = \left\{ (1-x)^2 + \frac{n_L}{n_0}\left[1-(1-x)^2\right] \right\}^{-1}, \qquad (1.9)$$

where $x = 2L_D/X$.

Thus, the model of "bottleneck" qualitatively explains why S increases sharply when D approaches $2L_D$. Quantitatively, this model allows you to analyze experimental results in the case, if you know the size of the grain, the Debye screening length is determined, and measured the temperature dependence of the electrical parameters of the film (the resistance, concentration and mobility of the major carrier) in air and test gas.

In the model of of ultra-particles [42] it is considered that the space charge region completely covers the grain polycrystalline sample (Fig. 1.9). In this case, a conductivity modulation is greatest films when they are placed into the air and gas in the atmosphere, and therefore the highest gas sensitivity of metal oxide semiconductors.

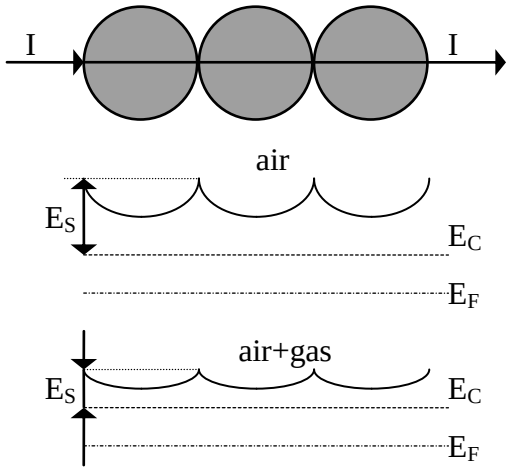


Fig.1.9. The scheme is illustrate the model of ultra-particles and profile of the conduction band [42]. Indications are the same as in Fig. 1.7

Thus, to obtain maximum sensitivity of the gas is necessary to synthesize $SnO_2$ film with minimal grain size of polycrystals and low concentration of free carriers, which increases the space charge and the degree of modulation of the height of potential barrier film by reacting with the gaseous medium.

## 1.6. Mechanisms of recombination of non-equilibrium carriers in transistors after light generation

Depending on the energy of light quanta of semiconductors absorption leads to the generation of non-equilibrium charge carriers of one sign - unipolar generation from impurity levels ($h\nu < \Delta E_g$) or electrons and holes - bipolar generation with self-absorption - ($h\nu \geq \Delta E_g$). After turning off the light there is recombination of non-equilibrium charge carriers.

It has been established that the impurities and defects play a crucial role in the recombination processes. The mechanism of recombination through impurity centers have long been used to explain the results of the study of the photoconductivity, for example, [45 - 48]. More experimental studies of the early $60^{th}$ carried out on materials germanium group (Ge, Si) and a group of CdS (CdS, CdSe, CdTe), clearly established that the recombination of these substances is mainly determined by the number and variety of impurities. Thus, recombination through impurity centers is one of the most important is effectively implemented mechanisms [49].

We consider the case contaminants that can be charged only once and that create in the forbidden band of the semiconductor single impurity level. In this case, each impurity center can be characterized by only two gripping sections: section of electron capture (when the level of the center is free) $q_n$ and hole capture cross section (when the center of the level occupied by an electron) $q_p$ [49].

We can expect that these sections are not the same. If we consider the donor center, it is in a neutral condition, it can capture a hole and being positively charged, - the electron. In the latter case, the capture process contributes positively charged electrostatic attraction and the center of the electron. Therefore, the capture cross section is then more [49].

Consider kinetic processes (Fig.1.10), which may occur in the semiconductor with one type of traps.

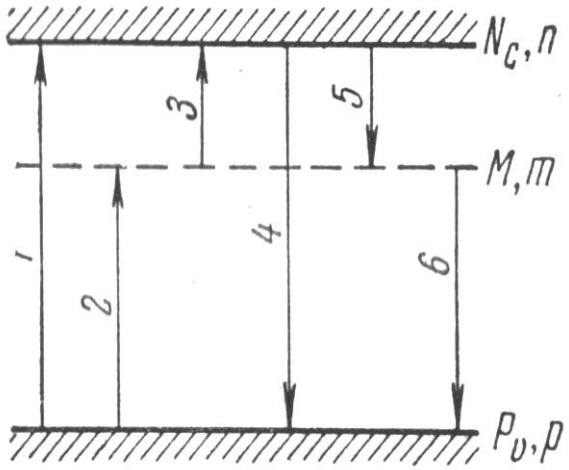


Fig.1.10. Possible transitions of electrons in the semiconductor with one type of trap [49].

Complete concentration of traps will be denoted by M, and the concentration of electrons onto them - by m (Fig.1.10.). The effective density of states in the zones will be denoted by Nc and Pυ, and the concentration of free electrons and holes - by n and p. In this scheme which is comprising three types of states (upper zone, a lower zone, traps), there are six possible transitions (1 - 6), which are shown in Fig.1.10. The six transitions can be divided into two groups [49]:

a) the transitions 1, 2, 3 under the action of light or heat motion requiring expenditure of energy;

b) the passages 4, 5, 6, leading to the seizure or recombination and coming from heat or light energy release.

Since the mechanisms of transition under the action of light and heat are different and there are several possible mechanisms of recombination transitions with heat and light, each one marked by the arrow of transitions in Fig.1.10 may consist of several, and complete a detailed diagram of possible transitions is very complex. For interpretation of results are usually analyzed circuit, which takes into account only a limited number of transitions that have experience in the conditions of the greatest intensity and able to explain the observed phenomena. [49]

We now consider the scheme shown in Fig. 1.11, where some of the most important and typical transitions is considered.

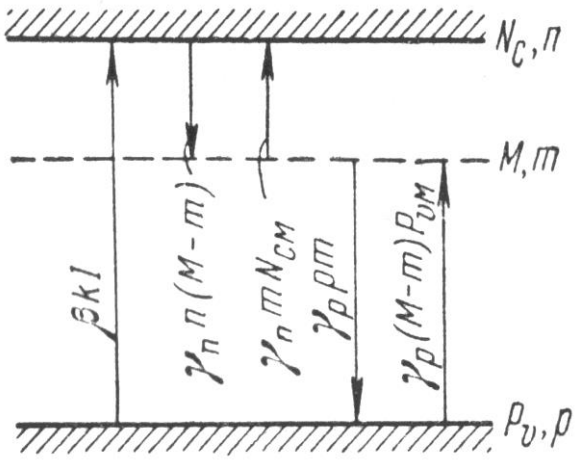


Fig.1.11. The scheme the most important transitions in a semiconductor with a wide band gap at presence the traps of the sam kind

In the scheme of Fig. 1.11 light transfers electrons from the valence band to the conduction band. An electron from the conduction band can be captured with traps M. trapped electrons or re-emitted into the conduction band by thermal motion, or recombine with a hole in the valence band, which is equivalent to the level of the capture holes M. Finally, the possible thermal transfer holes from the M levels in the u-area,i. e. the thermal electron throw from u-band to levels M. The scheme in Fig.1.11 is taken into account only one phototransition from zone to zone (phototransitions with traps unlikely because of the low concentration) and is not considered recombination transitions from the conduction band to the valence [49].

Phototransition intensity from zone to zone can be written in the form βkI where I - intensity of light, k - absorption coefficient, β - coefficient of proportionality. If I measure the number of photons per second, β is the meaning of "quantum yield", i. e. it determines the number of pairs formed by one light quantum [49].

Consider the calculation of the lifetime of nonequilibrium carriers in the stationary state for a scheme with one type traps. Let us consider two limiting cases of low and high concentration of traps.

Fig.1.12 shows a plot of the logarithm of the lifetime, at low light intensities, the position of the equilibrium Fermi level at a predetermined position traps (top band) [49].

On the curve in Fig. 1.12 there are four straight sections (two for two for the electronic and hole area), the variation τ which can be explained on the basis of visual physical representations [49].

While the Fermi level is closer to the conduction band than the trap level M (Fig.1.12, the 1st section) $\tau \cong \tau_{p0}$ i. e. τ is a constant, which is determined solely by the number and properties of the traps when they are completely filled with electrons [49].

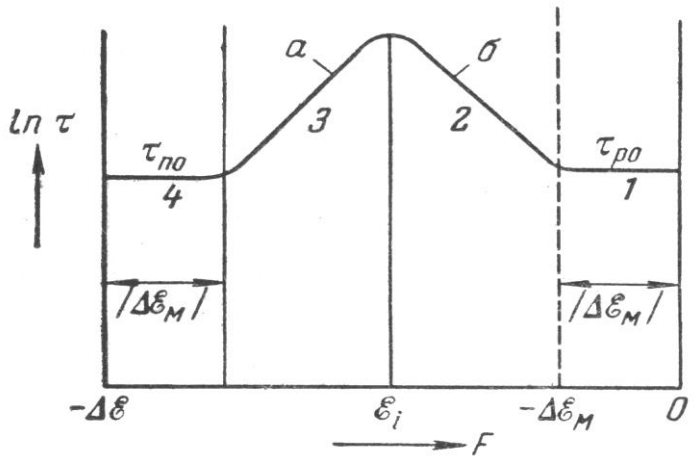


Fig.1.12. The dependence of the lifetime on the Fermi level [49].

In this case, all the traps are filled with electrons and the electron density is high in the upper area in equilibrium. The appearance of nonequilibrium electrons and holes in the zones leads to the fact that the holes are beginning to be gripped filled traps. Thus it is clear that the lifetime of the holes (and electron-hole pairs) is determined by the total concentration of traps (which in the described conditions are always filled), i. e. equal to $\tau p_0$ [49].

In the case where the Fermi level is further away from the conduction band than that of the traps, but closer than the level εi (i. e. $n_0$ electron density is still greater than the concentration of holes $p_0$), the lifetime increases exponentially when the Fermi level shift down. In this area is still the number of electrons in the conduction band is large and each hole captured a trap quickly "hammered" by an electron from the zone. Now, however, in equilibrium, all the traps are not occupied by electrons. The Fermi level is located below the trap, hence their low filling [49].

Thus, the increase in the lifetime of the holes (and couples) with a decrease in the Fermi level is determined at the site decrease filling traps electrons and a corresponding decrease in the probability of capture holes. Subsequent electron capture occurs "immediately" and thus do not affect the value of τ [49].

During the moving of the position of the Fermi level on the 3rd section (Fig. 1.12), the semiconductor becomes a hole. The lifetime is reduced by lowering the Fermi level. In this case, in equilibrium, is almost completely empty trap and readily capture zone of nonequilibrium electrons. Later, however, are not always trapped electron recombines with the hole. As the number of holes is not very large, with the recombination process competes process thermal transition of an electron from the trap back into the conduction band. By reducing the Fermi level of the hole concentration increases, the relative role of thermal transitions of electrons from the traps in the area decreases, and the lifetime falls [49].

If the Fermi level is closer to the valence band than the level of the traps to the conduction band (Fig.1.12, the 4th section), then $p_0 >> N_{cM}$. Lifetime does not depend on the position of the Fermi level. In this case traps are empty, and the lifetime of the nonequilibrium electrons is $\tau n_0$. An electron captured by the trap, immediately recombine with holes, which are many. Reverse thermal transfer of electrons from the traps to the conduction band does not play an important role [49].

Between four straight sections considered on the position of the depending lnτ Fermi level are transitional area width on the order of several kT, which should be used by the general expression (1.11) [49].

### 1.7. Influence of lighting on gas sensing properties of transistors

In 1973, J. Pankow wrote in his work [55] that the gas adsorption process of the semiconductor surface is faster with optical excitation, creates an increased concentration of electrons and holes, which can be captured respectively gas, the atoms of which have a large electronegativity, or substances having donor properties. Fig.1.13 shows that white light illumination accelerates the process of adsorption of oxygen on the surface of CdSe (n-type semiconductor).

*(Темновой ток = The dark current, Начальный темновой ток = The initial dark current, Время/мин = Time/min , В азоте = In nitrogen, В воздухе = In the air, В темноте = In the darkness , На свету = On the light )*

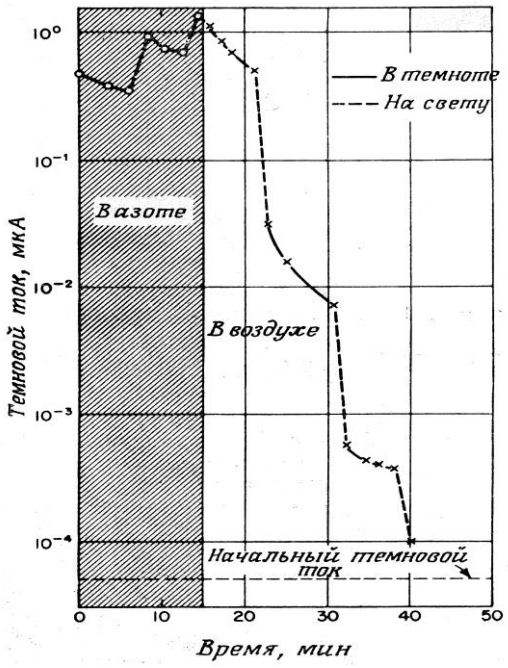


Fig.1.13 Photostimulated oxygen adsorption on CdSe crystals at room temperature [57]: the measurements were made only in darkness

When the zinc sulfide surface illuminated ($h\nu > \Delta E_g$) has been shown [56] that the oxygen absorption rate increases with increasing intensity of the emitted and oxygen pressure. In this case, the adsorption was monitored by changes in the contact potential is directly related to the magnitude of the surface potential [56].

Change in the surface potential was found in experiments with germanium, the surface of which is in contact with alternating wet and dry oxygen; while the greatest effect was obtained when the surface illuminated (Fig. 1.14). Water vapor and oxygen cause apparently opposite effects plate, whereby water is stronger. Changes in the value of the surface potential in Germany, the n- and p-type have different signs [58].

*(Влажный = wet, сухой = dry, тип = type, время/мин = time/min,* $\Delta_{mid} = \Delta_{cp}$*)*

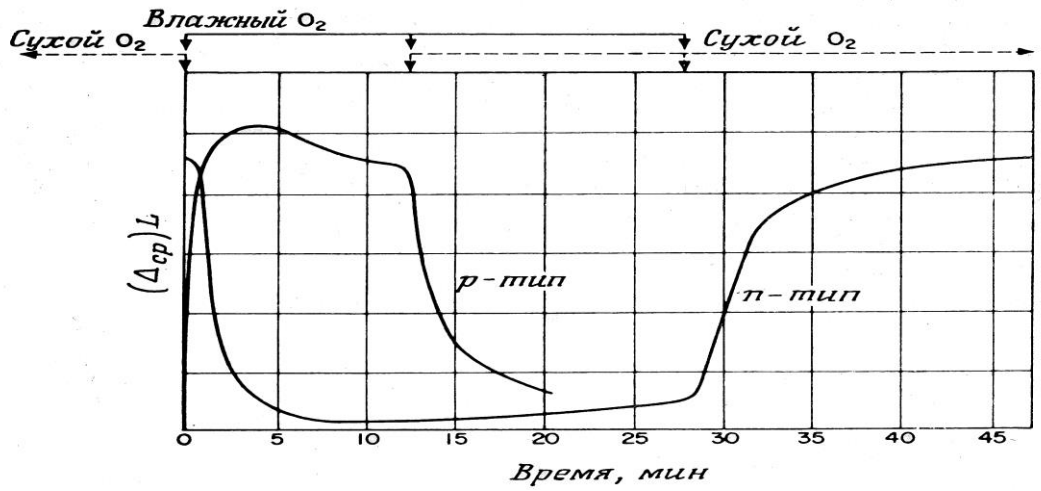


Ris.1.14. The change in the potential of the contact time $(\Delta_{mid})_L$ of Ge surface under illumination: at time t = 0, dry oxygen is replaced by damp, reverse replacement is made after 12 minutes. for p-type sample and after 28 min. the sample n-type [58]

Lighting can cause or increase the adsorption or, conversely, increased desorption [59]. It depends on the nature of the gas, semiconductor, its degree of doping character bending zones on the surface and the experimental conditions such as temperature and gas pressure.

The questions of what should happen when illuminated - adsorption or desorption, has been considered theoretically, at the same time analyzed the dependence of the effect on the position of the Fermi level (i.e., doping and temperature) and the band bending at the surface. The results of this review are summed in Fig.1.15 [59].

For example, the oxygen adsorption (acceptor) intrinsic semiconductor (Fermi level is in the middle of the band gap) causes upward bending zones. If the surface has a small amount of oxygen (low pressure), the bending zones is small, which corresponds to Fig. 1.15 area between points a and b. In this area, there is a positive photoelectric effect, i.e., photo adsorption occurs. At higher gas pressures increases the amount of adsorbed oxygen, the system shifts to a point illumination causes photo-desorption and [59].

*(Положительно заряженная поверхность (зоны изогнуты вниз) = The positively charged surface (zones are bent down), Отрицательно заряженная поверхность (зоны изогнуты вверх) = The negatively charged surface (zones are folded up), тип = type, изгиб зон = the bending of zones, Адсорбированные доноры = Adsorbed donors, Адсорбированные акцепторы = Adsorbed acceptors)*

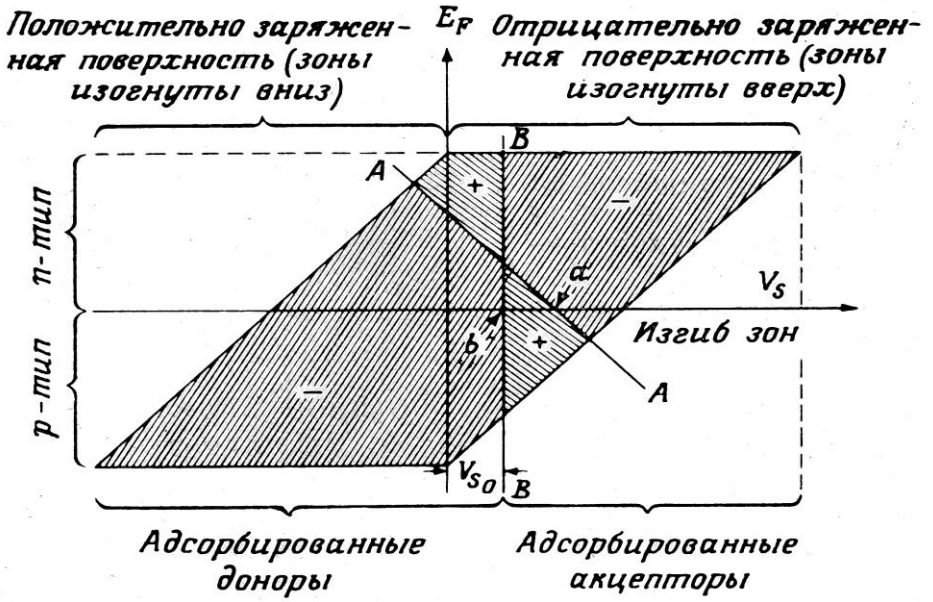


Fig.1.15. Possible $E_F$ the Fermi level position and the bending $V_S$ zones depending on the type of adsorbed particles [59]: Lines AA and BB obtained from theory; BB offset in relation to the zero line gives the initial value of band bending; the area marked with "+" correspond photoadsorption, and the sign "-" – photodesorption

In the case of ZnO oxidation and oxygen diffusion in the crystal leads to a gradual deviation from the stoichiometric composition on the surface. It can cause band bending in the opposite direction compared to the band bending at the oxygen absorption to the original surface [55].

Adsorption of oxygen on CdTe may cause a change in the polarity of the anomalous photovoltaic effect [60]. Oxygen is very strongly associated with CdTe surface, so its desorption and recovery of the sign of the photovoltaic effect requires heating under vacuum. However, it was observed that the adsorption of oxygen is accelerated by light.

In the paper [61] the effect of lighting on ZnO desorption of carbon dioxide and by the amount of surface conductivity of zinc oxide is described. The interrelation of the nature of change in these two processes. So when photodesorption $CO_2$ turns to the ZnO first rapid change, which slowed down with time. Also changed and the surface conductivity. The calculations of the dynamics of the process showed agreement with the experimental results. Then, for many years of research the effect of light on the processes of adsorption and desorption of gases surface of metal oxide semiconductors were not effective character.

In 1996 was published the paper [62] in which it is shown that the coverage of the ultraviolet (UV) light of $SnO_2$ films increases their sensitivity to oxygen gases - reducing agents (CO) at room temperature. At elevated temperature (T = 400 $^oC$), when the film is most sensitive to carbon monoxide, the influence of illumination on the sensitivity of tin dioxide was found.

Other Italian scientists E.Comini and etc. published in 2000 the paper [63], in which they described the effect of the illumination with UV light on the gas sensitivity of $SnO_2$ thin films and $In_2O_3$ to different concentrations of $NO_2$ and CO. Samples were prepared by spraying in Ar atmosphere reotaksial cultivation technology and thermal oxidation (RCTO) and reactive magnetron sputtering in an atmosphere of Ar and $O_2$,

respectively.The sensitivity to gases at room temperature in darkness in the air (Fig.1.16) and when exposed to UV light (Fig. 1.17).

Effect of UV radiation on the gas response of $SnO_2$ and $In_2O_3$ investigated in the study [63]. CO and $NO_2$ are used as gases. Sensitivity, different concentration of gas at room temperature in the dark (Fig.1.16) and the process of illuminating by ultraviolet light were studied. Irradiation was carried out UV lamp ($\lambda_{max}$ = 365nm, the power density of 0.5 mW / mm $^2$).

Without effect of light the gas response $SnO_2$ film to 3 ppm $NO_2$ rather slow (tens of minutes), and after stopping supply of tin dioxide $NO_2$ resistance does not return to the original values (~ 50% recovery).

Under the influence of UV gas faster response (ten seconds), and the resistance in clean air recovery is 80% of the initial value. At room temperature and irradiated with UV light a surface resistance value is not restored even after 20 hours. Therefore, the gas-sensor samples before each new cycle of irradiation was heated to 400 ° C one hour to avoid residual phenomena called "memory effect".

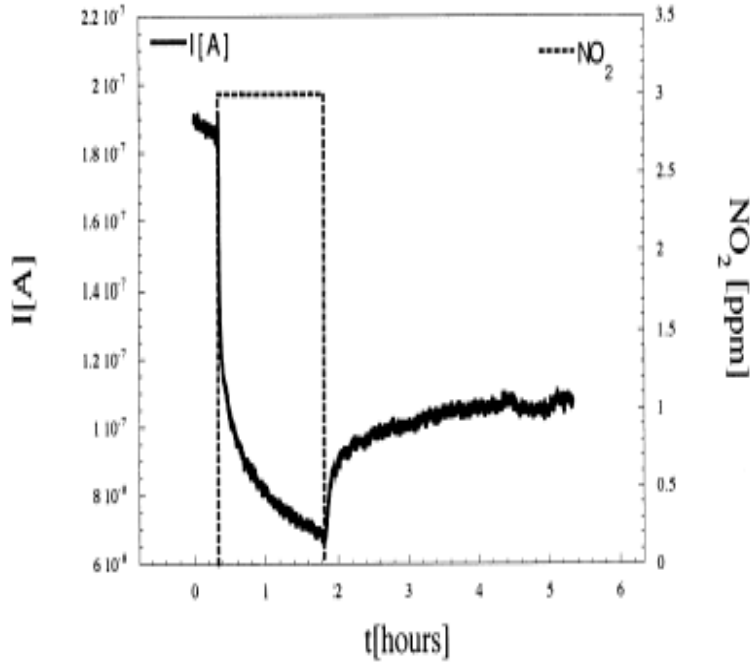


Fig.1.16. The kinetics of gas sensitivity in the darkness for 3 ppm NO2 at room temperature for the sensor based on tin dioxide

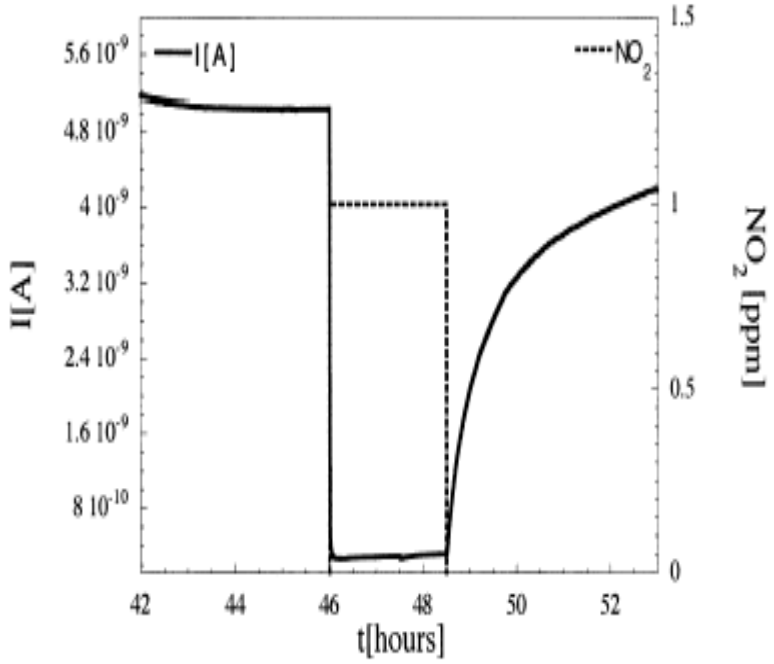


Fig.1.17. The kinetics of gas sensitivity to 1 ppm $NO_2$ under irradiation with UV light at room temperature for the sensor element based on $SnO_2$

Irradiation with UV light of a mercury-neon lamp power of 0.35 mW / $cm^2$ of thin films of tin dioxide and their response to $NO_2$ at room temperature has been studied in the paper [64]. As in the past [63] it was obtained by improving the performance ga sensor SnO2 films during exposing to UV light: a decrease in the response and recovery, the lack of effect «etched» of $NO_2$ gas. These results can be used to develop $NO_2$ sensors operating at room temperature.

In 2003 the team of authors of the Voronezh State Technical University [65] investigated the effect of optical excitation of the UV and visible range of the resistance film sensitive semiconductor gas sensor tin dioxide. For the study test structures of gas sensors, the sensor that consists of a thin (250 nm) of tin dioxide films produced by reactive magnetron sputtering are used. The film was deposited on a tin dioxide sensor pads interdigitated with the distance between the current collecting members 10 microns. The sensor was placed in the illuminator spectrophotometer SOM-2 at a distance of 0.4 m from the xenon lamp 150 watt. To focus the radiation between the lamp and the sensor placed collimator. The collector of the light flux is used in the

visible and near-ultraviolet light-sensitive sensor on the electrical layer. As a result, light sensor the electrical resistance decreases. These kinetics resistance recession when the lights have a complex form of these two groups can be distinguished: the first group of processes was obtained in the initial lighting cycles sample not subjected to preliminary thermal annealing. The shape of these curves is close to exponential. It was noted that the shape of the curves obtained is unstable and after a few switching cycles - turn off the light patterns are beginning to show the kinetics of the second kind, which were observed in the annealed samples were stable and samples immediately show them even after the break between measurements in a few days. The curves of the second type were observed two sections: the first - the rapid decay of the resistance for a few minutes; the second - a slow increase of the resistance, which is not typical for the kinetics of the photoconductivity of the classic semiconductors. The temperature dependence (T = 20 - 100 $^{o}$C) have shown that increase in temperature weakens processes responsible for increasing the resistance on the second portion relaktsionnyh curves.

After switching off the lighting, the recovery resistance of the samples is relatively long. Time constants of the resistance recovery process at room temperature is approximately equal 10 - 15 min. When the sample temperature resistance slowed the recovery process. As well as the curves of the resistance recession, there were observed two types of specific sections of the curves corresponding to the not annealed samples in the first and subsequent lightings, and the samples recovered faster after the first lighting, and two sections of fast and slow recovery observed curve. Subsequent measurements explicit separation was not observed in the two regions. Quick site was not more than 10% recovery soprotivleniya.Takim way exposure to light in a complicated way affects the resistance of the film of tin dioxide. They also studied the photoconductivity depending on the light intensity of the lamp power 56 and 64 Watt. It was found that the irradiation light intensity value does not affect the shape of the curves, and depth changes only effects.

In the paper [66] the use of the effect of low-power light violet LED ($\lambda_{max}$ = 407nm) to the electrical properties of $SnO_2$ films is described. When you turn on and off slowly light-emitting diode resistance film was set in and in the paper [66] Studies suggest mechanisms relaneation processes. It was found that the processes of change in the electrical resistance of tin dioxide films can be described by three exhibitors, each of which corresponds to a particular physical process.

After turning off the LED a slow relaxation of the electric resistance is happen, and it can also be described by three exponentials with characteristic relaxation times, different from the relaxation parameters of resistance changes when the film coverage. Prolonged annealing the film of tin dioxide in the air considerably reduces all 3 observed characteristic times of relaxation resistance when you turn on the LED, and when you turn off the light changes only one relaxation time compared to non-annealed films of tin dioxide.

It has been shown that one of the exponents can describe electronic processes associated with the levels of adhesion and deep defects, the second - ion processes associated with surface states, and the third - diffusion processes associated with the drift in an electric field [66].

The effect of action of light depends on the initial value of the resistance film of tin dioxide and the more evident the higher the initial resistance.

Theoretical description of the effect of UV light on the electrical properties of the metal oxide films have been applied in the paper [67], which was based on the results of studies [62, 63]. It was a model of the effect of light on the gas sensitivity at room temperature, based on the combined effect of "grain boundaries" and "bottleneck." At the respective light absorption leads to the generation of electron-hole pairs in the depletion region of polycrystalline grains, which reduces the height of the grain barriers and increases the concentration of free carriers in the sample. Calculated according to the relaxation curves of the electrical correspond to the previously obtained experimental data.

In the study [68] we published the results of research of the effect of radiation of red, yellow, green, blue LEDs on the sensitivity of gas sensors based on tin dioxide films. Tin dioxide films produced by reactive magnetron sputtering a tin target with additions of Sb, in and catalytic Pd and Pt coatings were tested for sensitivity to vapors of ethyl, isopropyl alcohols, acetone, and benzene. It was shown that all types of radiation whose energy ($h\nu < \Delta E_g$) for all these reactants increased sensitivity gas sensors with reagents doses 1 - 10 ppm of an amount of 2 to 100 times that the sensors have a low sensitivity without irradiation with light. It was shown that the dependence of sensor sensitivity on the intensity of light irradiation depends on the type of the catalytic coating, for example in the case of a linearly increasing impurity Pd and increases sharply at a maximum light intensity in the case of an impurity Pt. However, in this work, there are many contradictions, for example, it is unclear how it is possible to low-voltage LED diameter 3mm apply voltage from 5 to 15, do not understand the mechanisms of nature exposure of red, yellow, green, and blue light ($h\nu < \Delta E_g$) on the thin silica film tin, it is unclear why the light affects the film only in the presence of atmospheric trace gas concentrations and has little effect at high concentrations of gases, unclear error in determining the sensitivity of the gas, as the authors claim that they were dealing with a sensitivity to the vapors of ethyl alcohol 1%.

Summarizing the currently known data on the effect of light on gas sensing properties of semiconductors, we can conclude that they are quite contradictory. In some studies write that ultraviolet light decreases the temperature of the maximum gas sensitivity, others reported that UV light increases the value of the maximum gas sensitivity, the third - that both red and yellow, and green and blue light increases the value of the maximum gas sensitivity. At the same time we can say for sure that today we know very little definitive experiments, which can be judged on the mechanisms of light exposure on the gas sensitivity of thin films of metal oxide semiconductors.

**Conclusions of the 1st chapter.**

Using the analysis of the literature data we can point the general principles of the application of $SnO_2$ films in gas sensory. $SnO_2$ films which characterized by a high level of gas sensitivity (in ppm level), but have a low selectivity to controlled gases. The maximum response of the gas is achieved at high (200 - 400 ° C) temperatures, which means a high energy consumption and measurement explosiveness most reducing gases ($H_2$, CO, $CH_4$, etc.). The work temperature of the sensor can be reduced by activation of adsorption processes on the surface of the $SnO_2$ film by its doping-catalysts or by exposure to a light source of a particular wavelength.

The purpose of this study was to determine the features of SnO2 films photoconductivity mechanisms in interband transitions of electrons and impurity one, when activated by light exposure of adsorption processes on surfaces and in the bulk of the film, and as a result of the surface modification of $SnO_2$-alloy catalysts.

To achieve this goal it is necessary to solve the following tasks:

1. To characterize mechanisms of photoconductivity of $SnO_2$ films illuminated by LEDs with different energies of photons.
2. To study the effect of surface and bulk optical activation of the gas sensitivity of $SnO_2$ films for gas-reducing agent.
3. To investigate the activation process gas sensitivity of $SnO_2$ films surface modification sensors salt catalysts of silver and palladium.
4. To investigate the possibility of improving the metrological characteristics of sensors simultaneously exposed to light and surface modification of films $SnO_2$ catalysts by salts of silver and palladium.

# Chapter 2.

# RESEARCH METHODS OF PHOTO-ELECTRIC AND GASO-SENSOR PROCESSES IN TIN DIOXIDE FILMS

## 2.1 Construction and technology of preparation microelectronic gas detectors

Research and development of semiconductor gas detectors were carried out on various materials ($SnO_2$, ZnO, $V2O_5$, $In2O_3$, CoO, MgO, etc..), But the basic material is considered $SnO_2$ [70]. $SnO_2$ films have high chemical stability, mechanical strength, heat resistance, good adhesion to glass and other substrates [69].

To be effective, the gas sensor must have a heating element to create the desired temperature (500 ° C), the current collecting contacts, the contact pads for connection of external leads, gas-sensitive layer [71]. It is desirable that the crystal had minimal thermal contact with the housing and the minimal geometrical dimensions, in order to touch layer maximize heat given heating element. B is selected silicon coated with an insulating layer of silicon dioxide as the substrate.

Structures of sensors gases were produced according to modern technologies of microelectronic products with thin-film gas sensing layer. The advantage of thin-film technology is that it can help to create a fully all elements of the gas sensor chip in a single technological cycle. Test patterns can create any modes and explore all the features of the sensor behavior in real working conditions [72, 73].

The effectiveness of most types of sensors depends on the uniformity of the temperature distribution over the surface of the sensitive area. Mechanical strength is needed to resist manufactured load sensor occurring during the subsequent treatments, when mounted in the housing and during subsequent operation.

The heating element should have a slight resistance to extend the life of the battery and its topology must provide optimum heat distribution over the surface of the sensor chip. As the contact group generally uses the anti - whip system that provides reliable contact to the gas sensing element of the sensor and the control over the change in its resistance. The gap between the current collecting contacts of the sensor (10 microns) is selected to produce an acceptable design for this sensitive layer resistance. Size pads optimized for splicing external leads of aluminum wire with a diameter of 35 microns. Functions of the heating element perform a thin-film resistor.

The design of the test gas sensor shown in Fig.2.1 is a rectangular crystal is thermally oxidized silicon thickness of 0.4 mm and a size of 1 x 1 mm. The chip formed thin film platinum resistor meander - 1, which acts as a heater and counter - interdigital electrodes - 2, which in some way is applied $SnO_2$ gas sensitive film - 3. Pads - 4 ultrasonic welding welded connecting lead wires. Workflows can use the standard for the modern semiconductor industry for the manufacture of gas sensor.

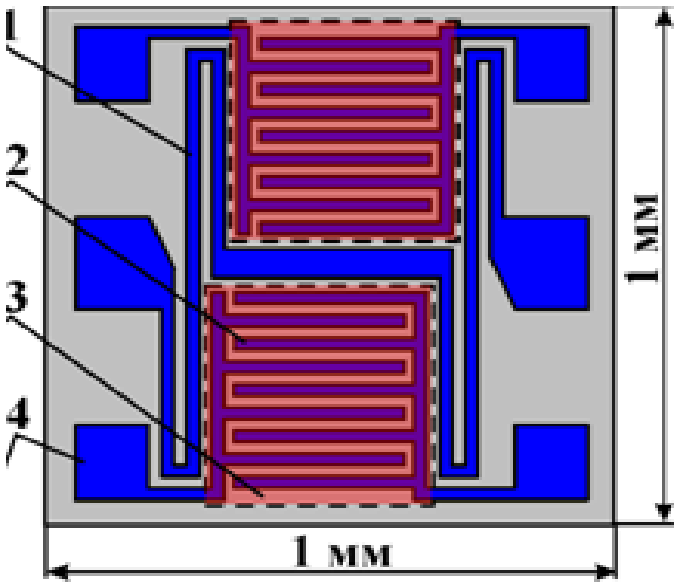


Fig.2.1. Test sensors Topology of structures (crystal 1x1 mm2, the scale is not observed): 1 - platinum meanders; 2 - counter - interdigital electrodes; 3 - $SnO_2$ gas sensitive film; 4 - contact pads.

The presence of two autonomous groups of current collector contacts allows detecting or measuring the concentration of two or more gases using different gas-sensitive films. If one of the sensitive areas of the gas to close the gas impermeable film can significantly increase the gas sensitivity of the sensor by using a measuring bridge circuit.

The thickness of the gas-sensitive film is (3) 250 nm.

To create a contact group platinum, which provides a chemically resistant, stable, well-conductive metal film is used. Sensor layers of tin dioxide can be "poisoned" photo resist, so their application to the contact group should be carried out by the blast photolithography.

The crystals can be mounted in a sintered metal body which has eight outputs. The installation should have high demands as gas sensor operates at temperatures up to 500 ° C. Mounting method should provide a high mechanical strength and good thermal connection between the housing of the crystal. Splicing of conclusions should be of aluminum wire (diameter 35 - 60 mm) by ultrasonic welding [72].

Technological route of the gas sensor output was as close to the silicon manufacturing technology of microwave transistors. All used process steps are used to produce of microwave transistors [73].

The following is diagram of the process flow of the gas sensor production with a brief description of the parameters and characteristics of technological operations (Fig. 2.2).

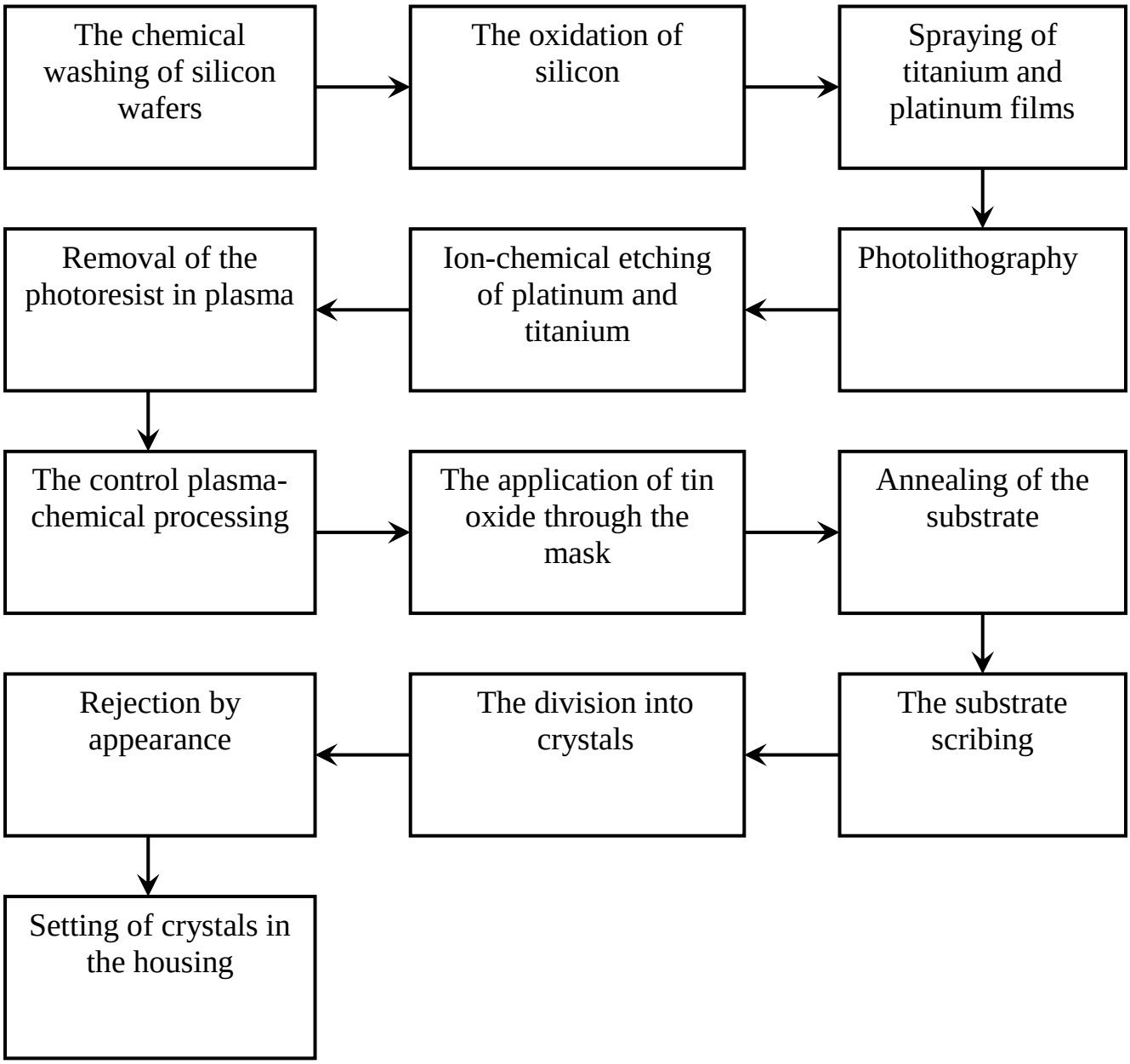


Fig.2.2. Diagram of the technological making process of the sensor [73]

To create a contact group platinum was used, and it provides a chemically resistant, stable, well-conductive metal film. Preparation of "windows" for contacts - 4 in the layer of tin dioxide using thumb maker used in producing Si transistors is difficult, and sometimes impossible because of the low chemical activity of tin dioxide in this case, the specificity consists in the fact that if a layer of tin dioxide located above

the slip contacts - 2, then prior to its application over the areas of contact pads 4 formed photo resist layer thickness of 3 - 5 times the thickness of the tin dioxide.

After applying a layer sensitive plate is placed in an acid or an organic solvent in which the photo resist layer is dissolved or after swelling "hacks" tin dioxide film remaining on its surface. Therefore, to create the desired pattern on it in the process flow we use the method of explosive photolithography.

The production process of each semiconductor device starts with the operation "Party Formation". Silicon wafer polished sensors of any type of conductivity around 0.4 mm thick used for manufacturing.

The chemical washing of plates was performed immediately before the basic operations. Before thermal oxidation unused cleaning process consisting of washing a mixture (KAPO) $H_2SO_4$ + $H_2O_2$ or peroxide - ammonia mixture (PAS) $H_2O_2$ + $NH_4OH$ + $H_2O$ (1:1:4) at 75 ° C for 5 min, then hydro mechanical washing of plates drying centrifuge using purified dry air stream in the plant.

Thermal oxidation is performed in order to create on the surface of a silicon wafer (the substrate), the dielectric layer SiO2, which will be further reliably isolate construction elements from each other and reduce the loss through the heating element substrate emitted heat. In the production structure of the gas sensor dielectric layer is formed by thermal oxidation in an oxygen atmosphere by the "dry - wet - dry oxygen." The thickness of the resulting oxide was about 0.5 microns.

The chemical washing of is carried out after thermal oxidation before the sputtering process of the plate subjected to a standard washing process in a mixture of PAS and KAPO.

Spraying Ti - Pt. Titanium provides good adhesion to the $SiO_2$ surface by the formation of a chemical bond. The thickness of the resulting composition was 0.45. This total thickness of the film provides the desired design parameters and allows for reliable welding leads. Spraying mask titanium Ti, about 0.2 microns thick is used as a masking coating at ion-beam etching Pt layer.

Positive photo resist is used in manufacturing technology gas sensor used. It is applied to the substrate by centrifugation, and then loses its solubility. The thickness of the resulting photo resist was 1.15 microns. In this case, we use the contact photolithography to create a topology of meanders and counter - pins.

Etching the titanium layer through the photo resist mask was produced in the acid etchant at room temperature. To remove the photo resist in gas sensor technology used, or chemical removal of the photo resist, or a plasma-chemical removal.

Ion-beam etching of Pt was carried out through a metal Ti mask. After ion - beam etching of the protective layer of platinum titanium mask on the platinum surface too decrease, resulting in masking and adhesive layers of titanium are approximately equal thickness. Therefore, chemical etching of these layers to complete removal is performed in one process step. After the operation on the surface of silicon oxide obtained fully formed Contact Group (thermistor and terminals for sensitive layer).

Photolithography. "Creation of the sensitive layer" in the films of materials that are difficult to etch, creates a method so-called "reverse" or "explosive" photolithography. On the substrate, first create a micro-relief of easily soluble material, which is a negative of the pattern to be obtained. Then the rest of the film and the film deposited substrate material and working the entire system is treated with a solvent. It dissolves readily soluble drags material lying on it a film which remains only at those places where it was deposited directly on the substrate. If the film thickness is easily soluble material is several times greater than the thickness of its coating layer, the process will be effective enough. The gas sensor technology as sensitive layer of SnO2 layer is used, which is difficult to etch, so to get the micro relief sensor used explosive photolithography. As a readily soluble material is applied a positive photo resists (FP 9120-1). For effective photolithography process needs a thick photo resist - 2.5 microns. To create a thick photo resist photolithographic all operations are carried out sequentially twice under standard conditions. SnOx sensitive layer sputtering is conducted in an atmosphere of argon and oxygen (oxygen content can be varied to

obtain the desired properties of the sensitive film). The thickness of the resulting film is 0.5 - 1 micron.

Removing the photo resist produced by chemical means. A solution of the photo resist drags him lying on the film SnOx. After surgery, the removal of the photo resist on the substrate surface film pattern are not removed particles of the photo resist, and many other dirty, so you need to carry out a chemical washing to complete the standard scheme.

Cutting is carried out on the crystals by scribing with a diamond disc. The assembly consists of a gas sensor mounted in the housing and crystal splicing conclusions. By mounting high demands as gas sensor operates at temperatures up to 500 ºC. Mounting method should provide a high mechanical strength and good thermal connection between the housing of the crystal.

## 2.2. Methodology of alloyage of sensitive elements of gas sensors using silver and palladium impurities

Alloying elements sensitive microelectronic sensors based on SnO2 gas was carried out by the method of a surface modification with alloy of palladium and silver.

Palladium is used as a catalyst in chemical reactions, which improves the selectivity to a specific gas, namely, to the pairs of ethanol. Palladium doping for 3 samples were also prepared mM, 6 mM, 9 mM and 12 mM solutions of $PdCl_2$ + $H_2O$. Upon formulation, solutions are placed in a special container, which does not allow penetration of daylight. 3 mM solution obtained by dissolving 25 mg of palladium chloride in 50 mL of distilled water. Before applying the admixture, gas sensors were pre-annealed at 450 ˚C for removing adsorbed molecules from the surface of the semiconductor [74, 75]. Local doping solution of palladium chloride was carried out by coating the surface of the sensor micro droplets sensor element solution is controlled under the microscope MBS-1 to 56-fold increase, followed by drying in air at room temperature for 30 minutes, and heating the admixture at a temperature of 350 ° C for 60 minutes. The second sensor element left undoped and used for comparative characteristics.

For doping samples by silver aqueous solutions AgNO3 of varying degrees of dilution from 25 mg to 100 mg in 50 ml water (0.003M, 0.006M, 0.009M and 0.012M respectively)were prepared and placed in a special vessel that does not allow penetration of daylight [76] .

Local application of the silver nitrate solution was carried out by a special technology controlled under the microscope by applying a solution onto the micro droplets sensitive sensor element, followed by drying in air at room temperature for 24 hours. The second sensor element left undoped and used as a control.

## 2.3. The settings for measuring of parameters and characteristics of gas sensors

For thermal stabilization of electric parameters (annealing) of test structures and the research of the parameters of gas sensors installation, a block diagram was used and it is shown in Fig.2.3.

Installation consists of the following modules: power supply unit (1) - the source HY3010E 0 DC stabilized voltage - 30 V / 0 - 10 A; a control unit (2) - switches the system is responsible for monitoring and measuring electrical parameters, pitch and adjust the sensor supply voltage; measuring stand (3) with a gas sensor and measuring instruments - ammeter METEX P-09 (4), a voltmeter, a built-in power supply (5) and an ohmmeter UT33D (6). The circuit includes also a timer to control the time of the experiment.

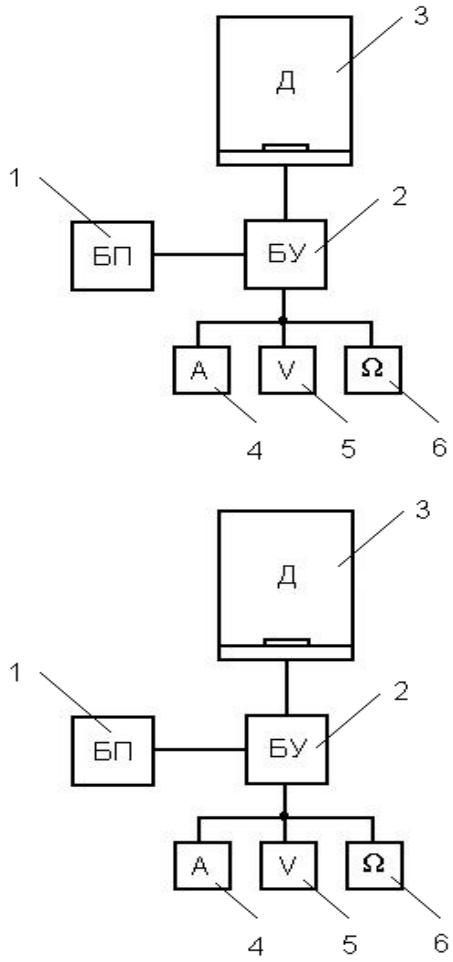

Fig.2.3. Block-scheme of the installation for research of gas sensors: 1 - power supply; 2 - control unit; 3 - measuring stand with a gas sensor; 4 - ammeter; 5 - voltmeter; 6 - ohmmeter.

Installation for measuring the parameters and characteristics of gas sensor is shown in Fig.2.4. This setup allows for the stabilizing annealing, the measurement of the electrical characteristics and parameters of gas sensors, gas measurement sensitivity, measurement of the effect of light on the parameters of the gas sensors.

The main elements that make up the unit for the measurement of gas gas sensor:

1 - Power supply NU 3010E

2 - Current in the indicator circuit.

3 - A voltage indicator, the power supply source (1).

4 - Handles for coarse and fine adjustment of the applied voltage

5 - Multimeter to measure resistance of the first sensor element (9).

6 - Multimeter to measure resistance of the second sensor element (8).

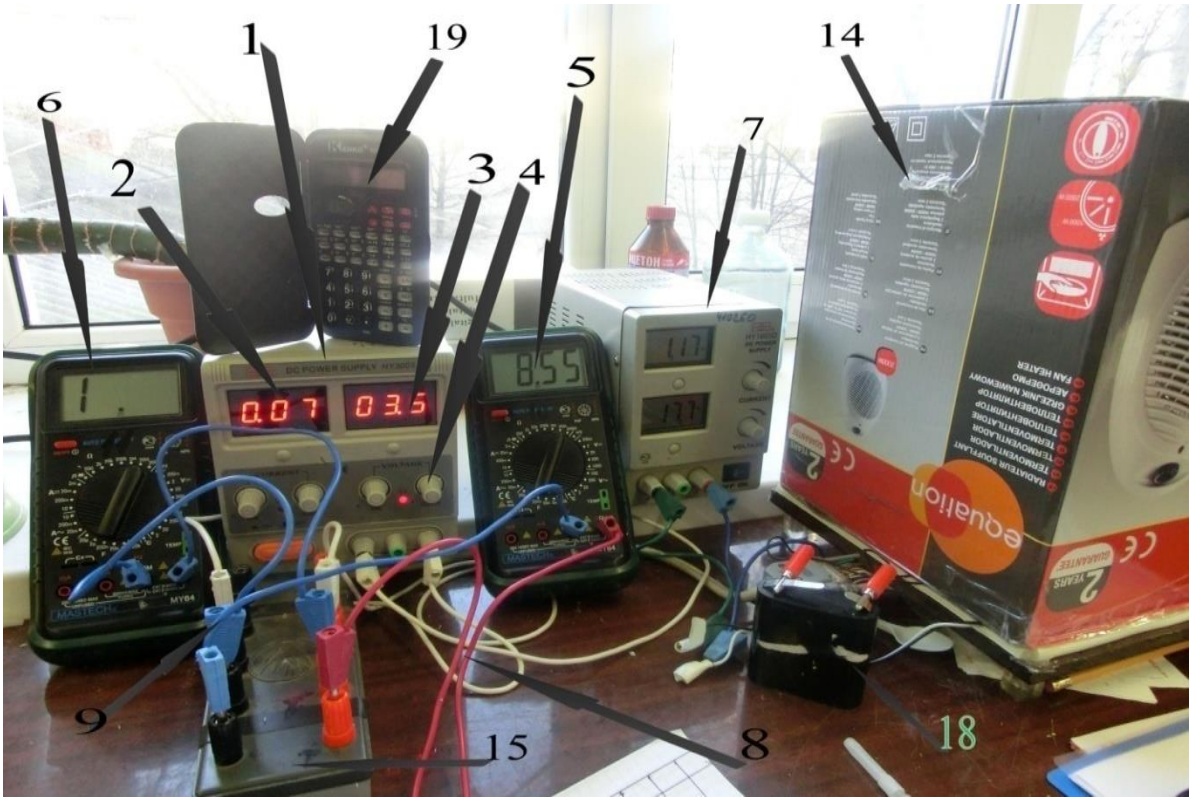

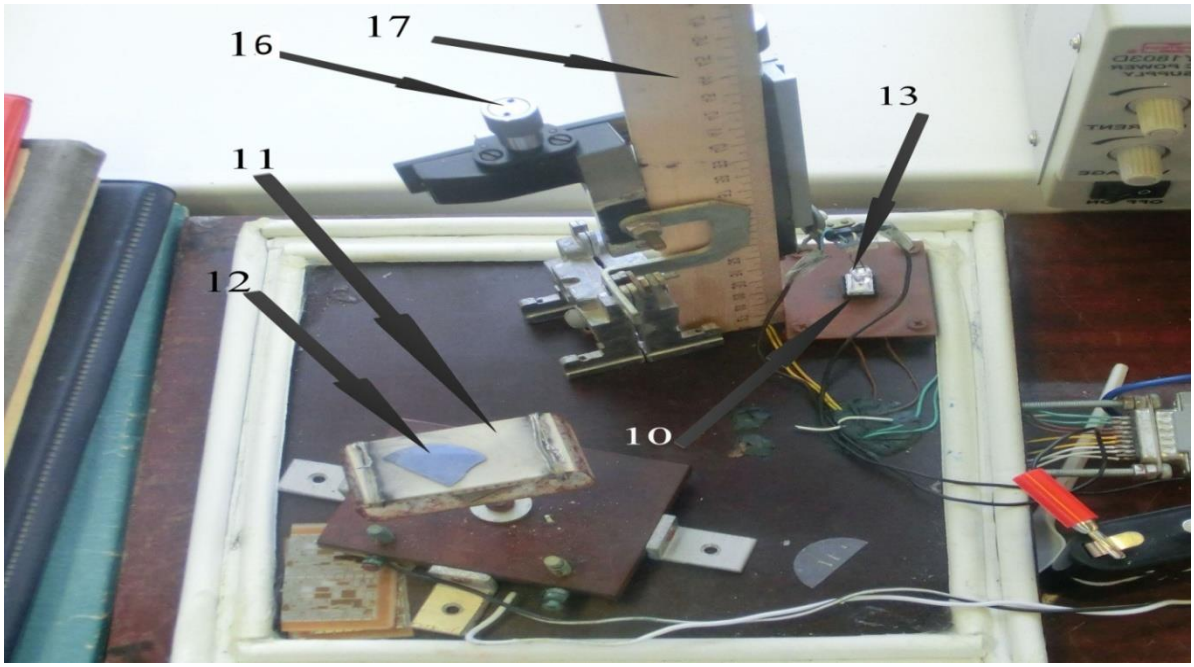


Fig.2.4. The elements of the installation of the measurement of gas sensitivity

7 - The output of block (15) for supplying power to the heating element power supply voltage

8 - The output of block (15) for removing from the second impedance sensor

9 - The output of block (15) for removal of resistance from the first sensor

10 - Sensor that is inserted into the connector, which is connected to the block (15).

11 - Furnace for rapid conversion of liquid substances in the pair

12 - The silicon wafer, on which is placed a liquid substance in order to avoid getting it on the heating element of the oven.

13 - LED (purple - blue – green - red light).

14 - Light-tight cap required to prevent external light on the sensor surface, as well as serving to isolate the leakage of gas vapors outside.

15 - the connector with the conclusions: 1 st and 2 nd sensors, the heating element.

16 - Handles for changing the distance between the LED and the sensor

17 - The ruler to measure the distance between the sensor and LED.

18 - Battery 4.5 V to run the LED.

19 - Hours to fix the time of the processes in minutes and seconds.

Getting started and the course of the experiment:

1. Setting gas sensor connector and check the quality of the contacts.

2. It then checks the electrical circuit includes a power source, exhibiting voltage of 5 V. At a given voltage occurs annealing, that is, from the surface of the sensors are removed adsorbed molecules. The workbook is compiled a table which includes the following values: resistor $R_{1\ SE}$, $R_{2\ SE}$, t - time, in minutes. The measurement is carried out every 5 minutes. When the values of the sensitive elements of resistance remain practically unchanged and their values do not differ by more than 5%, it is necessary to move to the next stage.

3. The sensor is getting cold to room temperature.

4. The cap is removed and the heater is placed a drop of the test substance. The hood is closed and turns on the evaporator.

5. Now you need to put pressure on the heater is equal to 1 and increments of 0.5 V to measure every 5 minutes, so to 6 V. The following measurements are recorded in the logs to the table: $R_{1SE}$, $R_{2\ SE}$, t - time, in minutes; $R_H$, U, I.

## 2.4. A measure method of gas sensitivity of microelectronic gas sensors

Studies of gas sensitivity of test structures were made using the same experimental setup as that of heat setting (Fig.2.3). The experiment involved pre-annealed sensors. The voltage applied to the heater for the purpose of setting the desired temperature of the crystal, depended on what happened in the test gas environment, and because the maximum gas temperature sensitivity is different for different gases.

Just as in the case of the annealing gas sensitivity studies were performed under a hermetic cap.

During the experiment we made the following

a) resistance measurement sensitivity of the sensor elements in the air at certain values of currents and voltages supplied to the heater;

b) termination of supply voltage, and cooling of the sensor chip;

c) run under the hood the desired concentration of the test gas;

g) resistance measurement sensitivity of the sensor elements in the test gas at a predetermined concentration for the same values of currents and voltages, as in the air;

d) determination of the sensitivity of the gas sensor at a certain concentration of the gas

$$S = \frac{R_{чв}}{R_{чг}} \quad , \qquad (2.2)$$

where $R_{PY}$ – resistance of sensing element in the presence of gas;

$R_{se}$ – resistance of sensing element in the air.

d) construction of the dependence S = *f* (N)

To obtain the desired concentration of the test gas cap was introduced under a calculated amount of the corresponding liquid evaporation which gave the desired gas concentration. Recalculation of the concentration of the liquid substance in the concentration of the gaseous substance by evaporation in a confined space was carried

out according to the formula Mendeleev - Clapeyron [78]. The error in the preparation of the desired concentration of the test gas is composed primarily of precisely the required amount of possibilities in terms liquid substance. Since the liquid in a syringe, the instrumental error was half the price of the syringe division, i. e. 0,005 ml, which was 150 - 200 ppm for the test in the gases. To increase the accuracy of experiments and preparation of small concentrations of gas liquid phase was stirred with water, the volume of liquid material was approximately 0.5 ml (approximately 15,000 ppm of gas), and thus obtaining the required accuracy of the test gas concentration was decreased to about 1%.

The error in the determination of sensitivity of the gas evolved from the error in determining the concentration of the test gas and temperature, as well as measuring multimeter resistance error, total error was ± 4,5%.

In the process of gas sensitivity studies were carried out measurements of the following characteristics:

• Relative resistance of the sensitive elements and the air temperature in the test gas at a predetermined concentration. According to this characteristic can be estimated how much the resistance of the sensing element of air resistance in the presence of gas, and the temperature at which the maximum contrast of the observed resistance. Sensor temperature was determined by monitoring the current and voltage of the heater, to calculate its resistance. Since the heater resistance depends linearly on the temperature, the temperature used to determine preavaritelno built calibration dependence of the resistance on the temperature of the heater.

• The dependence of the gas sensor sensitivity of the temperature at a constant concentration of the test gas. In this experiment the sensitivity of the gas was investigated in the temperature range from room temperature to 400 ° C which was controlled by changing the voltage applied to the sensor heater.

The measurement results were plotted against gas temperature sensor sensitivity. According to this feature, you can determine the temperature of maximal gas sensitivity to the test gas, which is the working temperature of the sensor.

• The dependence of the maximum sensitivity of the gas sensor of the concentration of the test gas. In this case it is necessary to conduct several experiments to identify the gas sensor sensitivity depending on the temperature for different concentrations of the test gas. Then construct the dependence of the gas sensitivity defined at the operating temperature of the sensor on the concentration of the testing test gas.

There is dependence of the gas sensor sensitivity of the temperature in different gas environments. This experiment was conducted to determine the temperature of maximal gas sensitivity of the of test structures to detect different gases and gas environment to which the sensor has maximum sensitivity.

## 2.5. Research methodology of properties of microelectronic gas sensors under the influence of lightening

Researches of the nature of the electrical and gas sensitive properties change when exposed to different temperatures and illumination were carried out on test structures microelectronic gas sensors in the apparatus shown in Fig.2.3.

to identify possible mechanisms of the effects of light on the electrical properties of tin dioxide crystals the following experiments were conducted:

• Comparison of changes in the nature of the electrical sensing elements of test structures microelectronic gas sensors under the influence of light to heat setting sensor layers and thereafter. For this test the sensors structure, stored in air for several months from date of manufacture, were irradiated with violet LED L5013VC wavelength of 407 nm and a power of 76 mW.

For irradiation we uses the following: an ultraviolet LED with ARL2-5213 UVC energy $E_u$ = 3.1 eV and a capacity of 76 mW blue LED ARL-5213 UBC with energy $E_c$ = 2.64 eV and a capacity of 70 mW, the green LED ARL-5513 PGC with $E_z$ Energy = 2.38 eV and a power of 70 mW, the red LED ARL-URC 5213 with energy $E_c$ = 1.98 eV and a capacity of 48 mW, which are located at a distance of 2, 4, 6 mm from the gas-sensitive film.

After that the test samples were annealed in air at 400 $^oC$ for desorption of atmospheric gases from the surface of the tin dioxide and the complete stabilization of electrical resistance sensing element and again exposed to the LED radiation. LED is placed at a distance of 2 mm from the crystal [79].

• Identification of the nature of the changes of the electrical sensing elements test structures microelectronic gas sensors under the effect of different intensities of light. For this test sensor structure stored in air for several months from the time of manufacture, annealed in air at about 400 $^oC$ for atmospheric gas desorption from the surface of the tin dioxide and the complete stabilization of electrical resistance sensing

element and then illuminated LED, which was located at a distance of 2 to 6 mm in increments of 2 mm from the gas sensitive film.

• Studying of a gas sensitivity test structures microelectronic gas sensors exposed to light at different temperatures (20 ÷ 200 oC). To test this sensor structure, stored in air is long, were annealed at 400 $^{o}$C for desorption of atmospheric gases from the surface of the tin dioxide. Sensors were then subjected to irradiation of light-emitting diode at room temperature, the crystal and at 50 °, 100 °, 125 °, 150 °, 175 ° and 200 ° C in air while measuring the magnitude of the resistivity sensor, and then at the same temperature in an atmosphere of the test gas. The LED located at a distance of 2 mm from the gas-sensitive film.

It was experimentally found that when exposed to light of tin dioxide film resistivity decreases to a minimum value depending on the complex, and after turning off the light resistance of tin dioxide increases.

To compare the results obtained in the presence of air and gases were plotted relative minimum values of resistance sensing element when exposed to radiation from LED temperature. Then, from the formula (2.2) was determined by the gas sensor sensitivity at different temperatures (room temperature, at 50 °, 100 °, 125 °, 150 °, 175 ° and 200 ° C), and were plotted against gas temperature sensitivity.

The error in the experiments described above, consisted of the error in determining the voltage drop by means of the data acquisition board, which is ± 1 mV (about 0.5%) and error in determining the temperature. Overall accuracy was about ± 5%.

## Chapter3.

## Research of light and gas influence on– reductants on the electrical resistance $SnO_2$ films at room temperature

### 3.1. Light influence on the electrical resistance of undoped sensitive gas sensor element based on $SnO_2$ films

Metal oxide gas sensors are based on $SnO_2$ and ZnO films and are widely used in air monitoring [80]. Because of the slow and unobtrusive interaction with the surface of metal oxide gas at room temperature, solid-state gas sensors typically operate at high temperatures (300 - 400 $^oC$), which is dangerous under the control of the content in the air of explosive gases. One way to reduce the operating temperature based on $SnO_2$ gas sensors is activated adsorption processes on the semiconductor surface and the manifestation of ultraviolet light gazosensornyh properties for CO and $NO_2$ at room temperature [64 - 81]. The theoretical model of the mechanisms of interaction of ultraviolet light to the surface of the metal oxide semiconductor, proposed in [84] allows you to qualitatively assess the nature of the change in resistance and gas sensitivity of sensor layers, depending on light intensity and ambient temperature.

However, sources of optical radiation (used in the early studies) in the form of powerful stationary xenon and mercury lamps are not suitable for practical use with portable gas detectors with battery. In this case it is convenient to use the LED blue and violet wavelength ranges.

This chapter presents the results of studies of the effect of radiation of low-power light-emitting diodes on the electrical sensor layers of test structures $SnO_2$ gas sensors at room temperature.

As it was noted in Chapter 2, in the study we used the following LEDs: UV LED ARL2-5213 UVC with a wavelength of 407 nm and 0.02 A current, voltage V = 3,5 B,

the brightness (0.1 - 0.2) $E_f$ radiation energy = 3.05 eV and a capacity of 76 mW; blue LED ARL-5213 UBC with a wavelength of 458 nm and a current of 0.02 A, the operating voltage of V = (2,9 ÷ 3,3) V, the brightness (1.5 - 2.5) cd, energy Ec = 2, 71eV and a capacity of 70 mW; green LED PGC ARL-5513 with 526 nm wavelength and a current of 0.02 A, at a voltage V = (3 ÷ 3,5) B, brightness (5 - 6) kd energy Ez = 2.36 eV and power of 70 mW ; ARL-red LED 5213 URC with 631nm wavelength, a current of 0.02 A, the voltage V = (1,8 ÷ 2,5) B, brightness (9 - 10) with energy $E_k$ kd = 1.97 eV and power of 48 mW . LEDs are located at distances of 2, 4, 6 mm from the gas-sensitive film. Fig.3.1 shows the emission spectra of the LEDs used, obtained at the Department of Optics of the Voronezh State University.

(I, отн. ед. = I rel. u, Длина волны/нм = The wavelength/nm, УФ = UV, Синий = Blue, Зеленый = Green, Красный = Red)

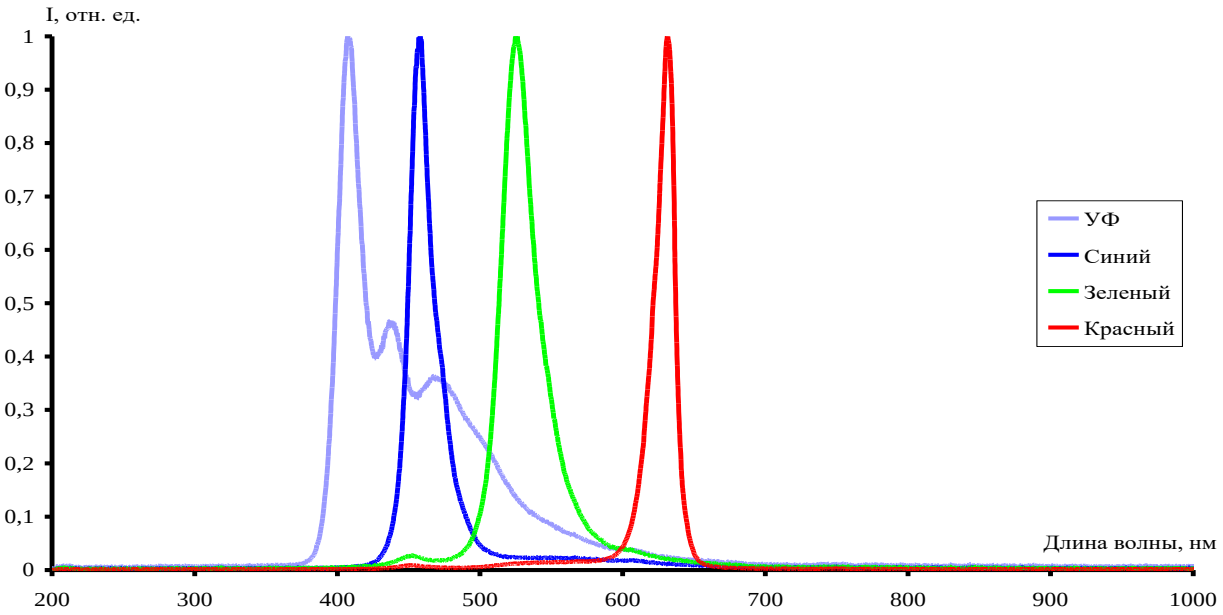


Fig.3.1. The emission spectra of LEDs

Table.3.1 shows the main characteristicswhich are used in LEDs.

Table 3.1

Basic characteristics of the LEDs.

| Characteristics of LED | Violet ARL2-5213 UVC | Blue ARL-5213 UBC | Green ARL-5513 PGC | Red ARL-5213 URC |
|---|---|---|---|---|
| The wavelength of a maximum of radiation, nm | 407 | 458 | 526 | 631 |
| The radiation energy, eV | 3,05 | 2,71 | 2,36 | 1,97 |
| Power of optical radiation, mW | 76 | 70 | 70 | 48 |

In the investigation of the effect of light exposure on the test measuring the structure parameters were carried out in a sealed measuring cell volume of 10 l with an opaque coating.

It was found that the light resistance of the sensor decreases rapidly at first, then decreases more slowly and after switching off the light increases, tending to its original value.

To simplify the analysis of the effect of light on the gas sensor we can considere effective relaxation times characterizing the duration of the rapid change in resistance when the light $\tau_{1ef}$, the duration of the subsequent slow relaxation $\tau_{2ef}$ $\tau_{3ef}$ and relaxation after the light is turned off. As shown previously [65], each of the effective relaxation time is described by several exponential functions.

The measurements were performed at a distance from the LED to the surface of the sensor 2 mm, 4 mm, 6 mm. At distances from the LED to the sensor 8mm noticeable changes electrical resistance was not observed, so further measurements are not a distance of 8 mm were not met.

For an exception of thermal effects of the LED on the sensor surface is performed by specially science experiments with the placement between the light source and the sensor

crystal filter 0.5 mm thick. It is found that the presence of the filter reduces the effect of a few percent of the LED, which indicates that the main role of the light and not heat.

During the exposing a purple light after the LED sensor resistance is reducing (about 8 - 10 min.) and reaches a stationary value. In accordance with the energy of light quanta violet light effect leads to the excitation of electrons from the valence band of the semiconductor $SnO_2$ into the conduction band (intrinsic photoconductivity). After switching off the LED has been a slow increase in the resistance to greater than baseline (Fig.3.2), which is characteristic of bipolar recombination involving deep traps. The phenomenon of long-term relaxation of the electrical resistivity of polycrystalline $SnO_2$ film after lighting the UV lamp was noticed earlier and called the "memory effect." Thus, samples violet LED illuminated radiation manifests the "memory effect."

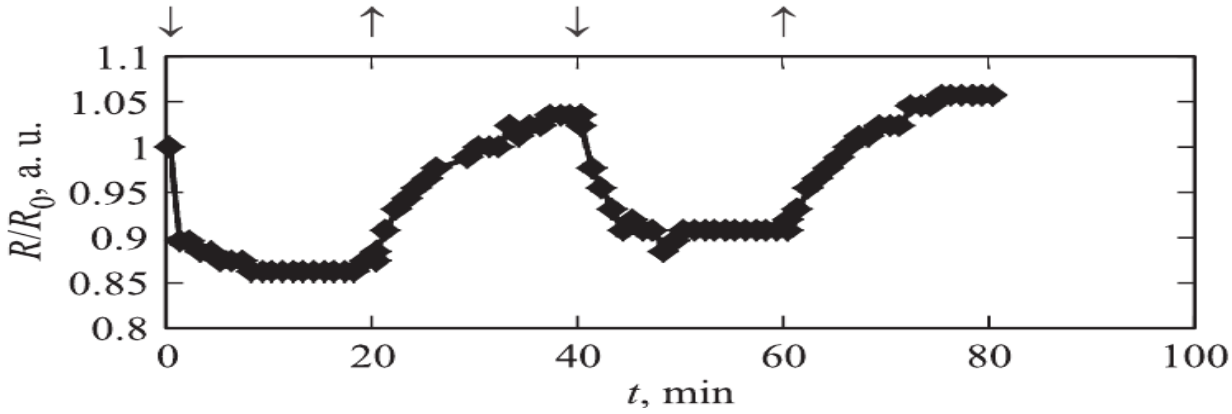


Fig.3.2. Influence of violet (λ = 407 nm) radiation on resistance of the sensor elements at room temperature: ↓ - turn on of the LED

↑ - turn off of the LED

*(вкл. = turn on, выкл. = turn off)*

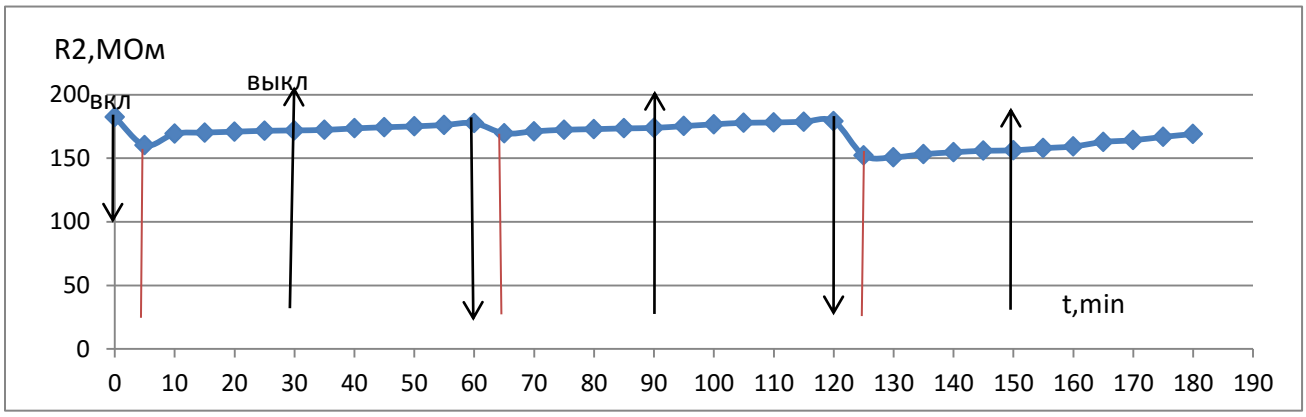


Fig.3.3. Changing the resistance of the sensor ($SE_2$) under the action of violet light. The LED is located at a distance of 2 mm from the film. The initial value $R_{SE2}$ = 182.4 MW

In Fig.3.2 and 3.3 points of switching on (↓) and switching off (↑) of the LED are indicated by arrows. Due to the fact that the initial values of the sensor resistance have a lot differences, we evaluated the changes in the relative resistance $SnO_2$ thin film under the action of light on the formula (ΔR / Ro).

Fig.3.4. shows the relative change of the sensor resistance (ΔR / Ro) under the effect of violet light. It is evident that the greatest changes at a distance of 2 mm occur when you turn on the light and make the value of (25 ± 5)%.

Fig. 3.5 and Fig.3.6 show the variation in the sensor resistance under the action of the violet LED located at a distance of 4 mm from the surface of the sensor, the nature of the sensor resistance change is the same as the LED at distances of 2 mm.

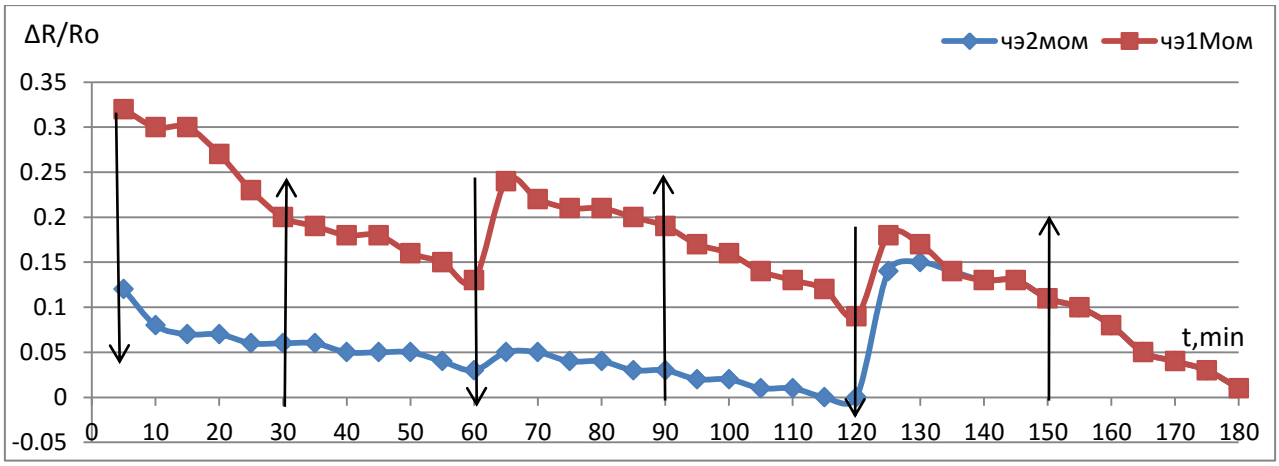


Fig.3.4. The relative changes in the sensor resistance under the action of the violet light, the distance from the LED to the SnO2 film is 2 mm.

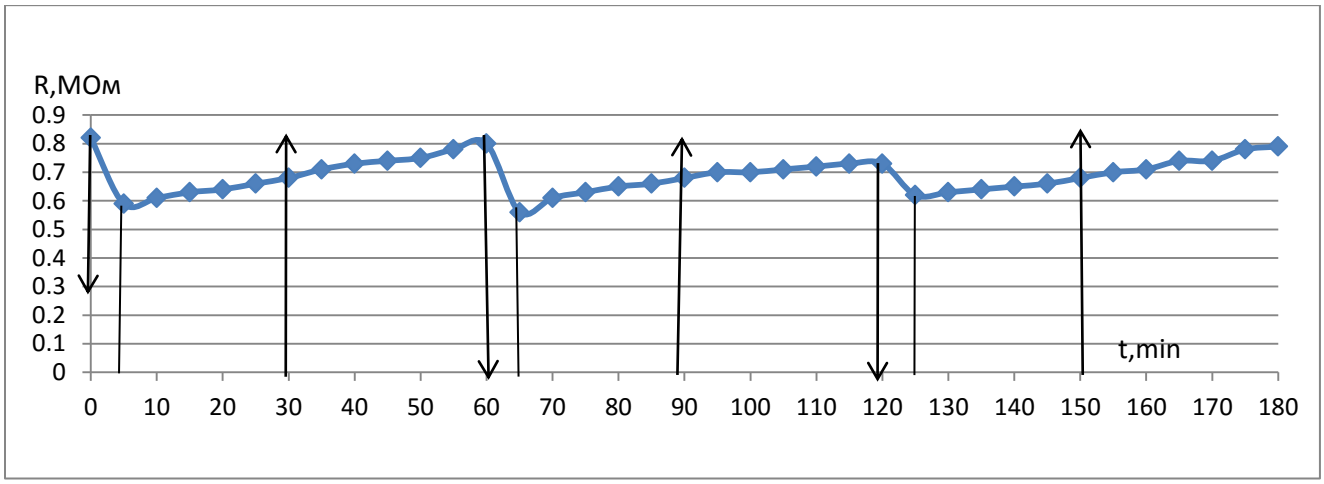


Fig.3.5. Changing of resistance of the sensor (SE1) under the action of light violet. The LED is located at a distance of 4 mm from the film. The initial value $R_{se1}$ = 0.82 megohms

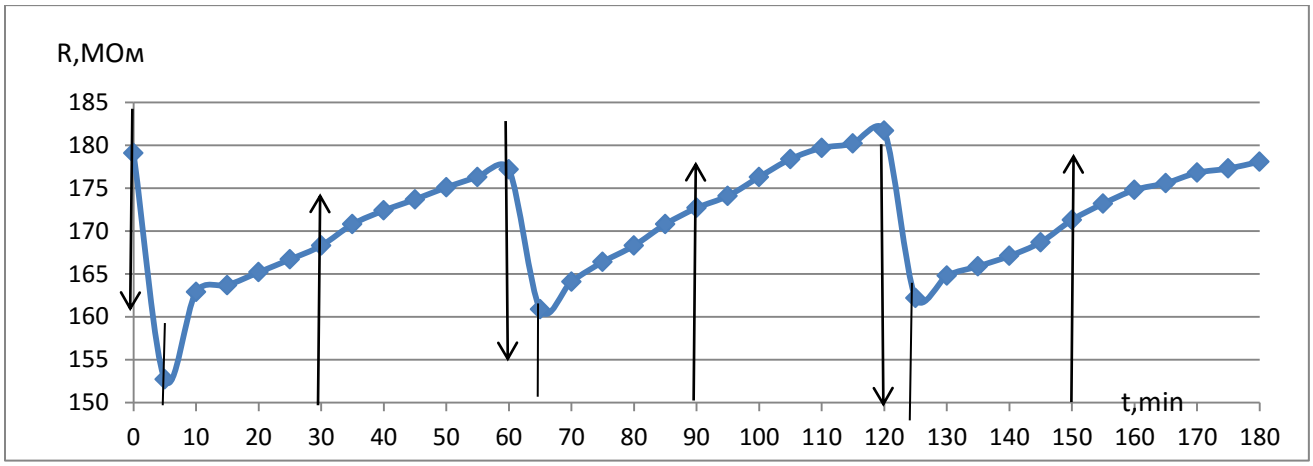


Fig.3.6. Changing of resistance of the sensor (SE2) under the action of light violet. The LED is located at a distance of 4 mm from the film. The initial value Rse2 = 179.1 MW

Fig.3.7 shows the relative change in resistivity $SnO_2$ films in the process of switching on and switching off of light. At a distance of 4 mm from the sensor the greatest change of the sensor resistance in this experiment is (25 ± 3) %.

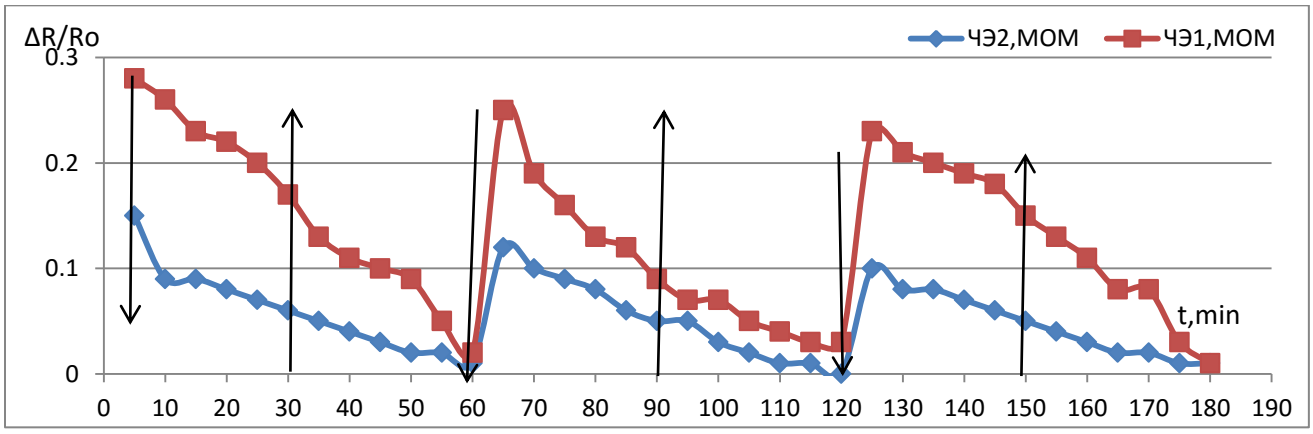


Fig.3.7. The relative changes of resistance sensors under the action of the violet light the distance from the LED to the $SnO_2$ film is 4 mm

Fig.3.8 and Fig.3.9 show the variation in the sensor resistance under the action of a violet LED, located at a distance of 6 mm from the transducer surface.

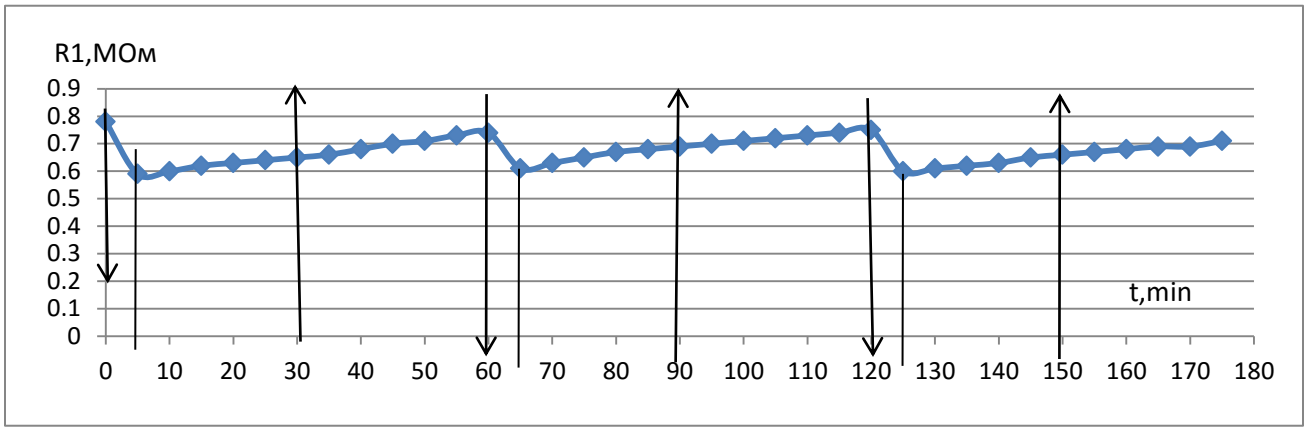


Fig.3.8. Changing the resistance of the sensor (SE1) under the action of light violet. The LED is located at a distance of 6 mm. The initial value $R_{se1}$ = 0.78 megohms

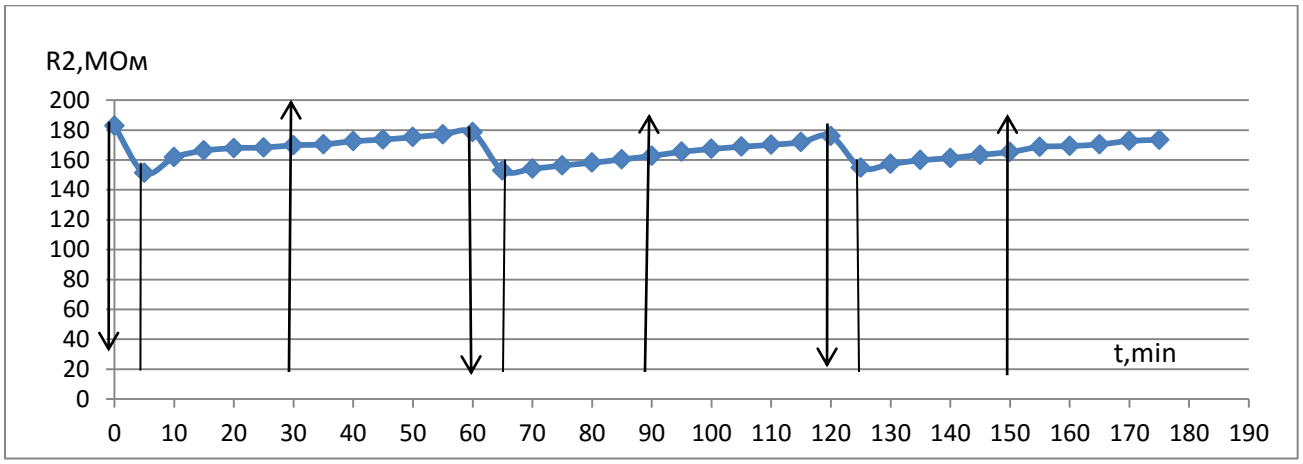


Fig.3.9. Changing of the resistance of the sensor (SE2) under the influence of violet light. The LED is located at a distance of 6 mm. The initial value $R_{se2}$ = 182.7 MW

Fig.3.10 shows the relative change of the resistance of SnO2 films in the process of switching on and switching off of light. At a distance of 6 mm from the sensor the greatest change of the sensor resistance in this experiment is (22 ± 2) %.

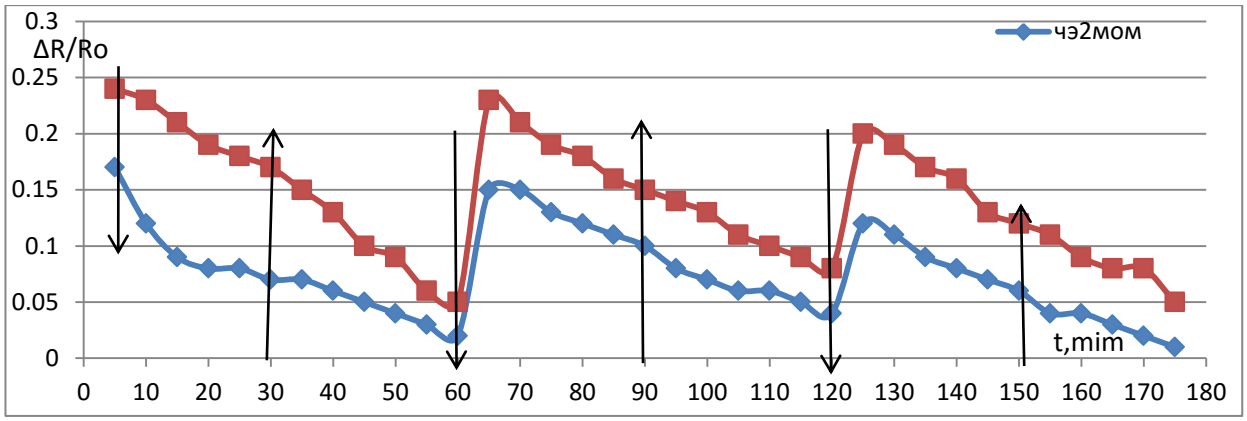


Fig.3.10. Relative changes in sensor of resistance under the influence of the violet light the distance from the LED to the film is (6 mm)

Fig.3.11. shows the average dependence of the relative changes in the sensor of resistance as a function of the distance from the LED to the surface of $SnO_2$ film.

*(уф2-4-6 мм = uv2-4-6 mm)*

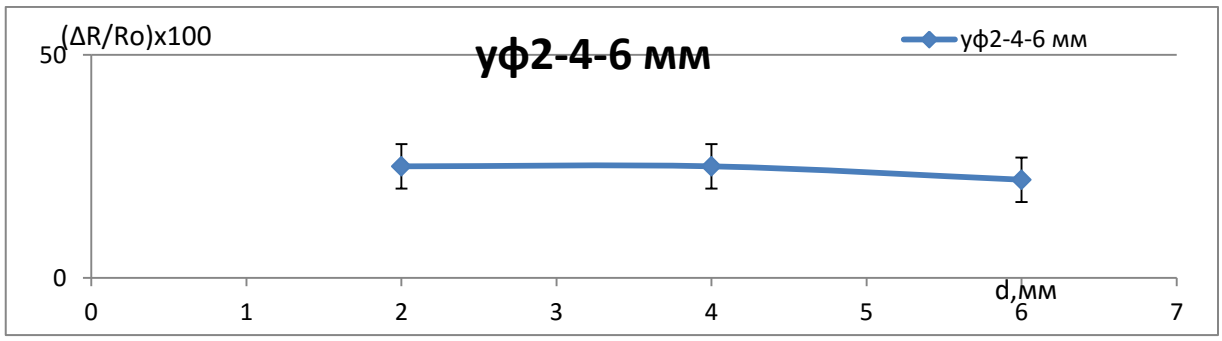


Fig.3.11. The average dependence of the relative change of resistance of sensors the distance from the purple LED

Thus, exposure to light from the purple LED reduces electrical sensor elements by an average of 25%. In accordance with the energy of light quanta effect of light leads to excitation of electrons from the valence band of the semiconductor $SnO_2$ into the conduction band (intrinsic photoconductivity). As a result, light absorption sensor resistance falls to a minimum value ($\tau 1_{ef} \sim 5$ min), and then begins to rise slowly,

trying to its original value ($\tau 2_{ef}$ ~ 25 min). This returns the value of the resistance continues after the light is turned off. However, the initial value for the foreseeable $R_{SE}$ measurement time is not reached, this phenomenon was named in the paper [64] the effect of "memory."

Form photoconductivity curve observed in the experiment typical for intrinsic photoconductivity in the presence of surface recombination [83]. This effect in polycrystalline samples is very important. Small dependence of the intensity of the photoelectric effect (the distance to the surface of the film $SnO_2$) low-power light source, as is characteristic of intrinsic photoconductivity [50] in the semiconductor.

The effects of blue LED on the electrical gas sensor shown in Fig.3.12 - 3.21. The LED is located at a distance of 2 - 6 mm from the surface of the $SnO_2$ film.

Fig. 3.14.shows a relative change of the sensor of resistance ($\Delta R$ / Ro) under the influence of of blue light. It is seen that a lot of changes happen when the distance is 2 mm and during switching on of light and have the value of (25 ± 5)%.

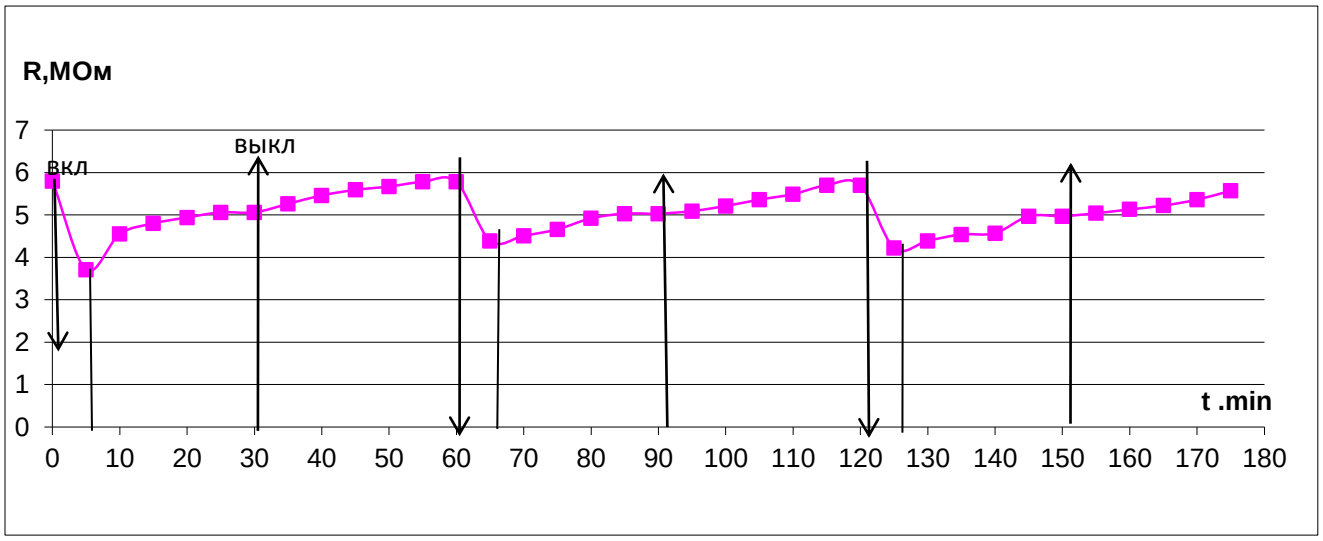


Fig.3.12. Changing of the sensor of resistance (SE1) under the influence of of blue light. The LED is located at a distance of 2 mm. The initial value $R_{se1}$ = 5.8 megohms

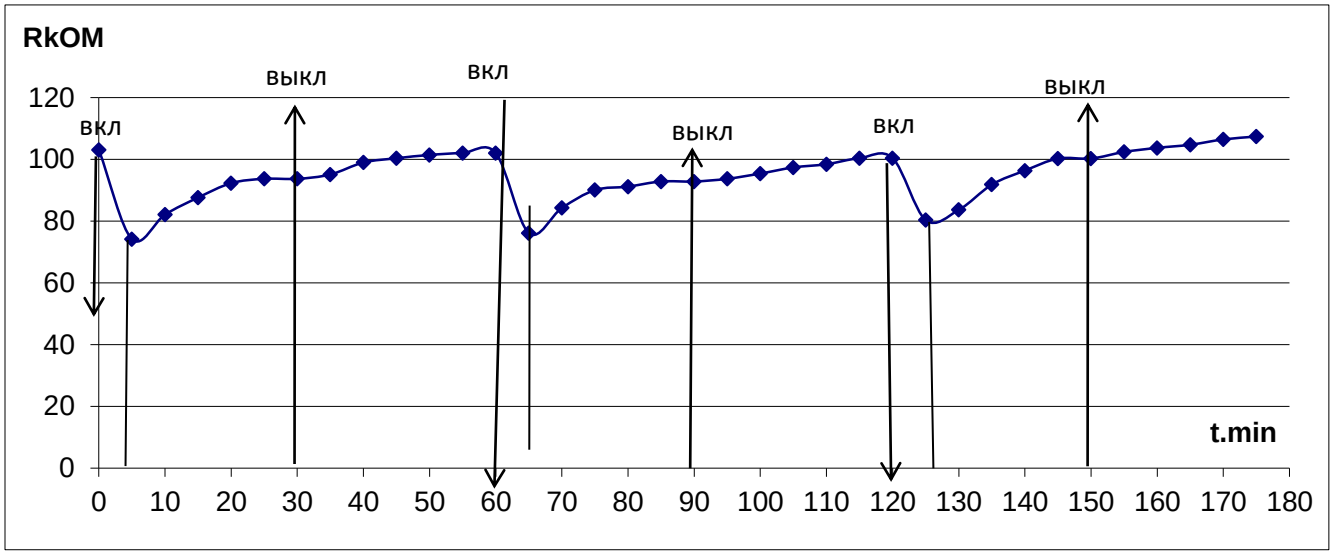


Fig.3.13. Changing of the sensor of resistance (SE2) under the influence of blue light. Distance from the LED to the film is 2 mm. The initial value Rse2 = 103.06 kOm

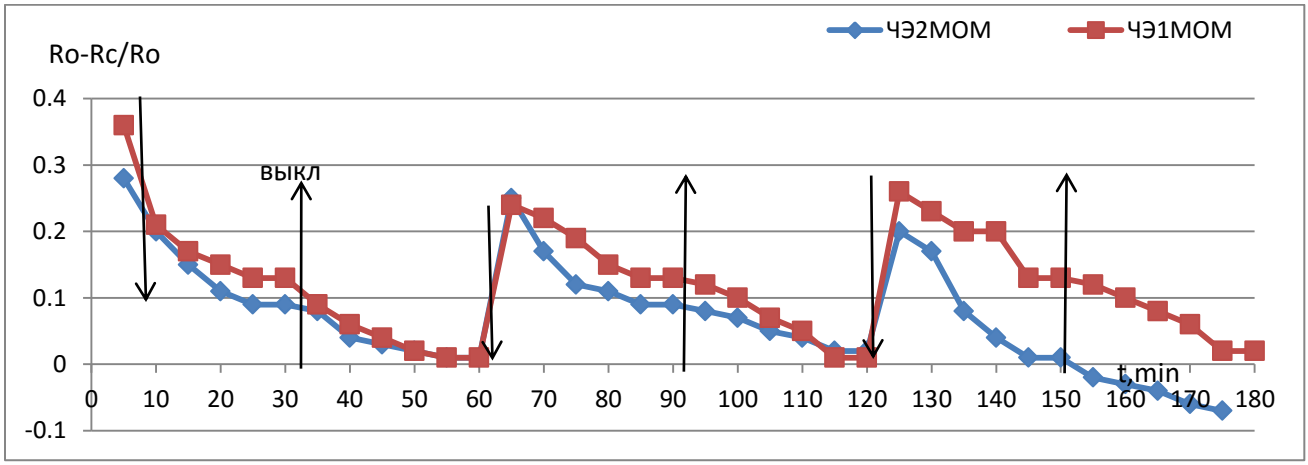


Fig. 3.14. The relative changes of resistance of sensors under the influence of blue light. The distance from the LED (2 mm)

Fig. 3.15 and 3.16 shows the variation of of resistance of the sensor under the influence of the blue LED, which is located at a distance of 4 mm from the surface of the sensor.

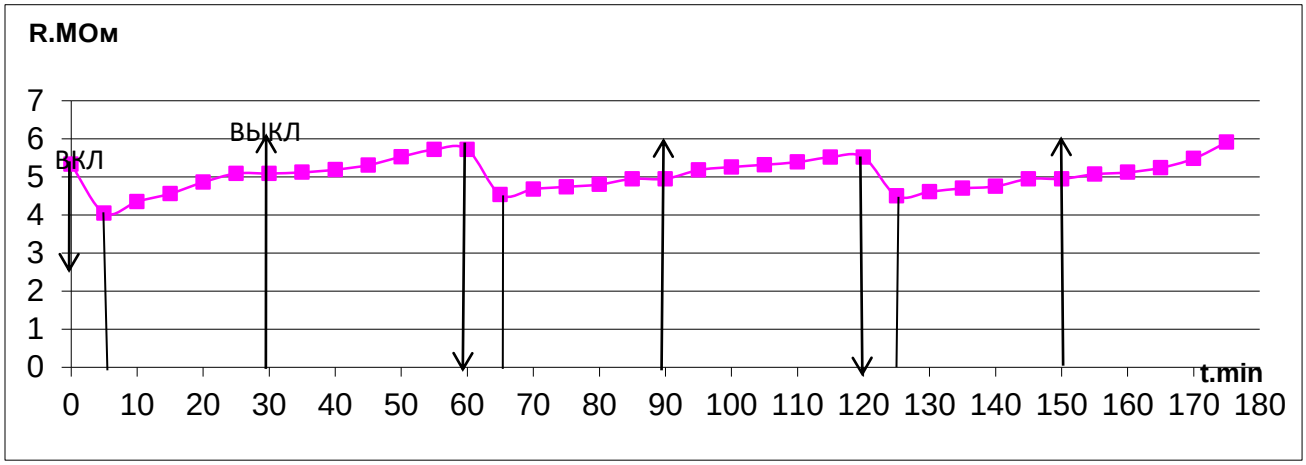


Fig. 3.15. Changing of the sensor of resistance (SE1) under the influence of blue light. Distance from the LED to the surface is 4 mm. The initial value $R_{se1}$ = 5.33 megohms

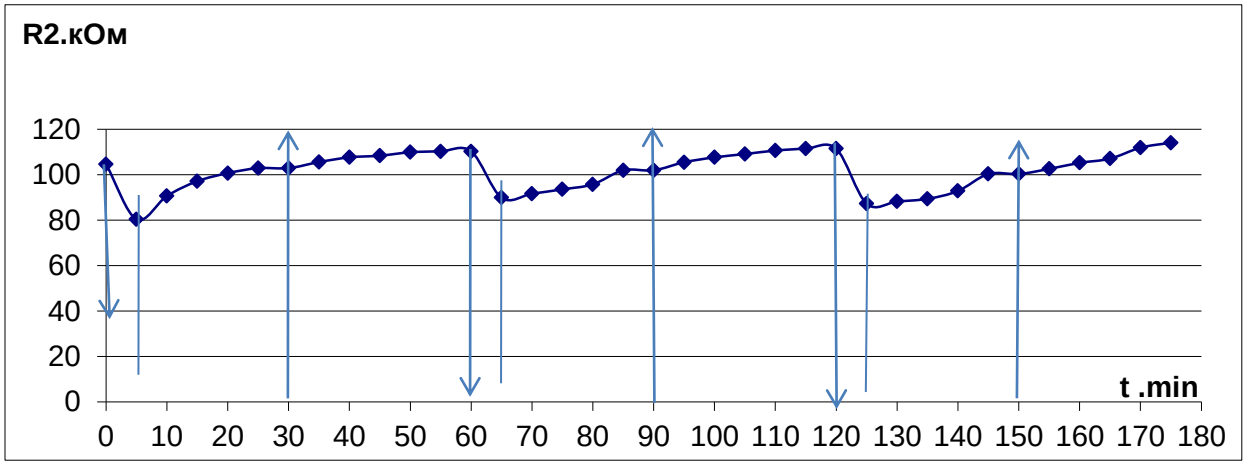


Fig.3.16. Changing of the sensor of resistance (SE2) under the influence of blue light. The LED is located at a distance of 4 mm. The initial value $R_{se2}$ = 104.62 kW

Fig.3.17 shows the relative changes of resistance SnO2 films in the process of switching on and off light. At a distance of 4 mm from the sensor the greatest change of the sensor resistance is (21 ± 4)%.

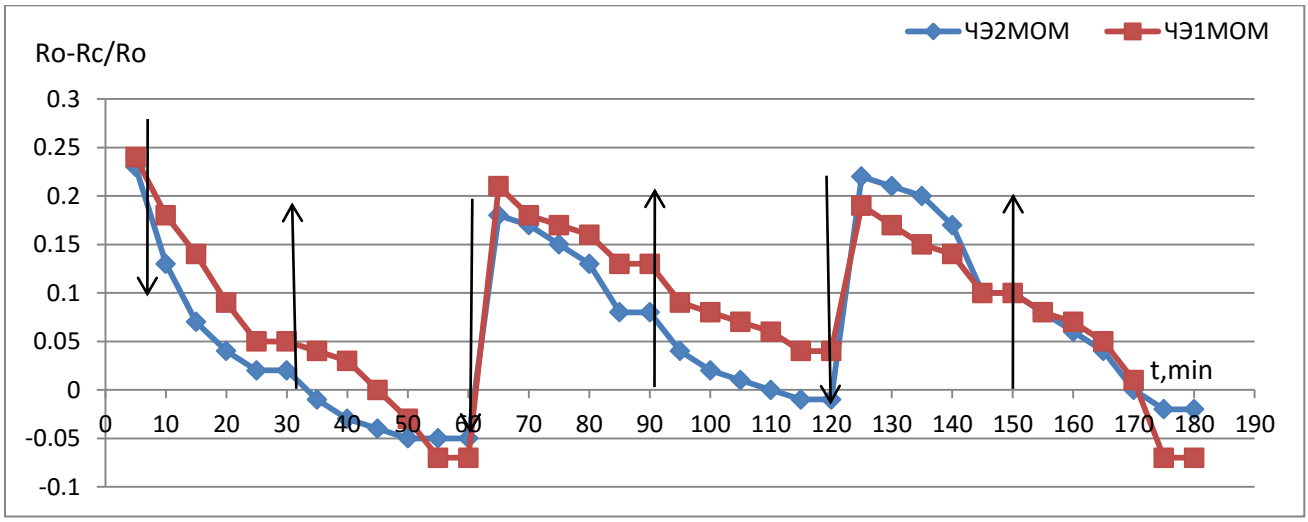


Fig.3.17. The relative changes of resistance of sensors under the influence of blue light. The LED is located at a distance of 4 mm from the sensor.

Fig.3.18 and Fig.3.19 show the variation of of the sensor of resistance under the influence of the blue LED, located at a distance of 6 mm from the transducer surface.

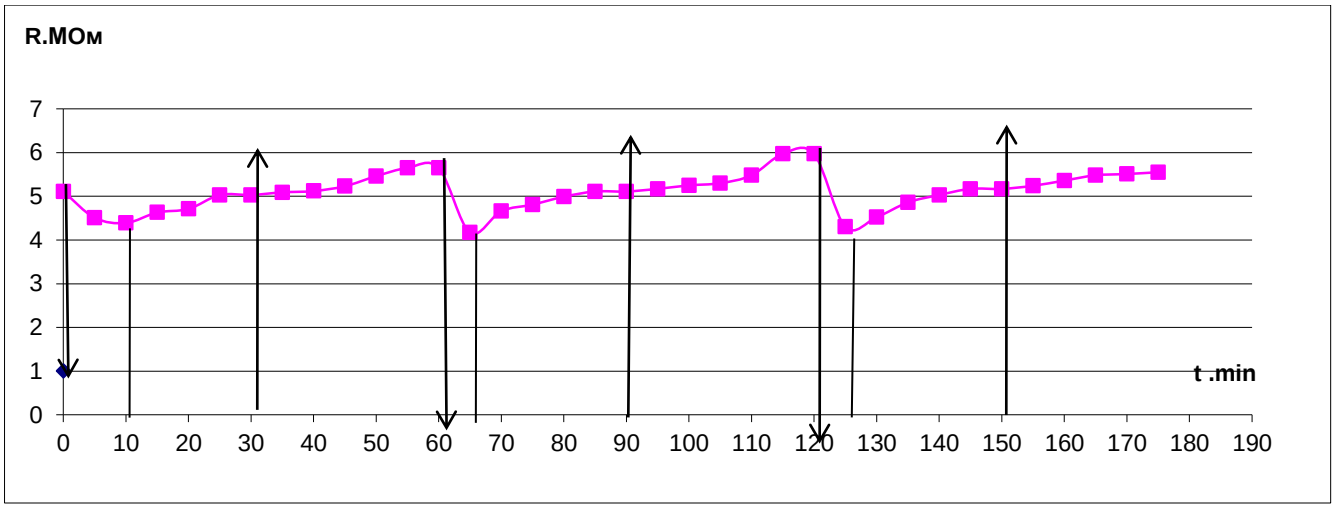


Fig.3.18. Changing of the sensor of resistance (SE1) under the influence of blue light. The LED is located at a distance of 6 mm. The initial value $R_{se1}$ = 5.11 megohms

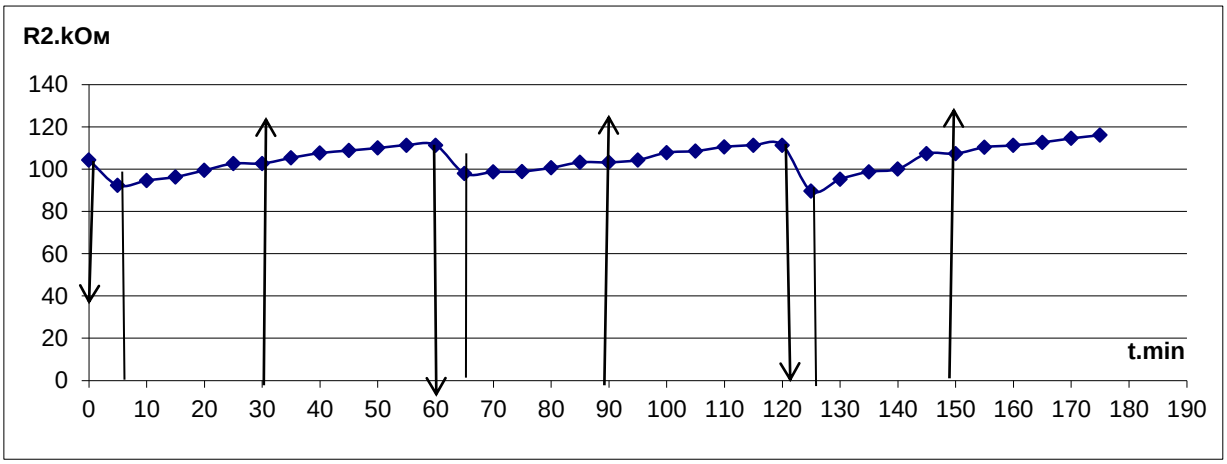


Fig.3.19. Changing of the sensor of resistance (SE2) under the influence of blue light. The LED is located at a distance of 6 mm. The initial value $R_{se2}$ = 104.34 kW

Fig.3.20 shows the relative changes of resistance of $SnO_2$ films in the process of switching on and switching off of light. At a distance of 6 mm from the sensor the greatest change of the sensor resistance is (15 ± 5) %.

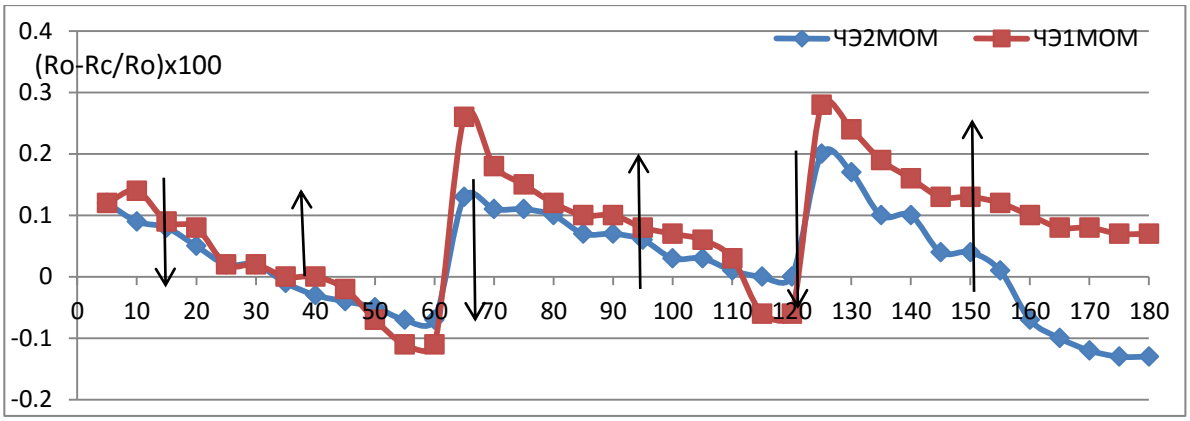


Fig.3.20. The relative changes of resistance of sensors under the influence of blue light. The LED is located at a distance of 6 mm

Fig.3.21. shows the average dependence of the relative changes of the resistance of sensors as a function of the distance from the LED to the surface of the film $SnO_2$ of sensors under the action blue light.

*(Синий = Blue)*

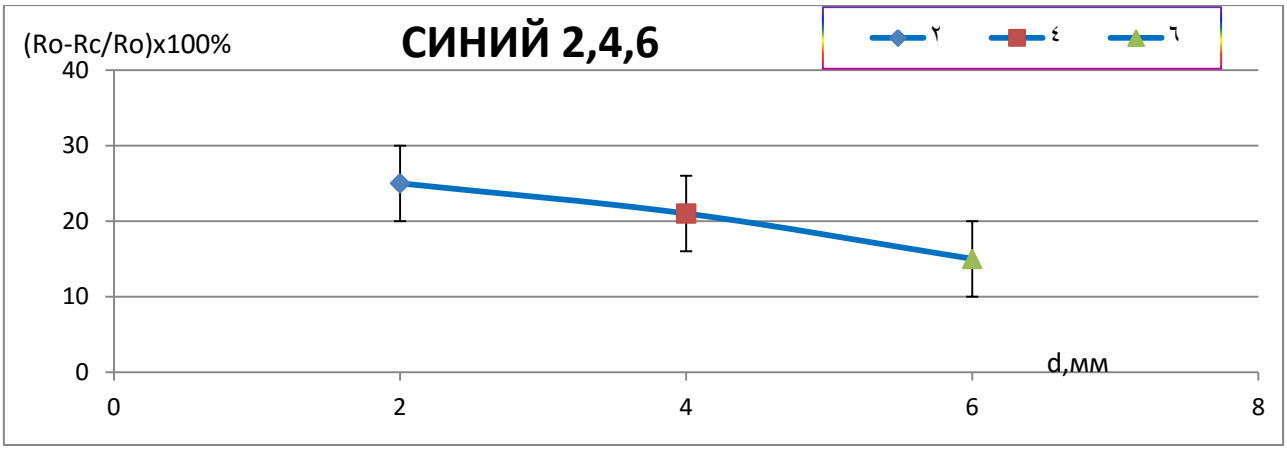


Fig.3.21. The average of the relative change of resistance of sensors under the influence of blue light on the distance from the LED

The effect of blue LED on the sensor element resistance value for its characteristic features similar to that of violet light on the gas sensors. Under the influence of blue light the sensor resistance reaches its first minimum value for 5

minutes, and then slowly increases. This resistance rise and the process does not stop after switching off the light. "Memory effect" is also stored on the sample illuminated with blue light. All of the features change resistance under the influence of the blue light, as in the case of purple light characteristic intrinsic photoconductivity in samples with surface recombination of non-equilibrium carriers. The average value of changes in the relative values of the sensor resistance under the influence of blue light of (20 ± 5)%, and allows us to recommend the use of blue LEDs for optical stimulation of working gas sensors.

The nature of changes of resistance of touch elements under the influence of the green light is different from the effects of exposure to violet radiation due to different mechanisms of generation of non-equilibrium carriers. When exposed to light after the green LED of the sensor resistance decreases (within 5 8 min.) and reaches a stationary value. After switching off the LED we can see a slow increase of resistance (40 -. 50 min) to less than the original (Fig.3.22).

The nature of resistance to change under the influence of the green light is different from the effects of exposure to violet and blue light-emitting diodes: after the light of the sensor decreases its resistance continuously until lights out. Perhaps this is a consequence of the unipolar generation of non-equilibrium charge carriers.

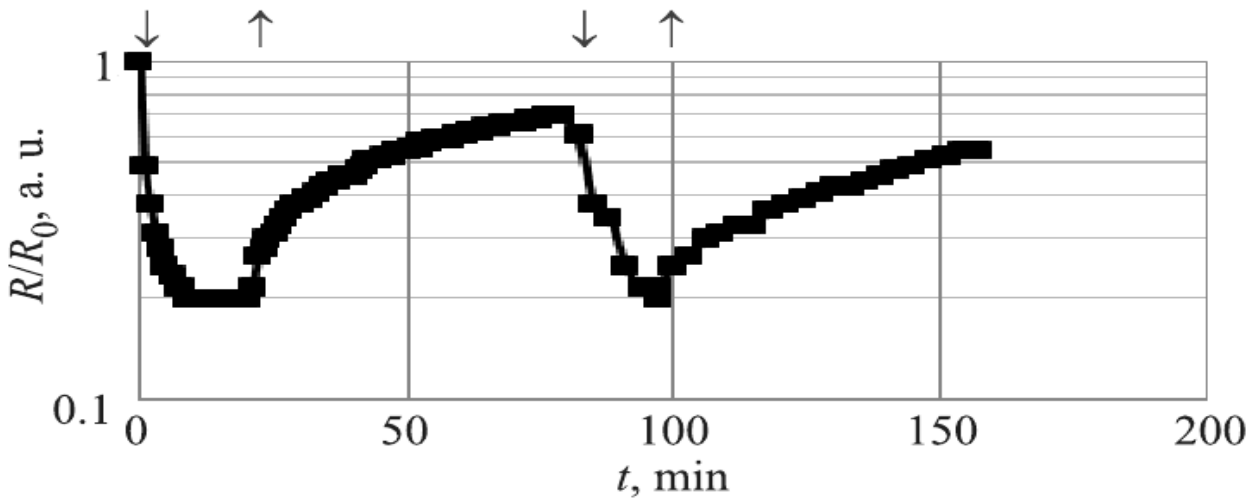


Fig.3.22. The influence of green ( = 526 nm) radiation resistance of touch elements at room temperature: ↓ - switching on of LED, ↑ - switching off of LED

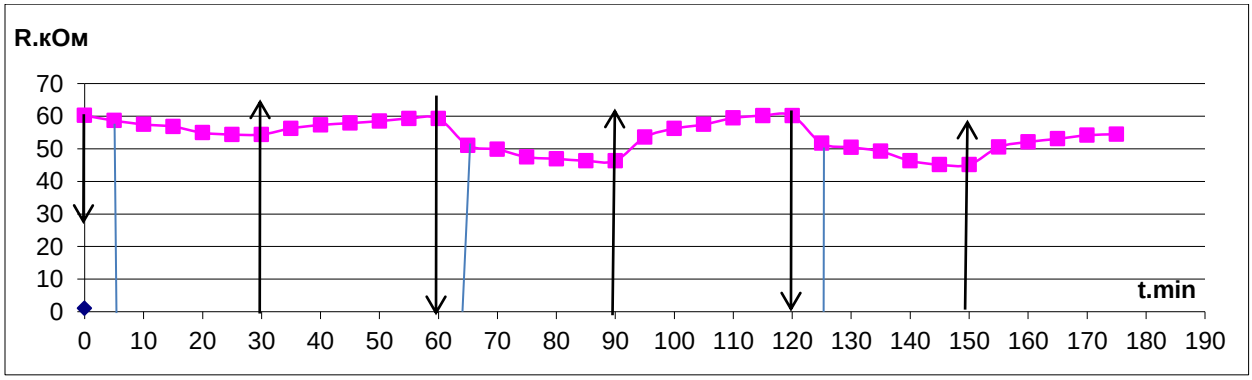


Fig.3.23. Changing of the sensor of resistance (SE2) under influence of the green light. Distance to the LED 2 mm. The initial value $R_{se2}$ = 60.23 ohms

Fig. 3.24 shows the relative changes of resistance $SnO_2$ films in the process of switching on and switching off of light. At a distance of 2 mm from the sensor the greatest change of the sensor resistance is (20 ± 5)%.

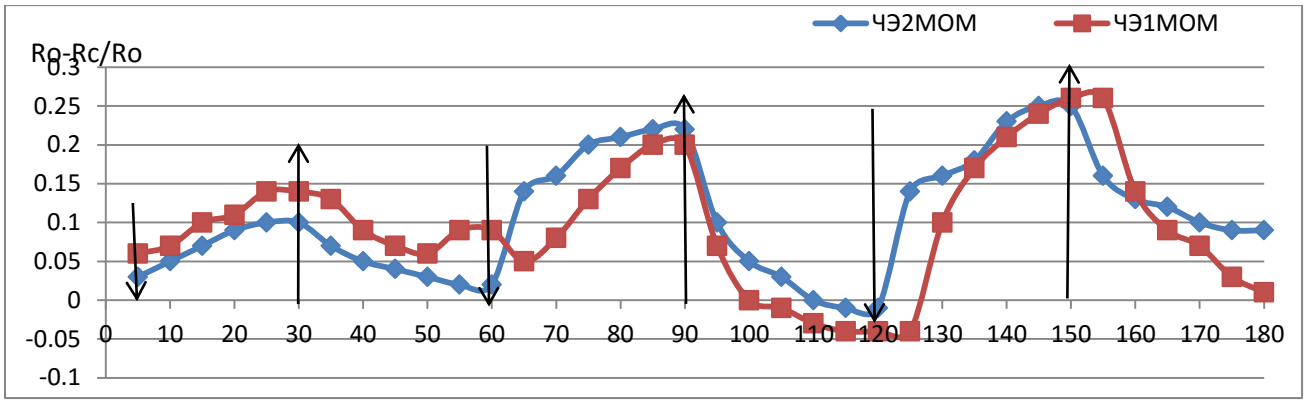


Fig.3.24. The relative changes of resistance of sensors under the influence of green light. The distance from the LED is 2 mm

Fig.3.25 and Fig.3.26 shows the variation of resistance of the sensor under the influence of the green LED, which is located at a distance of 4 mm from the surface of the sensor.

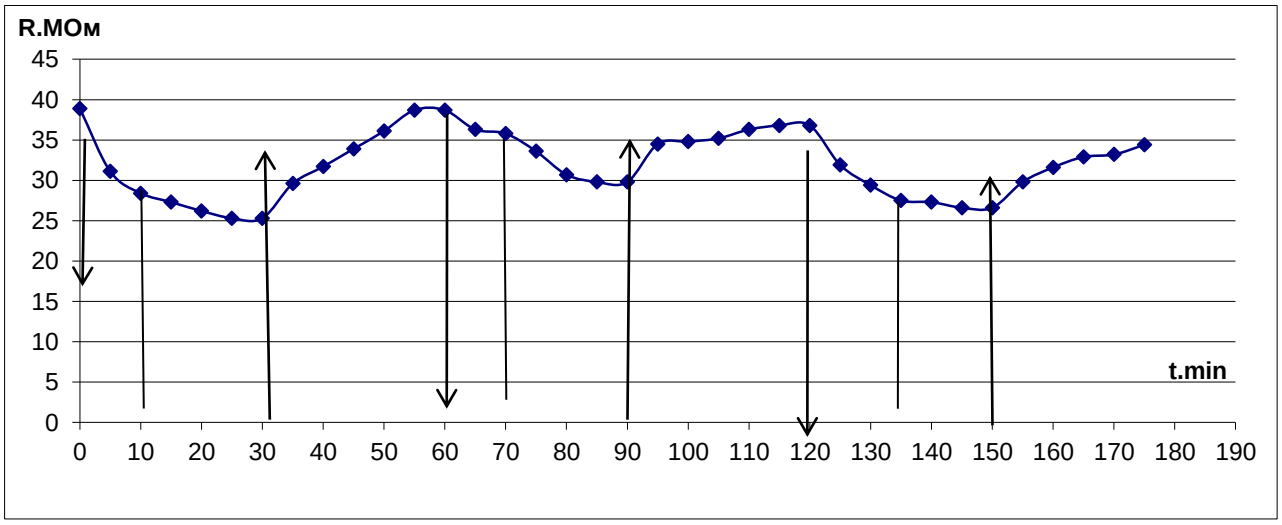


Fig.3.25. Changing of the sensor of resistance (SE1) under the green light. LED is on the distance of 4 mm. The initial value $R_{se1}$ = 38.9 MW

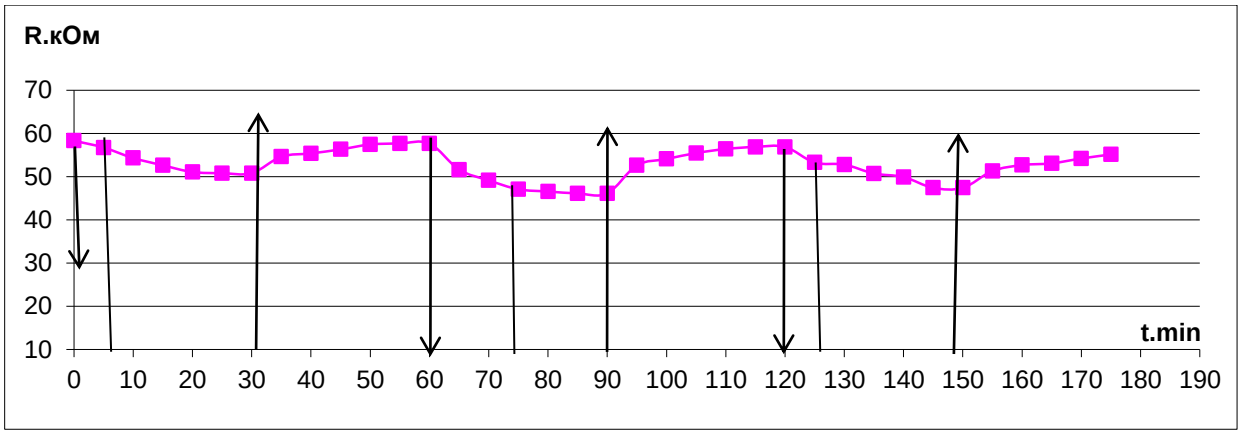


Fig.3.26. Changing of the resistance of the sensor (SE2) under the green light. The LED is located at a distance of 4 mm. The initial value $R_{se2}$ = 58.33 ohms

Fig.3.27. It shows the relative change of resistance of the sensor (ΔR / Ro) under the influence of green light. We can see that the greatest change is happen in the location of the LED which is 4 mm occurring 30 minutes after light is turned up and the size is (20 ± 5)%.

*(зеленый – green)*

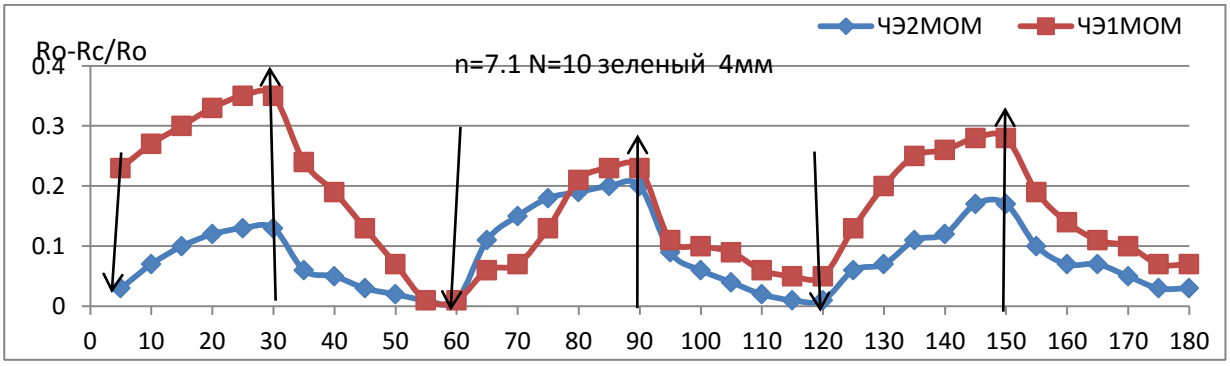


Fig.3.27. The relative changes of resistance of sensors under the influence of green light. The LED is located at a distance of 4 mm

Fig.3.28 and Fig.3.29 show the variation of the resistance of the sensor under the influence of the green LED, which is located at a distance of 6 mm from the surface of the sensor.

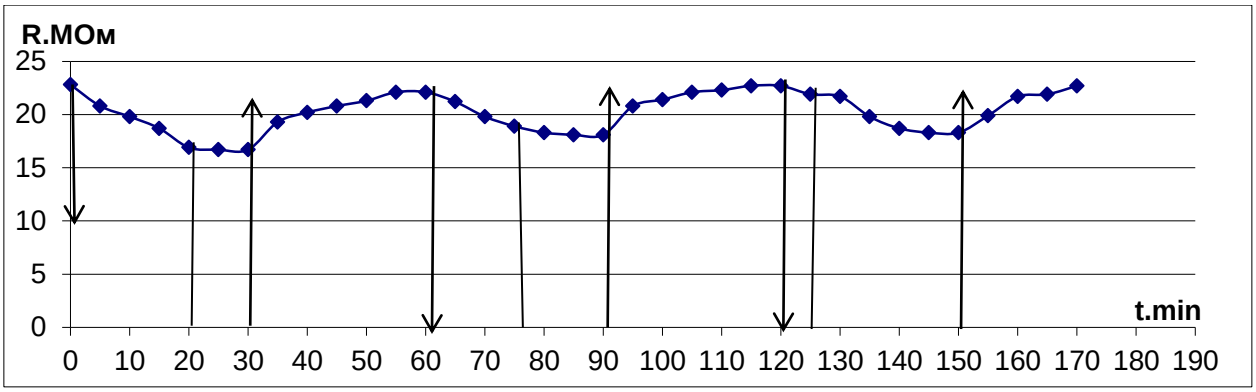


Fig.3.28. Changing of the sensor the resistance (SE1) under the influence of the green light. The LED is located at a distance of 6 mm. The initial value $R_{se1}$ = 22.8 MW

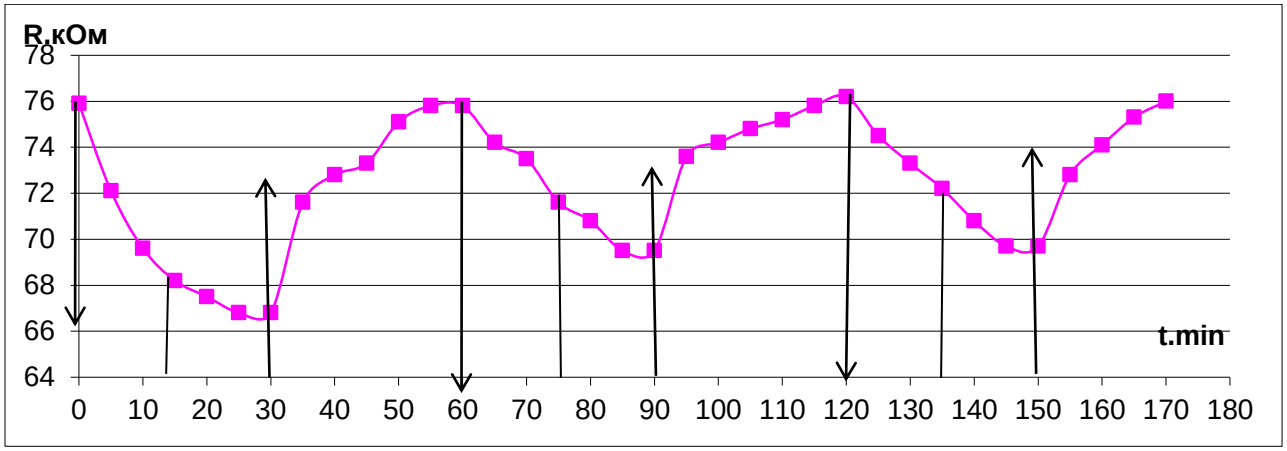


Fig.3.29. Changing of the sensor the resistance (SE2) under influence of the green light. The LED is located at a distance of 6 mm. The initial value $R_{se2}$ = 75.9 ohms

Fig.3.30. shows the relative change of the resistance of the sensor (ΔR / Ro) under the influence of green light. It is seen that the greatest change is in the location of the LED of 6 mm occurs 30 minutes after light is turned up and the size is (12 ± 5)%.

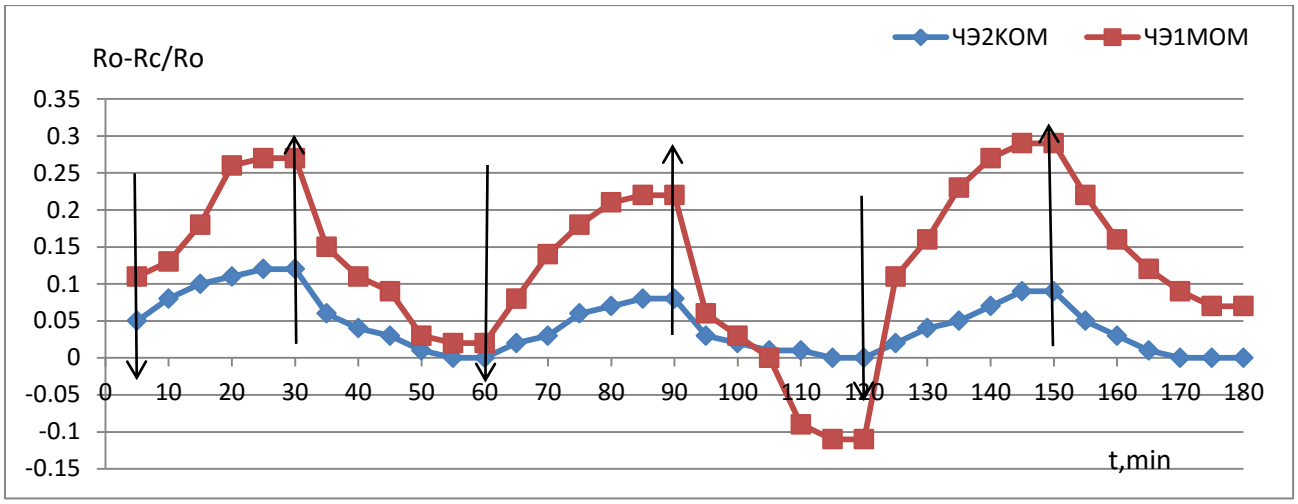


Fig.3.30. The relative changes of resistance of sensors under the influence of green light. The LED is located at a distance of 6 mm

Fig. 3.31 shows the average dependence of the relative changes of the resistance of sensors under the influence of green light, depending on the distance from the LED to the $SnO_2$ film surface.

*(зеленый = green)*

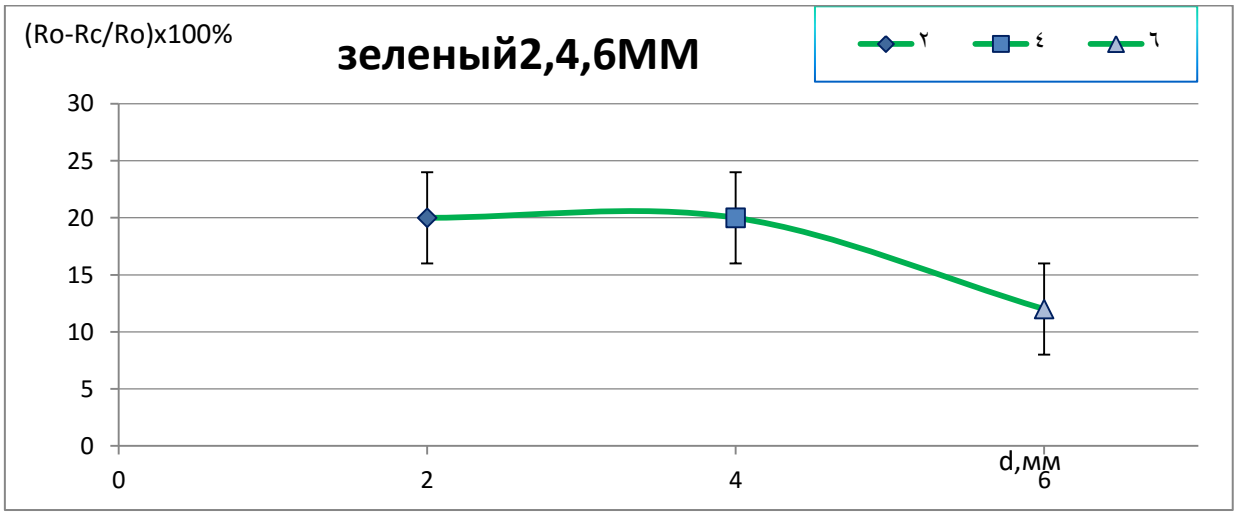


Fig.3.31. The average dependence of the relative change of resistance of sensors under the action of green light from the LED to the distances

The energy of light quanta, the green LED is not sufficient to drive the transition zone, the zone of the electrons, so green or red light can lead to impurity photoconductivity of $SnO_2$, which can participate impurity states in the band gap such as oxygen vacancies and the status of surface defects. This is manifested in the characteristics of the change of the sensor resistance when it is illuminated green and red light, both at the stage of turninig on, and at the stage of switching off the light. On the nature of the impurity photoconductivity is also indicated by the smaller value of the photoelectric effect and a marked dependence on the intensity of it (the distance to the sensor film) light. At a distance of 4 - 6 mm photoelectric effect is (15 ÷ 10)%, that is significantly less than for the blue and violet light.

It should be noted that the pattern of change of resistance under the influence of blue and green LEDs varies. When the green light is a continuous decline in the resistance until the moment of switching off the light. At the same time under the influence of a blue light the resistance decreases to a minimum for 5 minutes, and then starts to increase slowly. This may indicate a difference in mechanisms of action of green and blue light on the $SnO_2$ film. Plot most rapid change in the resistance under the effect of green light, and a blue one upon exposure, it takes about 5 minutes. However, in $R = f(t)$ graphs there are no features characteristic of intrinsic photoconductivity involving the surface recombination of non-equilibrium charge carriers.

Fig.3.32 - 3.41 show the results of the effect of the red LED light located at distances of 2 - 6 mm from the surface on the sensor resistance.

Fig.3.32 and fig.3.33 show the change of resistance of the sensor under the influence of the red LED light located at a distance of 2 mm from the surface of the sensor.

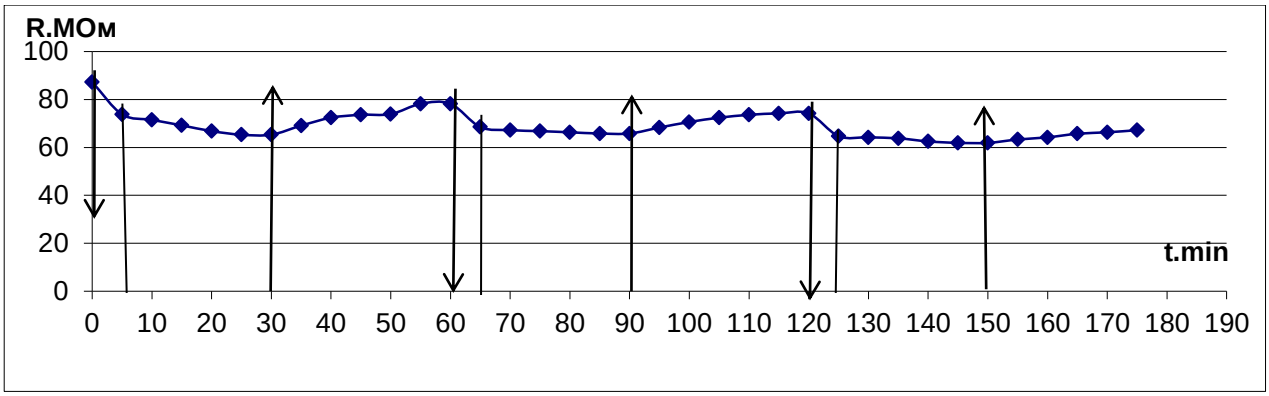


Fig.3.32. shows the change of the sensor resistance (SE1) under the influence of red light. Distance to the LED is 2 mm. The initial value $R_{se1}$ = 87.3 MW

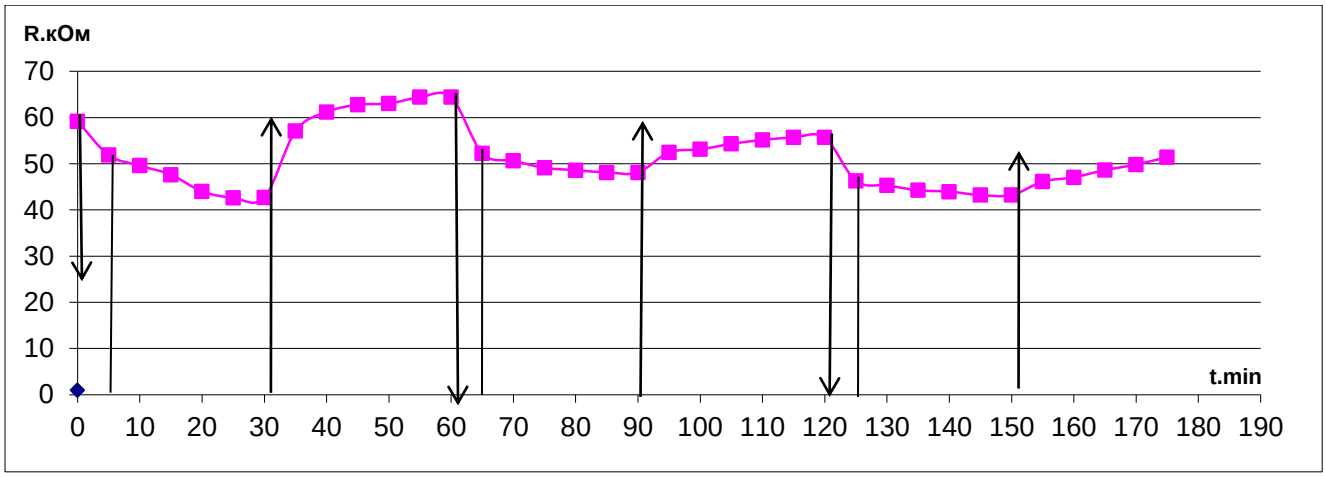


Fig.3.33. shows the change of the sensor resistance (SE2) under the influence of red light. The LED is located at a distance of 2 mm. The initial value $R_{se2}$ = 59.21 ohms

In the fig.3.34. it shows the relative change of the sensor resistance (ΔR / Ro) under the influence of red light. It is evident that the greatest changes at a distance of 2 mm from the

LED occurs during 30 minutes after turning on the light and make the value of (20 ± 5)%.

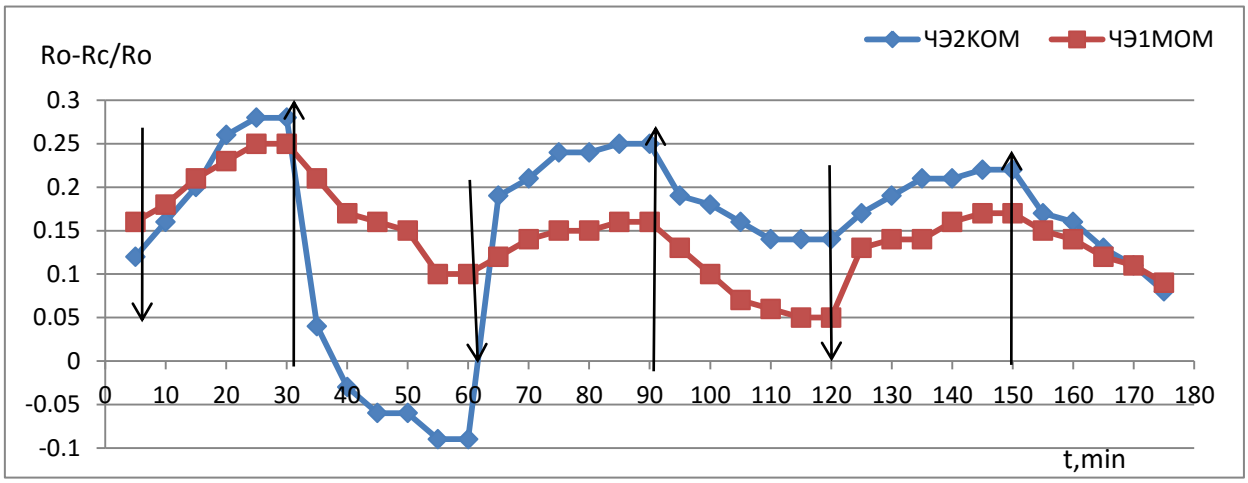


Fig.3.34. The relative change of resistance of sensors under the influence of red light. The LED is located at a distance of 2 mm

Fig.3.35 and fig.3.36 show the variation of resistance of the sensor under the influence of the red LED, which is located at a distance of 4 mm from the surface of the sensor.

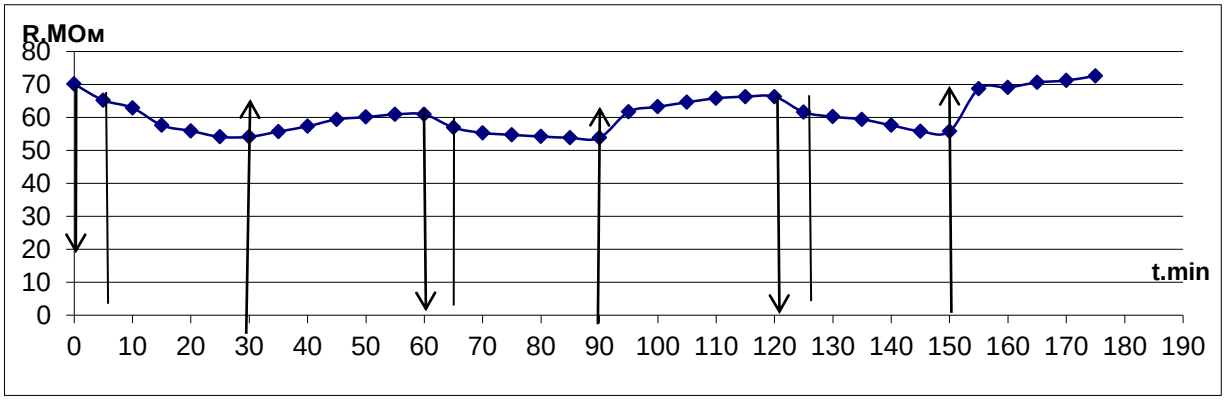


Fig.3.35. Changing of the resistance of the sensor (SE1) under influence of red light. The LED is located at a distance of 4 mm. The initial value $R_{se1}$ = 70.1 MOhm

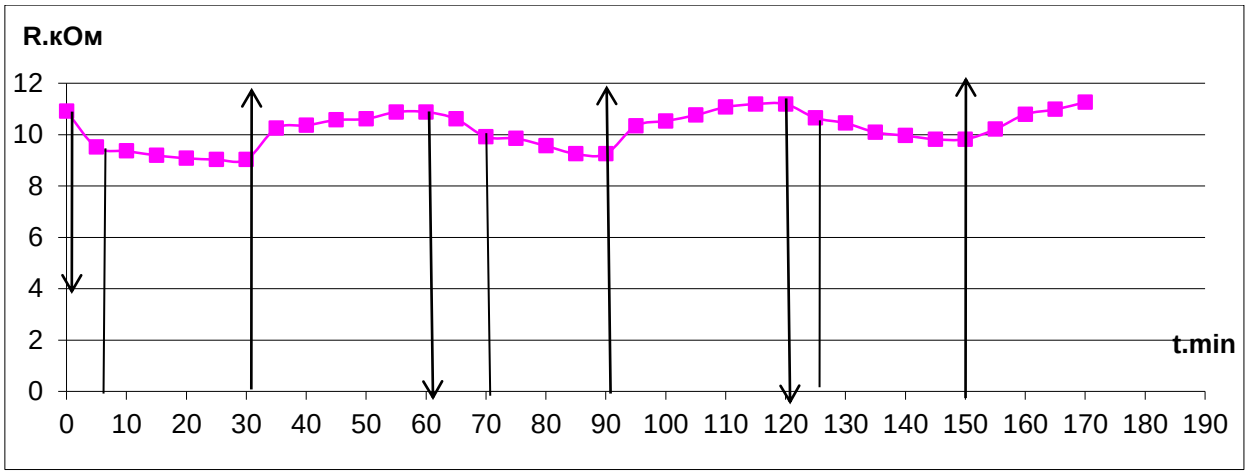


Fig.3.36. The change of the sensor resistance (SE2) under the influence of red light. The LED is located at a distance of 4 mm. The initial value $R_{se2}$ = 10.91 ohms

Fig.3.37 shows the relative change of the sensor resistance (ΔR / Ro) under the influence of red light. It can be seen that the greatest changes in the distance of 4 mm occurs when the light is switching on and make (13 ± 2)%.

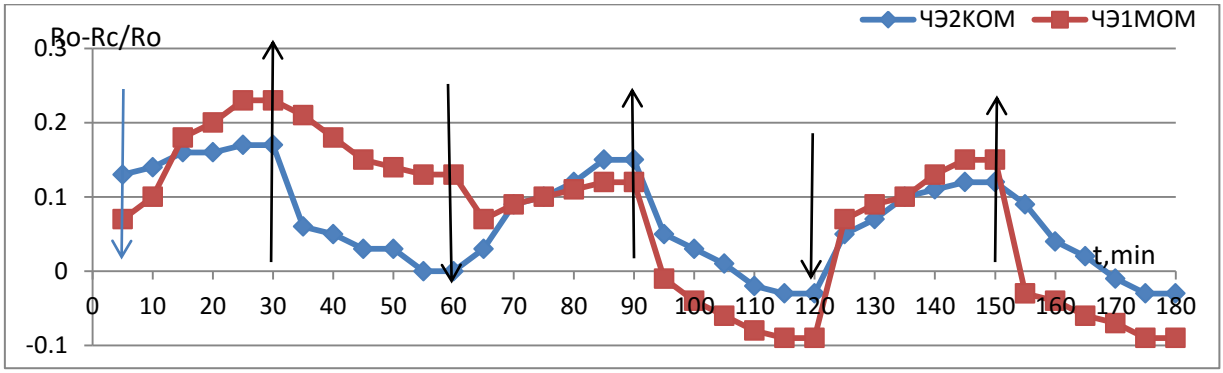


Fig.3.37. The relative change of resistance of sensors under the influence of red light. The LED is located at a distance of 4 mm

Fig.3.38 and fig.3.39 show the variation of resistance of the sensor under the influence of the red LED, which is located at a distance of 6 mm from the surface of the sensor.

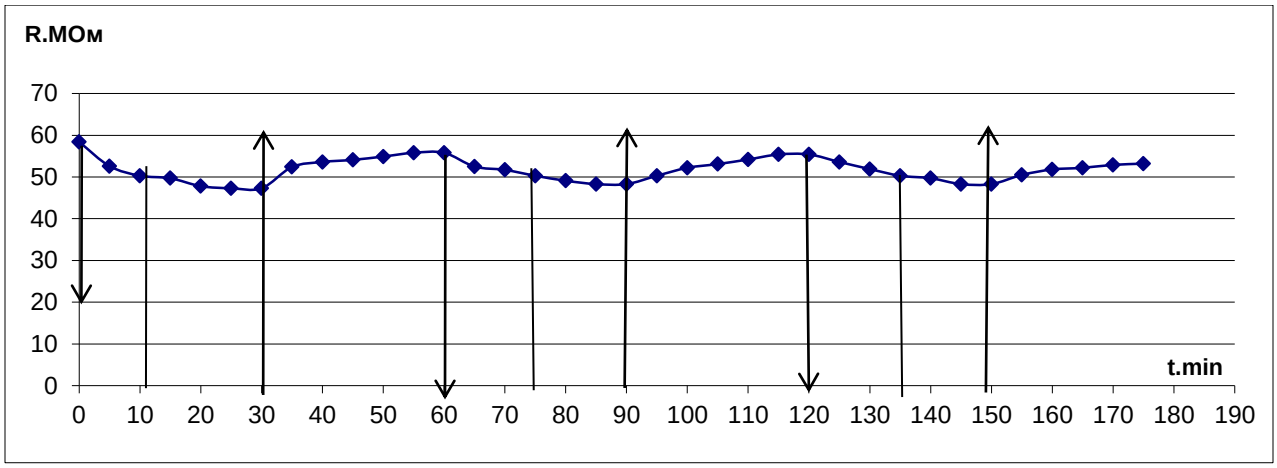


Fig.3.38. The change of the sensor resistance (SE1) under the influence of the red LED, which is located at a distance of 6 mm from the surface of the sensor. The initial value $R_{se1}$ = 58.4 MOhm

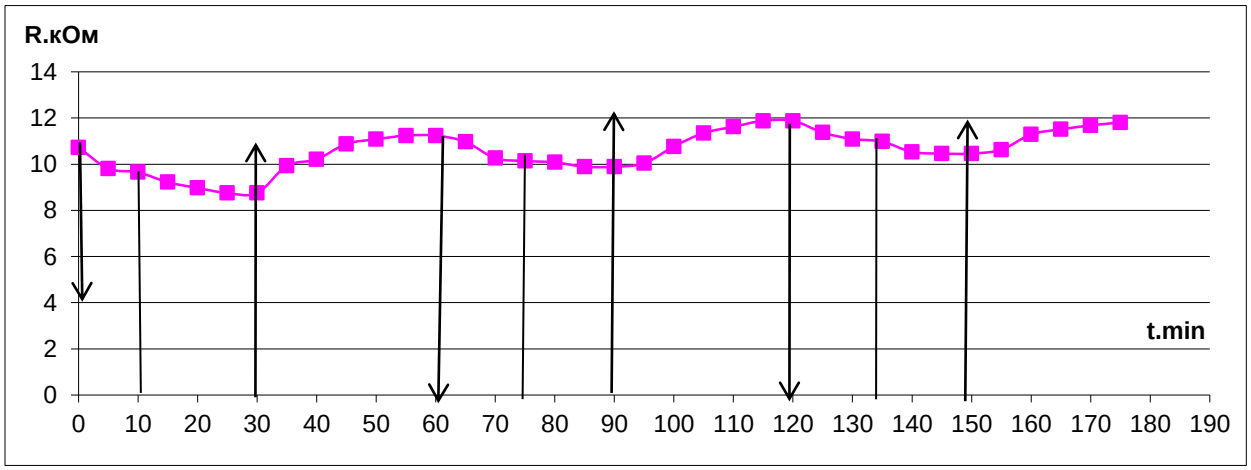


Fig.3.39. The change of the sensor resistance (SE2) under the influence of red light. The LED is located at a distance of 6 mm. The initial value $R_{se2}$ = 10.73 ohms

Fig.3.40. shows the relative change of the sensor resistance (ΔR / Ro) under the influence of red light. It is evident that the greatest changes at a distance of 6 mm occur when you turn on the light and make the value of (12 ± 1) %.

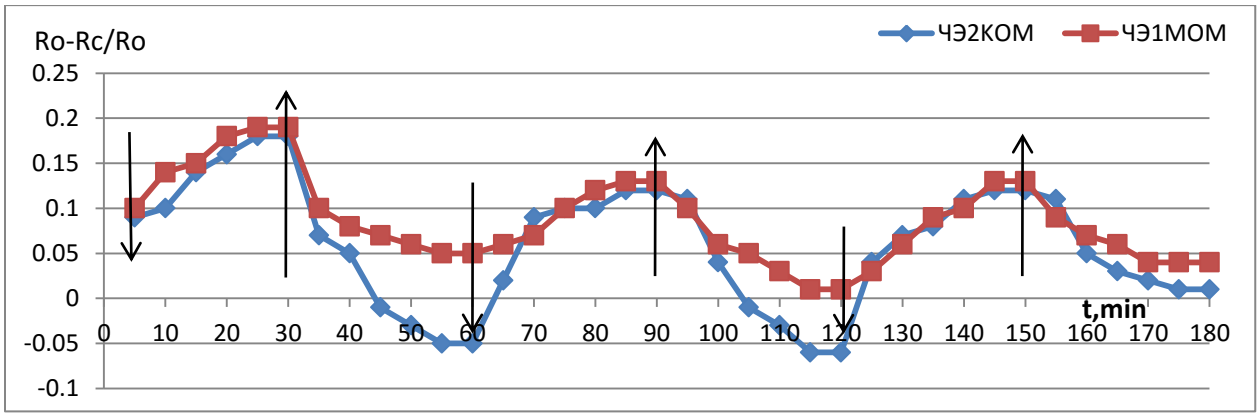


Fig.3.40. The relative change of resistance of sensors under the influence of red light. The LED is located at a distance of 6 mm

Fig.3.41. shows the dependence of the relative changes in the average of sensors resistance as a function of the distance from the LED to the surface of the $SnO_2$ film of sensors under the influence of red light.

The nature of changing of the resistance under the influence of red light is the same as under the influence of green light. The highest value of the relative change of resistance is about 20%, and with increasing distance from the LED which is from 4 to 6 mm is even less.

(Красный = Red)

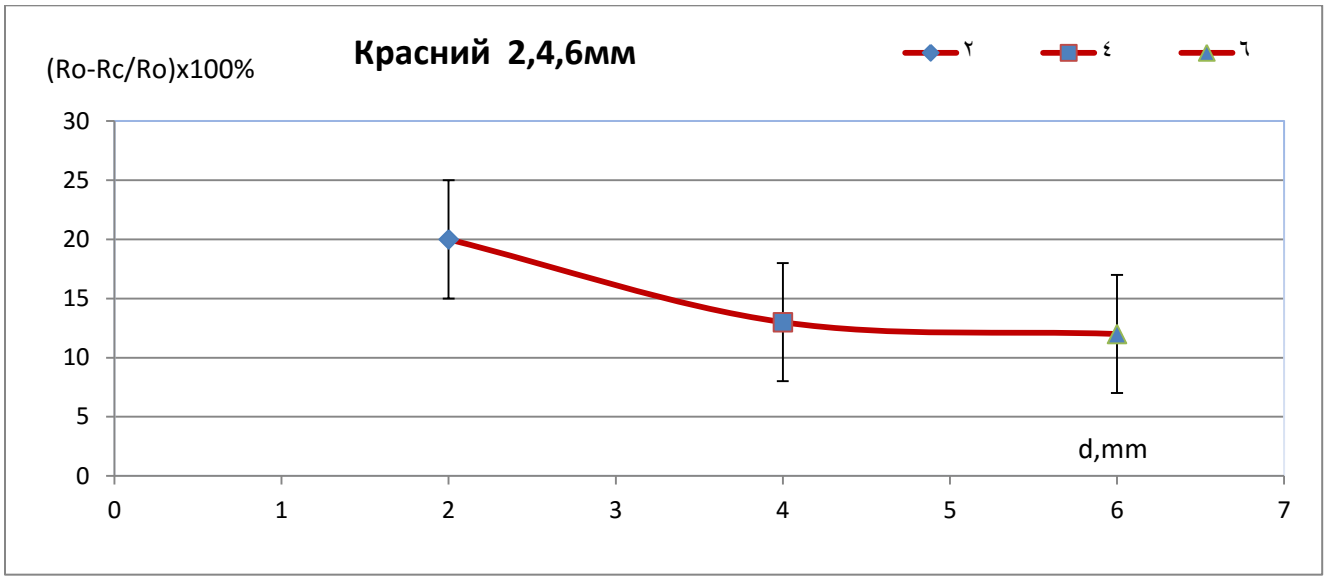

Fig. 3.41. The average relative change of resistance of sensors under the штадгутсу of red light on the distance from the LED to the sensor surface

In further researches we mainly used the exposure of purple or blue light at a distance from the sensor which is about 2 mm as purple and blue LEDs have the most powerful influence on the resistance of the $SnO_2$ film.

Table. 3.2. presents us the duration of the effective time of relaxation of sensors resistance when exposed to light-emitting diodes of different wavelengths. On the duration of the effective time of the sensor resistance relaxation effect of light is detected. The experimental results on the change in the electric gas sensors under the influence of purple, blue, green and red LEDs do not contradict the experimental data of the study [68]. The analysis of change features of the resistance during prolonged influence of the light indicates that the lighting $SnO_2$ film by purple and blue LEDs leads to the similar parameters of changes of the resistance.

Table 3.2

Effective relaxation times of sensors resistance under the influence of different color LED at a distance of 2 mm

| **The light** | $\tau_{1ef}$ | $\tau_{2ef}$ | $\tau_{3ef}$ |
|---|---|---|---|
| **Violet light 407 nm 3,05 eV** **λ = 407 mm, E = 3,05 eV** | 5 min | 25 min | 30 min |
| **Blue light 458 nm 2,71 eV** **λ = 458 mm, E = 2,71 eV** | 5 min | 25 min | 30 min |
| **Green light 526 nm 2,36 eV** **λ = 526 mm, E = 2,36 eV** | 5 min | 25 min | 30 min |
| **Red light 631 nm 1,97 eV** **λ = 631 mm, E = 1,97 eV** | 5 min | 25 min | 30 min |

Also we can note the similar effects of green and red light to change of the gas sensor resistance. It can be assumed that the violet and blue light generate non-equilibrium

carriers by band-band transitions and create two types of non-equilibrium carriers - electrons and holes. At the same time, the energy of green and red light is not sufficient for excitation of interband transitions and, most likely, their impact excites transitions of electrons in the conduction band of the system of surface states and impurity levels of oxygen vacancies lying in the forbidden band of the semiconductor. Therefore, at about the same power of LED effect of purple and blue colors noticeably superior to the effect of green and red colors. Since most the effect observed at a distance of 2 mm from the LED to the $SnO_2$ film, in future, all experiments were performed at a distance of 2 mm.

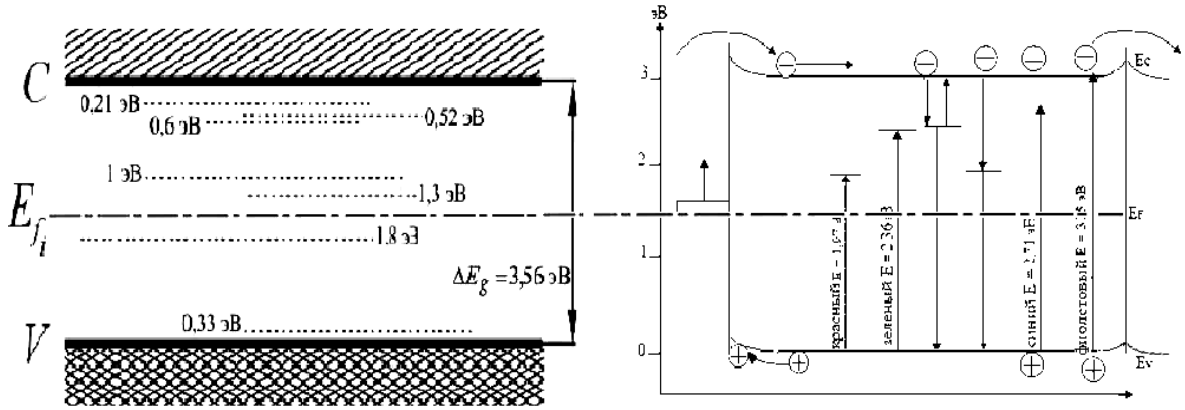


Fig.3.42. The energy band diagram of $SnO_2$ and an optical transitions scheme $SnO_2$ film in the interaction with the radiation of LEDs and processes bipolar and monopolar generation of charge carriers [82]

Because of the gas sensor was made by microelectronic technology using reactive magnetron sputtering method gas-sensitive $SnO_2$ film, its structure may deviate from stoichiometry, contain a high concentration of oxygen vacancies and other defects, and characterized by a bandgap of not more than 3 eV [8, 9]. Therefore own optical transitions can be stimulated by not only the purple light E = 3.05 eV, and blue E = 2.71 eV, which are indirectly confirmed by the similar behavior of resistance sensors under the influence of the violet and blue LEDs. Optical excitation of own electrons transitions do not exclude the possibility of impurity unipolar diodes generate violet light and blue light.

The quanta energy of green (E = 2.36 eV) and red (E = 1.97 eV) LEDs are not sufficient to excite the transition zone. Because the green emission energy band gap less then $SnO_2$ zone, it may be the result of non-equilibrium generation of unipolar charge carriers with impurity levels on the surface and in the bulk of the semiconductor. Previously, it has been found [82] that in single crystals of $SnO_2$ there is a large collection of shallow and deep energy levels due to multiply charged oxygen vacancies and other defects, with the distance from the bottom of the conduction band of 0.21; 0.52; 0.6; 1; 1.3 and 1.8 eV (Fig.3.42). In the $SnO_2$ films the concentration of these defects may reach values of the order of 1018 - 1019 $cm^{-3}$ and the number of these levels in the n-$SnO_2$ may participate in processes of photoconductivity and relaxation of non-equilibrium carriers.

### 3.2. Influence of fumes of gas-reducing on a gas response of sensitive gas sensor element on the base of $SnO_2$ films

It is known [1], when placing gas sensor to air containing impurities gas - a reducing agent (Ethyl alcohol, acetone, ammonia, etc.), electrical resistance sensing element composed of SnO2 film decreases. Reducing the resistance is proportional to the value of the gas concentration - reducing agent and this fact is the basis for measuring the gas sensitivity of the sensor elements.

This section describes the results of studies of the gas sensor sensitivity at room temperature. Method for determining $S = \frac{R_B}{R_Г}$ gas response is described in Chapter 2. Before starting the measurement sensors annealed in the air at about 450 ° C to desorb the gases and stabilize the sensor resistance. Method of air-gas mixtures are also described in Chapter 2.

We studied the effect of various substances on the vapor sensitive elements resistivity of gas sensors manufactured by microelectronic technology, having one heater and two sensors based on $SnO_2$ films. The silicon substrate in this design has dimensions 1.0 × 1.0 × 0.12 mm. The thickness of the gas-sensitive film is 250 nm [72].

Gas sensitivity $S_g$ defined as the ratio of the resistance of the film in air ($R_B$) to the film resistance when admitted into the measuring chamber volume of 10 liters of known concentration test gas ($R_g$): $S_g = R_B / R_g$ [89]. A film resistance measured multimeters company Mastech MY64 series. The concentration of gaseous mattern is determined by the controlled dilution. The basis of his supposed equation Mendeleev-Clapeyron, namely the conversion of concentration of a substance from a liquid to gaseous state [78].

We studied the effect of vapors of ammonia, water, ethanol, acetone concentration of 500 - 10000 ppm in the air on the electric sensors sensing gases elements at room temperature. Gas feedback pairs of ethyl alcohol and acetone at room temperature with the indicated concentrations was detected.

The process of interaction of water vapor at a temperature of 21 ˚C with the surface of the $SnO_2$ film takes a few minutes, during which the sensor resistance decreases, reaching a minimum value. The ratio of the initial resistance to the minimum resistance patterns will characterize the gas sensor response at a given concentration of water vapor. After each experiment, the samples were annealed at a temperature 450˚S to remove water molecules from the surface of the $SnO_2$ film. Gas response measurements are performed in the concentration range (1000 - 10,000) ppm $H_2O$ in the air that meets the values of relative humidity with an accuracy of ± 1%: 56% - 1000 ppm, 74% - 3000 ppm, 82% - 5000 ppm, 94% - 10000 ppm.

Preliminary studies showed that the water vapor concentration less than 3000 ppm stable gas sensor response at RT absent, i. e. humidity less than 75% on electrical resistance of SnO2 film at room temperature is not affected.

Fig. 3.43 shows the change of sensor resistance in water vapor (3000 ppm) at room temperature according to the time indicated by arrows closing time (↓) and the opening (↑) of the measuring chamber. Elektrosoprotiivleniya time reducing to a minimum value under the influence of water vapor takes about 5 minutes and then gradually relaxes resistance to the initial value (about 10 minutes). Relaxation resistance may be due to the saturation of the surface states and partial desorption of water molecules. The magnitude of the response of the gas S = RB / Rg = 1.72 RLU

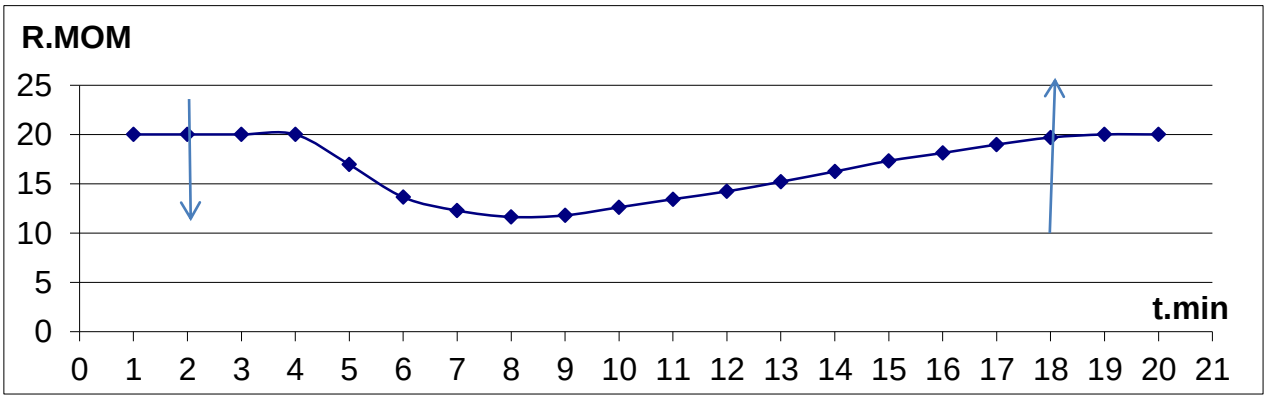


Fig.3.43. The change in resistance of the sensitive element of water vapor 3,000 ppm (74% relative humidity) at room temperature

With increasing concentration of water vapor up to 5,000 ppm (relative humidity 82%) the variation of the sensor resistance changes (Fig. 3.44). The resistance decrease to the minimum time during about 2 minutes, then the resistance is reached saturation and relaxation to the initial value only after removing a hermetic cap.

When the concentration of water vapor in the air 5000 ppm (82% relative humidity) sensor is sensitive equal S1 = 20 / 7.43 = 2.69 RLU After 23 minutes the experiment semiconductor surface is saturated, and the resistance begins to increase.

Similar phenomena are observed in water vapor at a concentration of 10,000 ppm, (relative humidity - 94%). When the water vapor concentration of 10,000 ppm in air sensor is sensitive equal S1 = 20 / 3.29 = 6.07 RLU After 37 minutes of the experiment the semiconductor surface is saturated with water and the resistance begins to increase. The whole interaction process takes approximately 132 minutes. Duration achieve the lowest value $\tau_{1ef}$ resistance is about 20 minutes slow relaxation $\tau_{2ef}$ = 30 min and relaxation before returning to baseline values $\tau_{3ef}$ = 80 min.

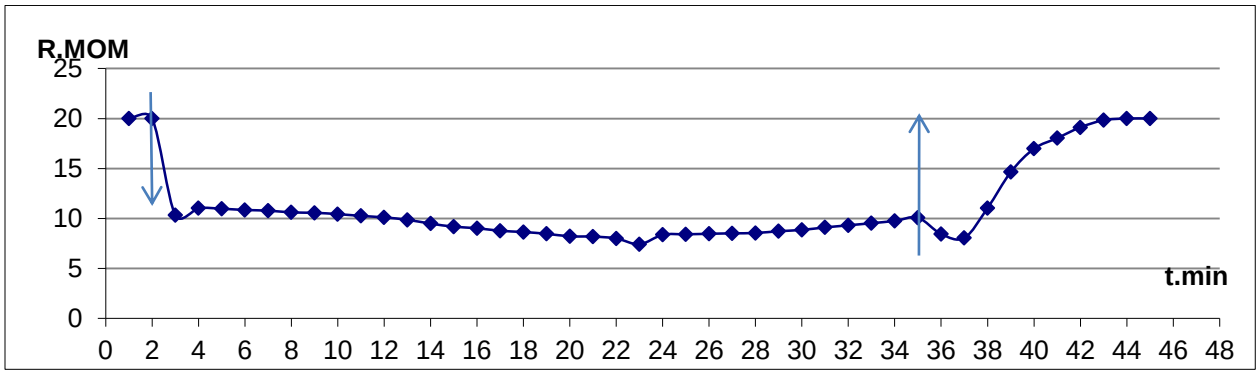


Fig.3.44. Changing of the resistance of a sensitive element of the water vapor of 5000 ppm (82% - relative humidity) at room temperature.

The dependence of sensor response to concentration of water vapor in the air at room temperature is shown in Fig. 3.45. The maximum response value is S = 6 RLU water vapor at a concentration of 10,000 ppm, (relative humidity - 94%), which corresponds to 1% of the volume content of water in the air.

Thus investigated sensors may be used to determine the humidity of 75% at room temperature.

The nature of changing of the resistance of $SnO_2$ film under the influence of vapors of 10% aqueous ammonia at room temperature is similar to the impact of water vapor, but much more evident.

*(чэ1 = se1)*

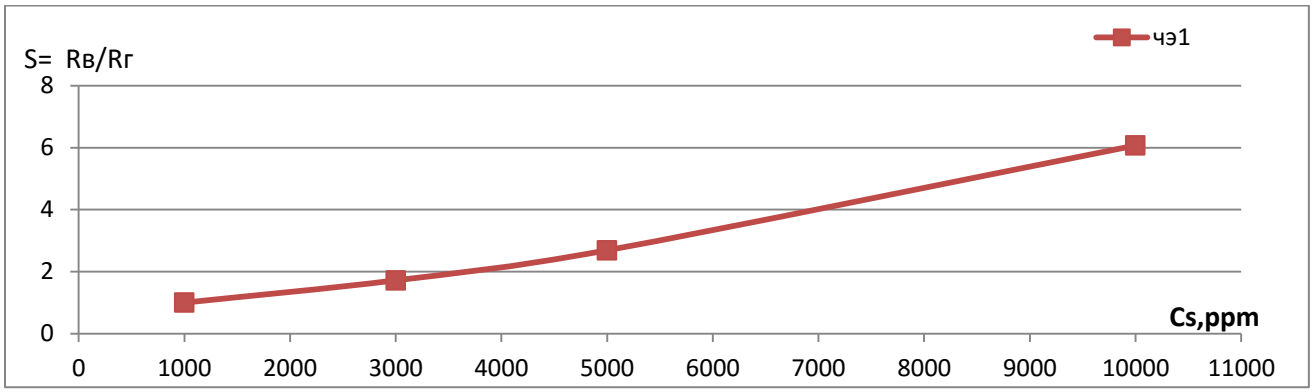


Fig.3.45. The dependence of sensor response on the concentration of water vapor in the air at room temperature

We studied the effect ammonia vapors with a concentration of 500 - 10,000 ppm on the resistance of gas sensors. Sensor resistance begins to change when the concentration of ammonia vapor in the air is 1000 ppm, Fig. 3.46.

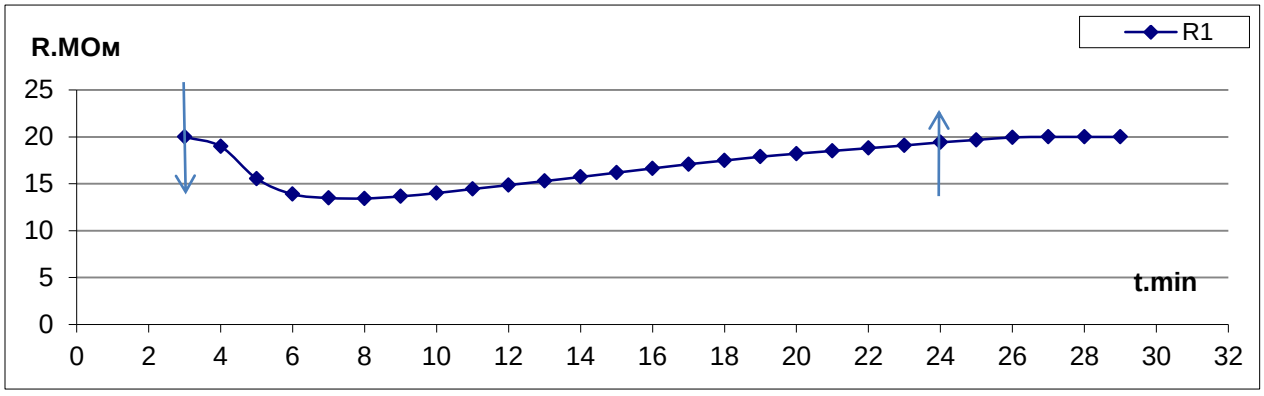


Fig.3.46. The change of the resistance of the sensitive element 1000 ppm ammonia vapor at room temperature.

At the same time there is a sensitive, which is equal to S1 = 20 / 1.48 = 13.44 RLU after 7 minutes of the experiment the semiconductor surface is saturated with ammonia and the resistance begins to increase. The interaction process takes approximately 30 minutes. Duration achieves the lowest value $\tau_{1ef}$ resistance is about 5 minutes of slow relaxation $\tau_{2ef}$ = 10 min and relaxation before returning to baseline values $\tau_{3ef}$ = 15 min.

Fig. 3.47 shows the change of the resistance of the sensitive element in 3000 ppm ammonia vapor at room temperature.

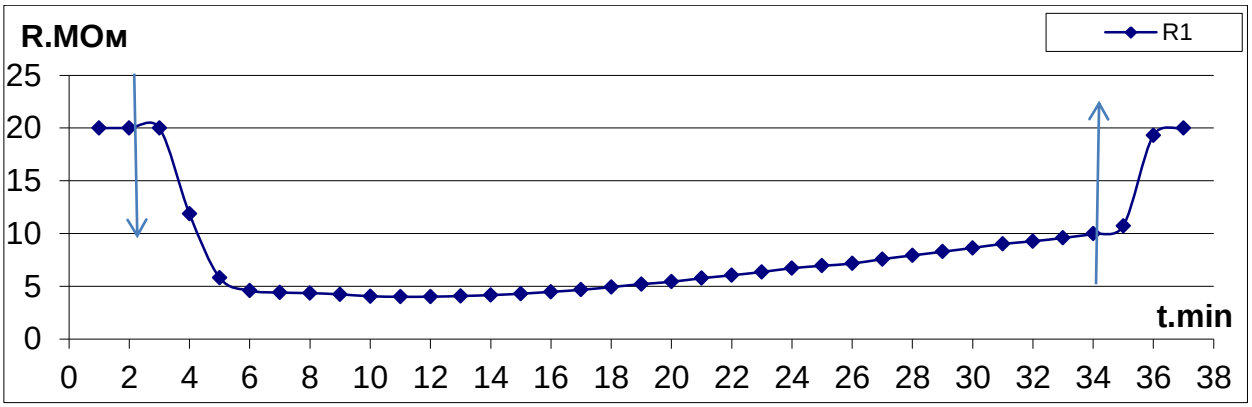


Fig.3.47. The change of the resistance of the sensitive element 3000 ppm ammonia vapor at room temperature.

When the concentration of ammonia vapor in the air of 3000 ppm sensitivity is S1 = 20 / 4.01 = 4.98 RLU after 11 minutes of the experiment is saturated with ammonia semiconductor surface and the resistance begins to increase. The interaction process takes approximately 38 minutes. Duration achieve the lowest value of $\tau_{1ef}$ resistance is about 5 minutes of slow relaxation $\tau_{2ef}$ = 10 min and relaxation before returning to baseline values $\tau_{3ef}$ = 20 min.

The change of the resistance of the sensitive element 5000 ppm ammonia vapor at room temperature is shown in Fig. 3.48.

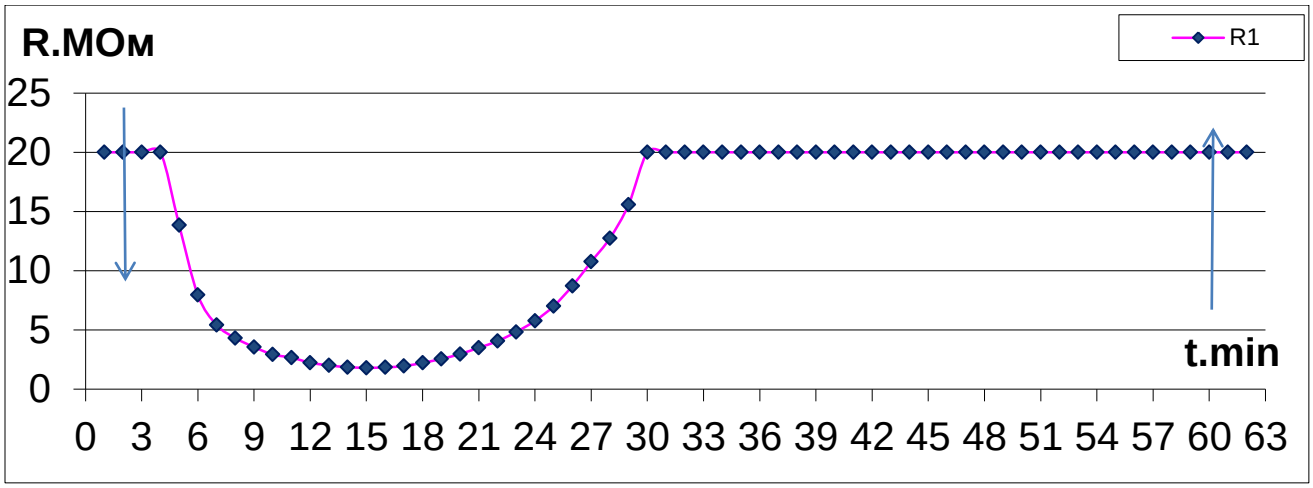


Fig.3.48. The change of the resistance of the sensitive element 5000 ppm ammonia vapor at room temperature.

At the concentration of ammonia vapor in the air of 5000 ppm sensor has a sensitivity equal to $S_1$ = 20 / 1.81 = 11.04 RLU after 15 minutes the experiment is saturated with ammonia semiconductor surface and the resistance begins to increase and reaches a baseline value after 30 minutes. Duration achieve of the lowest value $\tau_{1ef}$ of resistance is about 10 minutes of slow relaxation $\tau_{2ef}$ = 20 min and relaxation before returning to baseline values $\tau_{3ef}$ = 35 min.

Fig. 3.49 shows the dependence of sensor response on the ammonia concentration of 500 - 5000 ppm at room temperature. The highest response value of the gas is 11 units, and is achieved at 5000 ppm ammonia in air at room temperature.

*(чэ1 = se1)*

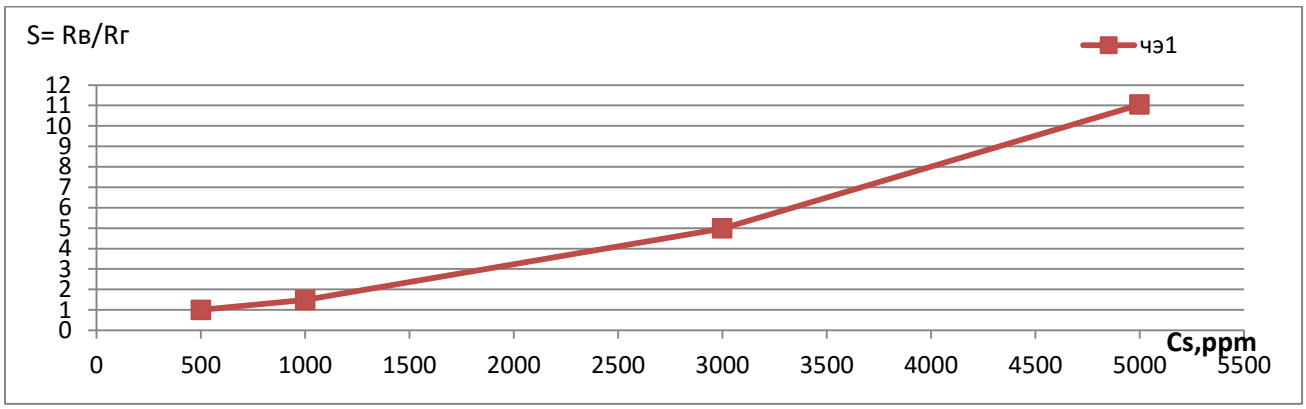


Fig.3.49. The dependence of sensor response on the concentration of ammonia vapor in the air at room temperature.

In our studies we used 10% ammonia water, so along with the ammonia vapors manifested effect of water vapor on the gas sensor. Fig. 3.50 shows the dependence of the gas sensor response at room temperature, water vapor and aqueous ammonia, and the difference of these responses illustrating the effect on sensor only ammonia vapors. As it follows from Fig. 3.50, the confident detection of ammonia vapor at room temperature can be carried out on the concentrations of 2000 - 3000 prm in the air.

*(чэ1 вода = se1 water, чэ1 аммиак-вода = se1 ammonia-water, чэ1 аммиак = se1 ammonia)*

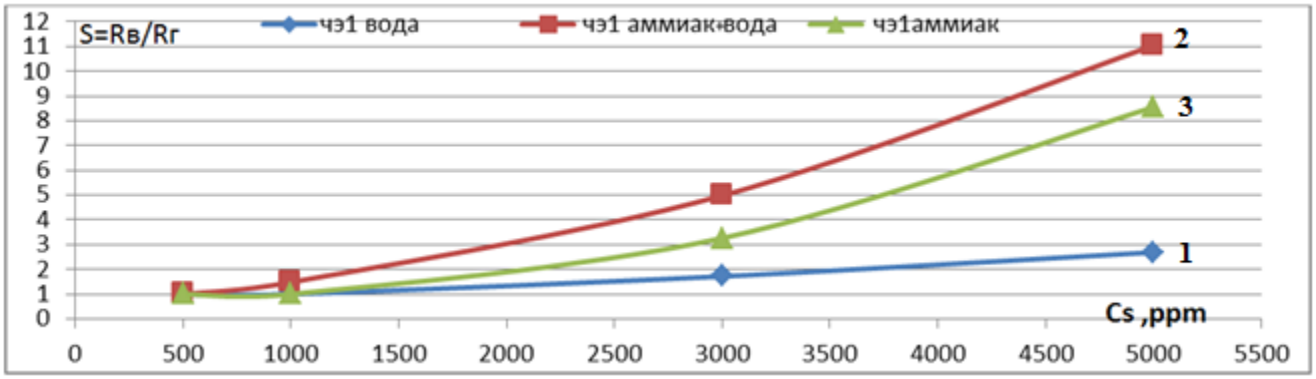


Fig. 3.50. Sensor response to concentration of ammonia vapor in the air at room temperature with allowance for the contribution of water vapor.

Such concentrations (0.2 -. 0.3% by volume) of ammonia in the air can be achieved in the areas of production, transportation and storage of ammonia, where a gas leak indicators can be installed, operated at room temperature.

Table.3.3. shows the values of response of $SnO_2$ gas sensor at room temperature, to the vapors of ammonia based on the influence of water.

Table 3.3

Gas sensor sensitivity at room temperature, to the vapors of aqueous ammonia, water and ammonia.

| The concentration of ammonia Cs,ppm | Aqueous ammonia $S_{SE1}$ | Water $S_{SE1}$ | Ammonia $S_{SE1}$ |
|---|---|---|---|
| 1000ppm | 1.48 | 1 | 0.48 |
| 3000ppm | 4.98 | 1.72 | 3.26 |
| 5000ppm | 11.04 | 2.69 | 8.35 |

**Conclusions of the 3rd chapter.**

As a result of studies of the impact of light and gases in the value of the resistivity of $SnO_2$ sensors at room temperature, it is possible to make the following conclusions:

1. It is found that a result of the effect of light of low-power LEDs with energies of 1.97 eV (red) to 3.05 eV (purple) electrical resistance of the sensor element based on $SnO_2$ is reduced by the generation of optical equilibrium charge carriers. The highest values of resistance to change are 20 - 25%, at a distance of 2 mm from the LED to the sensor layer.

2. Under the influence of the violet and blue light sensor changes the resistance characteristics are similar in nature, due, apparently, its own interband optical transitions of electrons and the bipolar light generation of nonequilibrium charge carriers. Resistance to change under the influence of the green and red LEDs also have similar laws due, probably, monopolar impurity light generating charge carriers with the impurity levels in the volume of the crystal and surface states. The differences in the dynamics of change in resistance in case purple and green light are caused by different mechanisms of optical generation of nonequilibrium charge carriers. Magnitude of the effect of green and red exposure light on the $SnO_2$ film is significantly less than the impact of the violet and blue LEDs.

3. The effective relaxation time characterizing the three stages of time sensor resistance dependencies when illuminated by LEDs, with all kinds of influences have similar values τef = 5 minutes (rapid process) $\tau_{2ef}$. = 25 minutes (slow) $\tau_{3ef}$. = 30 minutes (after the light is turned off). However, the nature of resistance changes when exposed to violet and blue LEDs is different from the characteristics of the relaxation curves under the influence of the green and red LEDs due to the different mechanisms of generation of non-equilibrium carriers. A scheme for the possible optical transitions in the $SnO_2$ film under the influence of LED radiation is studied.

4. Under the influence of water vapor on the SnO2 layer resistivity sensor at room temperature there is a marked decrease in resistance of the sensor at concentrations

exceeding 3000 ppm, which corresponds to 74% relative humidity. With further increase in the concentration of water vapor (up to 10,000 ppm or 94% RH) observed almost linear increase in gas SnO2 film response.

5. At room temperature the sensitivity of gas $SnO_2$ films to vapors of aqueous ammonia ($NH_4OH$), which is noticeably manifested when the ammonia concentration of 1000 ppm (S = 1,48) and above. At 5000 ppm the sensitivity to ammonia vapors of S = 11,04 RLU

6. Due to the fact that the gas sensitivity study to ammonia used an aqueous solution, was calculated sensitivity $SnO_2$ gas sensors based on the contribution of water vapor. These threshold measurement sensitivity of $SnO_2$ gas sensors to ammonia at room temperature increases from 1000 ppm to 1500 ppm. Sensors which are on the basis of $SnO_2$, operating at room temperature, can be used to control ammonia leak in the areas of production, transportation and storage, where the concentration of ammonia in air may exceed the threshold of 1500 ppm sensor sensitivity (0.15% by volume).

# Chapter 4.

## RESEARCHING OF INFLUENCE OFAN IMPURITY MODIFICATION OF SENSOR SURFACE THROUGH CATALYSTS AND LIGHT EFFECT ON THE LEVEL OF GAS RESPONSE

Active effect of the light of the fundamental absorption on the electrical sensor elements, as well as previously performed experiments [61, 62, 63, 64, 65] allow us to expect an increase in gas sensor response when illuminated with violet light. This chapter presents the results of studies of the effect of light purple low power LED on the amount of gas response $SnO_2$ films under the influence of gas-reducing acetone, ethyl alcohol and isopropyl alcohol.

This chapter also shows the experimental results of the effect of surface modification film $SnO_2$ by solutions of salts of Pd and Ag, which are known as the impurity-catalysts, the gas sensor response. Techniques for preparation of salt solutions with different molar concentrations of Ag and Pd are given in Chapter 2. It has been established [84] that the greatest impact on the response of the gas $SnO_2$ films have aqueous solutions of salts Ag and Pd, containing 6 millimoles of impurities. Therefore, for the surface modification of $SnO_2$ is mainly used 6 millimolar solutions of salts of silver and palladium.

Also we studied the simultaneous effect on the response of the gas sensor surface modification catalyst impurities and exposure to light of different wavelengths to establish mechanisms of interaction of gas molecules with the $SnO_2$ semiconductor surface states when excited by light with different energies.

**4.1. Researching of the influence of violet and green light on sensivity of gas sensor on the base of $SnO_2$**

The impact of violet light on the resistance of sensing element [79] leads to a decrease of the electrical resistance by nearly 25% due to the generation of non-equilibrium charge carriers (Fig.4.1). Duration of the achievement of least resistance values ($\tau_{1ef}$) is about 5 minutes of slow relaxation $\tau_{2ef}$ = 25 min and relaxation after the light is turned off $\tau_{3ef}$ = 30 min. It should be noted that the resistance is not returned to baseline values after light-off.

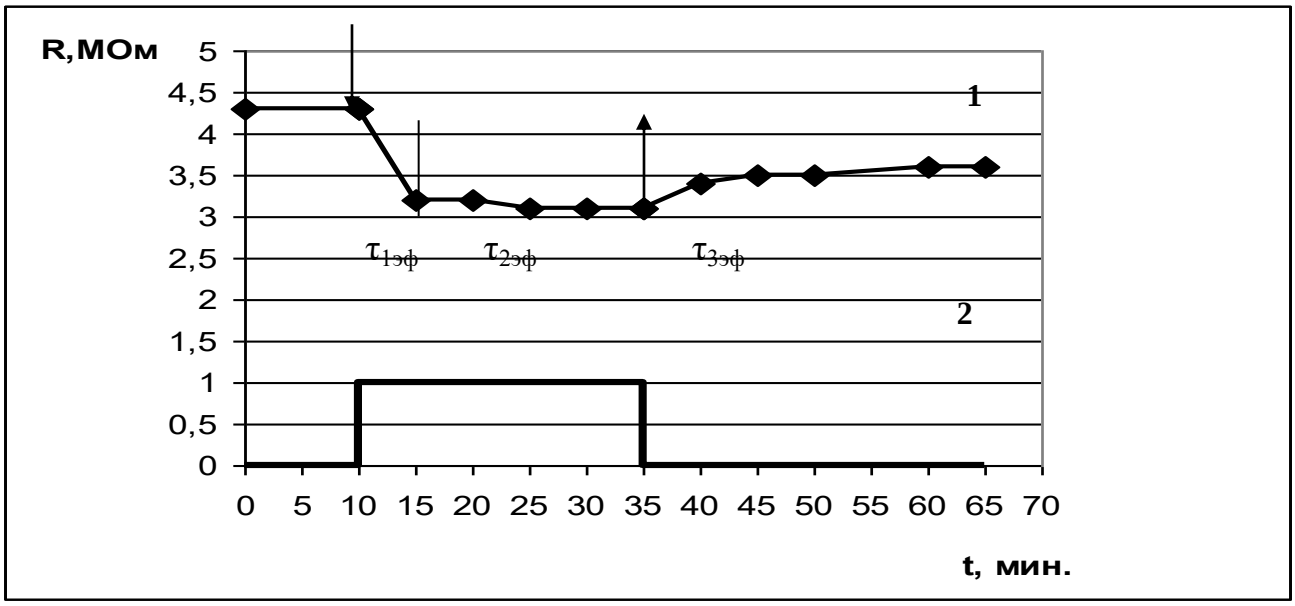


Fig. 4.1.The nature of change of the sensor resistance (1) under the action of the violet LED light pulses (2)

With simultaneous interaction with the gas and light can be recharged $SnO_2$ film surface states by exposure to light, which may lead to changes in the sensitivity of the gas. Therefore, the resistance change sensing elements gas sensors was investigated in cooperation with different pairs of substances in the air under the action of violet radiation. ALR2-513UVC brand LED with a wavelength of 407 nm and 76 mW output power was located at a distance of 2 mm from the surface of the sensor element. We investigated the sensitivity of gas sensors gas test structures to vapors of ethyl,

isopropyl alcohol and acetone in air at temperatures of 20 – 400$^{o}$ C. Sensors for temperature changes in the heater to a voltage of 1 to 5 V. The temperature was controlled datchka largest resistance heating element. Typical temperature dependence of the resistance on the temperature of the heater is shown in Fig. 4.2. The resistance of the heater is at room temperature RH = 22.3 ohms.

*(Расчитано = Calculated, Измерено = Measured)*

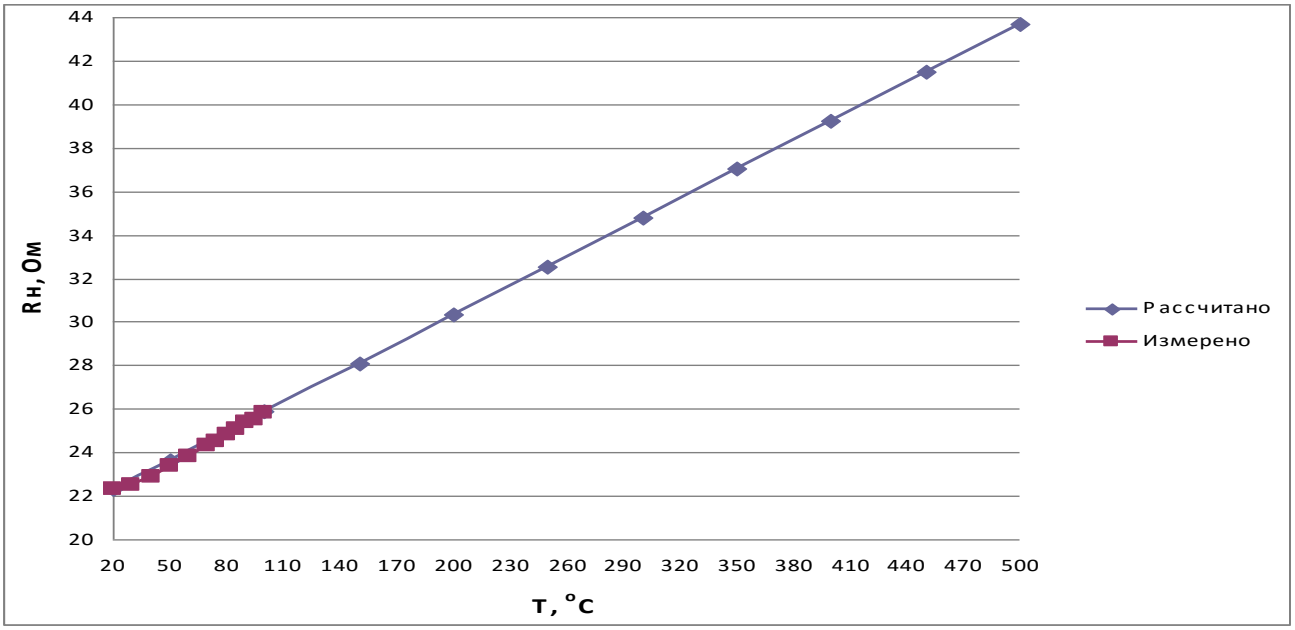


Fig.4.2. The dependence of the temperature of the resistance of the heater test structures for gas sensors [74].

The results of experimental measurements and calculated values are shown in Table. 4.1

Table. 4.1

The temperature dependence of the resistance heater at different values of the external voltage.

| $U_H$,V | $I_H$,мА | $R_H$,Ohm | T,˚C |
|---|---|---|---|
| 0 | 0 | 22,3 | 20 |
| 1 | 26,7 | 23,638 | 50 |
| 1,5 | 39,1 | 25,868 | 100 |
| 2 | 49,6 | 28,098 | 150 |
| 2,5 | 59,7 | 30,328 | 200 |
| 3 | 68,8 | 32,558 | 250 |
| 3,5 | 75,8 | 34,788 | 300 |
| 4 | 81,9 | 37,018 | 350 |
| 4,5 | 88,5 | 39,248 | 400 |
| 5 | 93,4 | 41,478 | 450 |
| 5,5 | 104,3 | 43,708 | 500 |

From the linear dependence R = *f* (T) calculates the temperature coefficient of resistance (TCR) of the formula

$$R(T) = Ro(1 + \alpha\Delta T),$$

where Ro is a resistance of the heater at room temperature To;

K (T) is the resistance at elevated temperature T;

$\Delta T = T - To$ – change of the temperature.

The value of TCR is $\alpha = 0{,}002$ 1/ K.

Temperature dependence of sensitivity of the gas sensor to the gas sensor element pairs of ethanol in the air, as well as optical effects in the presence of ethanol shown in Fig. 4.3. [90]. It is found that the maximum sensitivity of the gas to ethanol vapor in air (1700 ppm) without exposure to light is observed at a temperature of 330 ° C and 1.8 RLU The irradiation test structure violet light sensitivity of the maximum gas temperature is reduced to 290 ° C. At the same time the value of the gas sensitivity is 6 relative units, as well as an additional peak sensitivity at a temperature of 130 ° magnitude 4.8 RLU, thus, the violet light exposure sensitivity increases the main peak

gas in 3 times and reduces the temperature sensitivity of the gas at maximum of 40 ° C. Peak more sensitivity to ethanol at 130 ° C can be used to measure the low temperature ethanol content of the air at light exposure.

*(отн. ед. = RLU)*

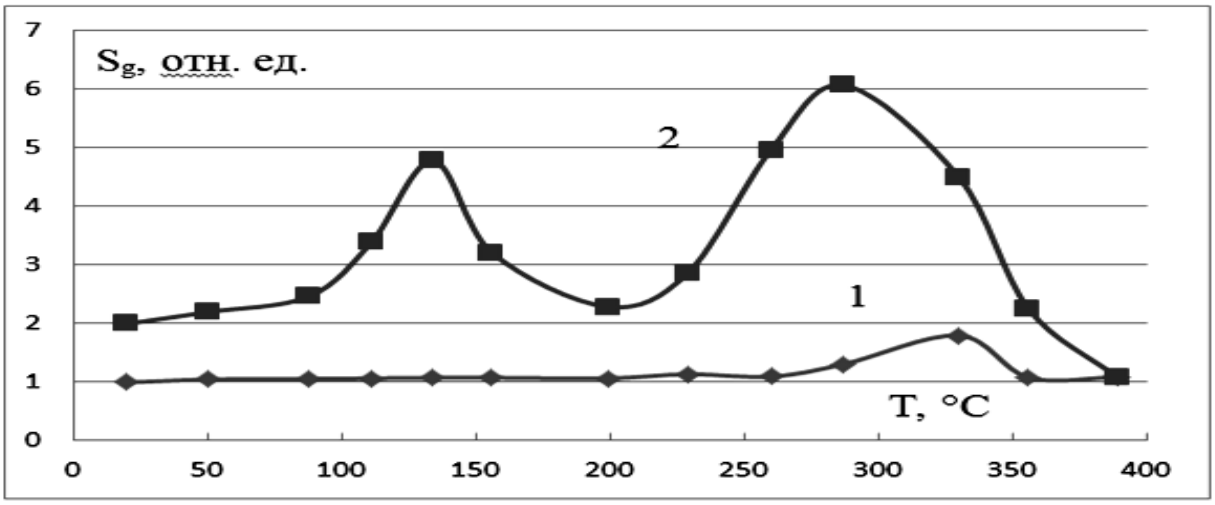


Fig.4.3. The temperature dependence of the sensitivity of the gas sensor element pairs to ethyl alcohol (1700 ppm) in the air by irradiation with violet light (1) and without illumination (2).

The temperature dependence of the sensitivity of the gas sensor to the gas sensor element isopropyl alcohol vapor in the air, as well as optical effects in the presence of isopropyl alcohol is shown in Fig. 4.4.

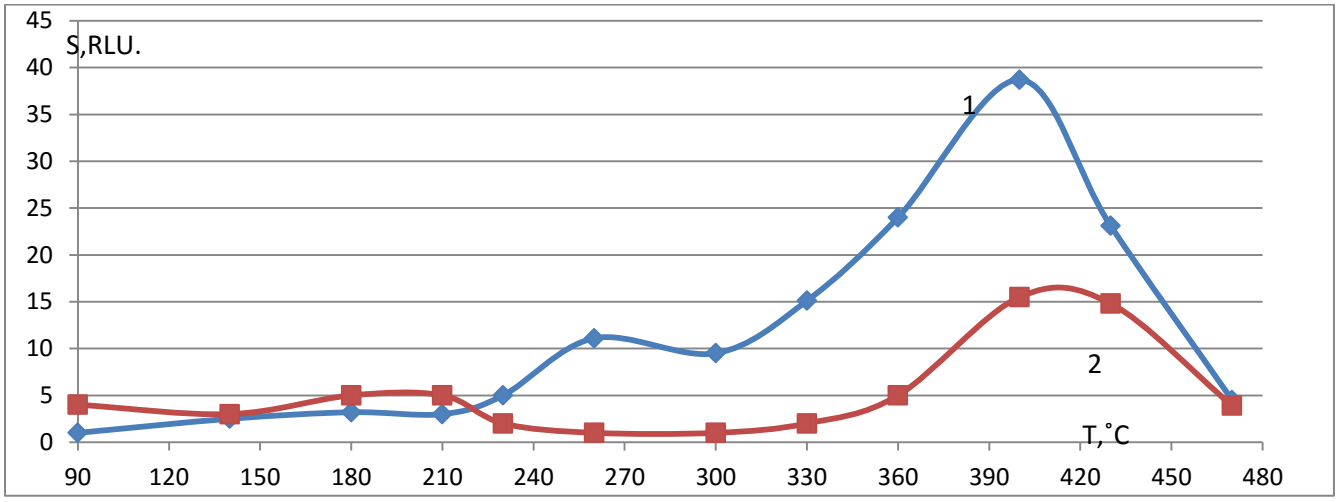


Fig.4.4. The temperature dependence of the sensitivity of the gas sensor to the gas sensor element pairs isopropyl alcohol (1300 ppm) in air by irradiation with violet light (1) and without illumination (2)

The maximum gas sensitivity of the sensor gas sensor element to the pairs of isopropyl alcohol (1300 ppm) in the air without exposure to light is observed at a temperature of 400 ° C and 15.5 RLU the irradiation test structure violet light sensitivity of the maximum gas temperature decreases to 10 ° C, and the gas sensitivity value increases to 38.7 RLU, as well as an additional peak sensitivity at a temperature of 260 ° C value of 11.1 RLU. In this case, the light quantity of gas at the main peak sensitivity is increased in more than 2 times. The additional peak at 260 ° C can also be used to determine the air content of propanol light when exposed to the gas sensor.

The temperature dependence of the sensitivity of the gas sensor to the gas sensor element of acetone vapors in the air, as well as optical effects in the presence of acetone are presented in Fig. 4.5. The maximum gas sensitivity to acetone vapors (1700 ppm) in the air without exposure to light is observed at a temperature of 360 ° C and 7.4 RLU. The irradiation test structure LED temperature maximum gas sensitivity remains

practically unchanged; the amount of gas sensitivity is 10.1 relative units, as well as additional peak sensitivity at a temperature of 136 ° C, the value of 8.6 RLU.

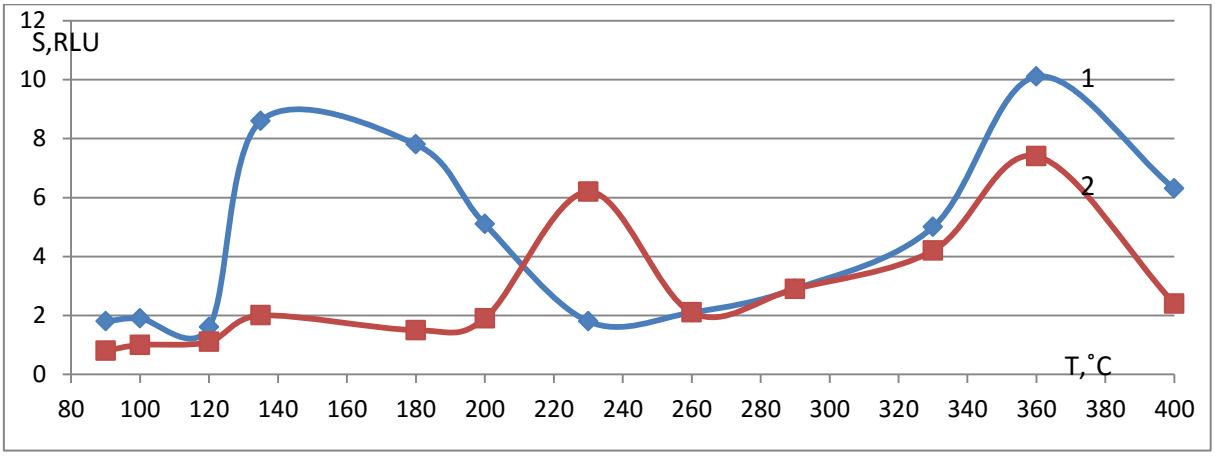


Fig.4.5. The temperature dependence of the sensitivity of the gas sensor to the gas sensor element pairs acetone (1700 ppm) in the air by irradiation with violet light (1) and without illumination (2)

At the green light emission value of the maximum gas sensitivity is practically not changed. However, when exposed to green light at temperatures of the order of 100 ° C, an additional peak gas sensitivity is practically coincides with the largest sensor sensitivity without lighting (19 RLU), But observed at a temperature of 330$^{o}$ C. The new peak gas sensitivity may be due to the interaction of green light with the energy levels of defects in the $SnO_2$.

*(отн. ед. = RLU)*

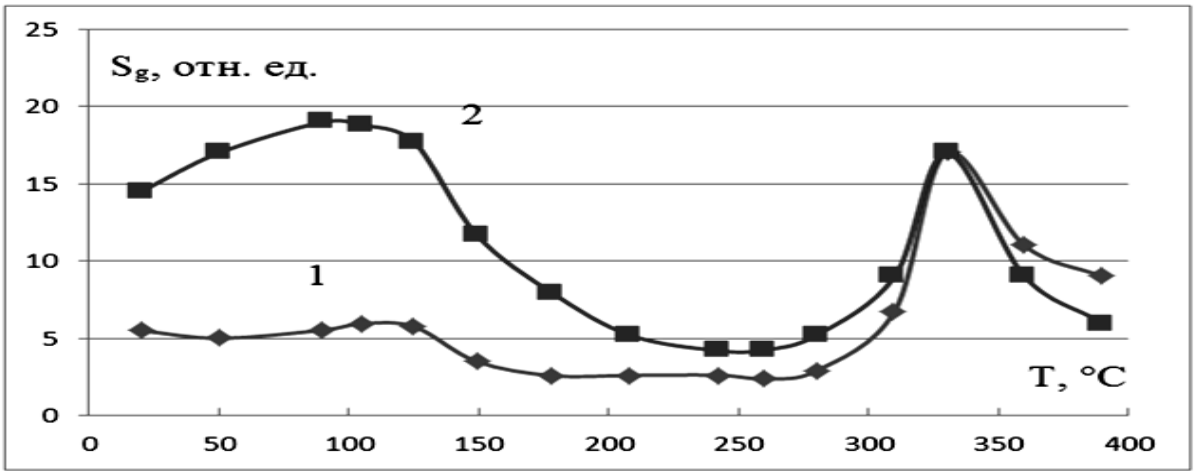


Fig.4.6. The temperature dependence of gas sensitivity to vapors of ethyl alcohol (2000 ppm) in the air without illumination (1) and at the illumination of green light (2)

Thus, in all experiments we performed light exposure increases sensitivity to gas vapors of ethyl, isopropyl alcohol and acetone in the main peak is 1.5 - 3 times. Maximal sensitivity gas temperature is reduced to 10 - 40 ° C, or does not change (acetone). Also, at lower temperatures of 130 - 260 ° C, an additional peak of largest gas sensitivity comparable to or superior to the sensitivity of the sensor without a corresponding gas lighting. The advent of low-temperature gas sensitivity peak indicates that light photons activate new mechanisms gas sensitivity missing samples in the darkness. These mechanisms can be attributed directly to the interaction of light with the charged surface states, such as oxygen vacancy and their activation, as well as interaction with the low-temperature light-controlled gas molecules. For additional peaks maximal sensitivity gas temperature sensor for ethyl alcohol and isopropyl alcohol and acetone is 2 - 3 times lower than the temperature of maximum sensitivity for the same gas, but in the absence of light exposure on the surface of the sensor. These additional peaks may be used to monitor ambient air at lower temperatures, resulting in lower power consumption of gas sensors.

### 4.2. Researching of the influence of a surface modification of sensor $SnO_2$ fibres through Ag and Pd impurities on a gas the gas response of gas sensors

For the surface modification of samples $AgNO_3$ aqueous solutions were prepared with different degrees of dilution from 25 mg to 100 mg in 50 mg of water (0.003 M, 0.006 M, 0.009 M and 0.012 M, respectively) and placed in a special vessel that does not allow penetration of daylight, due to the increased photosensitivity of silver ions. Before applying the impurity gas sensors are pre-annealed at a temperature of 450˚C to remove from the surface of the semiconductor adsorbed molecules from the air. Surface modification of the silver nitrate solution was carried out by a special process, under controlled microscope MBS-1 56-fold increase by applying a solution onto the microdroplets sensitive gas sensor element, followed by drying in air at room temperature for 24 hours. Droplet sizes of consistent with the size of the sensor element (200 x 200 mm2) were the same. Previously, [84] it was found that the response of the gas SnO2 films greatest effect vodnyy silver nitrate solution containing 6 mM silver. the temperature dependence of gas sensitivity studies were carried out to vapors of isopropyl alcohol 3000 ppm in air to the sensing element, the silver modified 6 mM solution (Fig. 4.7).

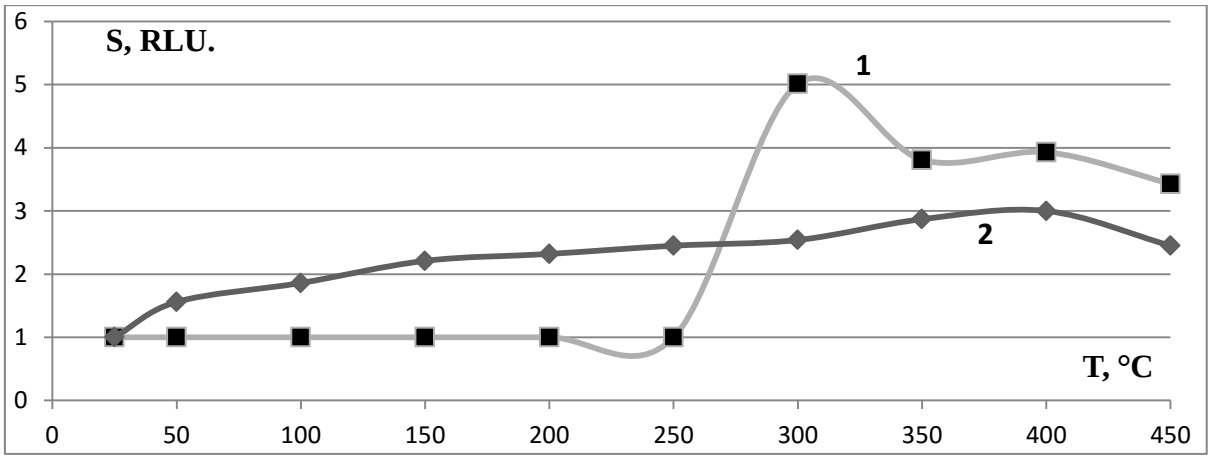


Fig.4.7. The temperature dependence of gas sensitivity to vapors of isopropyl alcohol 3000 ppm in the air for pickup modified 6 mM solution of silver (1) in the comparison with the undoped sample (2)

As we can see from the graph, the maximum gas sensitivity of silver salts of modified samples appears to the pairs of isopropyl alcohol at the temperature of 300 $^{o}$C crystal sensor, and is about 5 RLU.

The value of the reference sample gas sensitivity reached 3 RLU $^{o}$C at 400, 100 that $^{o}$C greater than for the sensing element, the doped silver solution 6 mM. Thus, modification of the silver surface of the sensor reduces the temperature of maximum sensitivity of the sensor is 100$^{o}$ C and increases the sensitivity of the sensor of 1.5 times.

The temperature dependence of gas sensitivity of 12 mM silver doped and undoped SE solution in pair's ethanol 2000 ppm in air (Fig. 4.8) were studied.

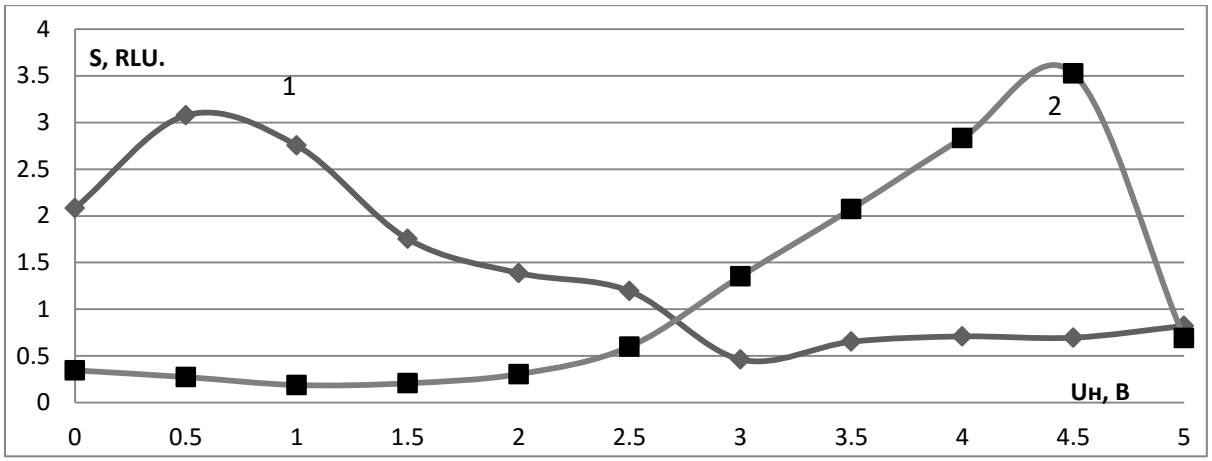


Fig.4.8. The dependence of the sensitivity of the gas sensor element 12 mM doped silver solution (1) and control (2) of pairs of voltage ethanol 2000 ppm in the air

The graphs in Fig. 4.8 is determined that the maximum gas sensitivity to $C_2H_5OH$ vapor on undoped sensing element is shown at 4.0 V, on the doped SE - at 0.8 V, which corresponds to a temperature of about 350 $^oC$ and 50 $^oC$. The amount of gas for the sensitivity of doped and undoped SE 3 is almost the same - 3.5 relative units, and a maximum sensitivity of the temperature sensor at the doped 7 times lower.

Fig. 4.9 shows the temperature dependence of gas sensitivity to 3000 ppm ammonia vapors in air for gas sensor, which surface is modified with a solution of 12 mM silver.

It was found that the temperature of maximal gas sensitivity to ammonia vapor control sensor is 400 $^oC$, which corresponds to the 4 on the power supply, while the 200 $^oC$, which corresponds to 2.5 V. The sensor doped with the silver value of the gas sensor sensitivity in doped it is much higher (60 RLU) than that of unalloyed senser (34 RLU).

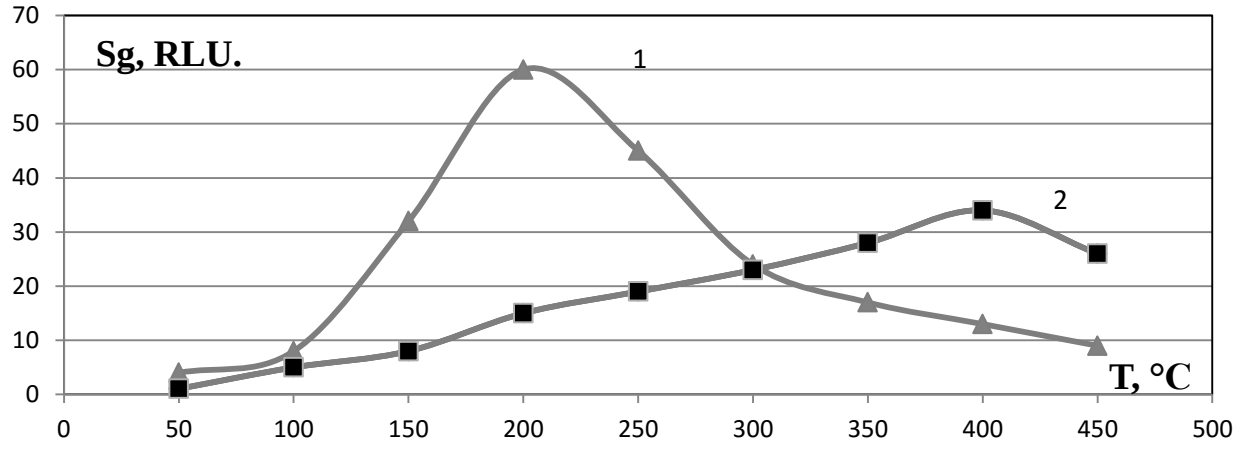


Fig.4.9. The dependence of gas sensitivity on temperature in the 3000 ppm ammonia vapors in the air: 1 - for the sensor SE doped silver solution of 12 mM 2 - undoped SE

Thus, as a result of the research mean that the sensor elements, surface modifying silver temperature is lowered maximum gas sensitivity to ethyl alcohol, isopropyl alcohol and ammonia at 100 and 300 and 200 ° C, respectively, the quantity of gas sensitivity varies slightly [85 ]. However, the ammonia vapor temperature not only reduces the maximum sensitivity of the sensor, but also almost 2-fold increase in the sensitivity of the sensor.

Because of the modification of the surface of $SnO_2$ silver allowed to lower the operating temperature of maximal gas sensitivity, it was decided to study at room temperature [86]. Effect of the surface modification of 6 mM solution of silver salt layer on a touch sensitivity of $SnO_2$ as compared to the unmodified layer was studied at room temperature and ammonia concentration Cs = 3000 ppm in the air.

It follows from the experiment that unalloyed $SnO_2$ film at room temperature has no pronounced peak sensitivity to ammonia. At room temperature, the ammonia process interaction with the surface-modified silver $SnO_2$ film is a lengthy process with a time delay, which is about 10 - 12 minutes, but the saturation process time was 16 minutes at the maximum value of sensitivity to ammonia 35 RLU. The peak in the modified sensor

silver, when the maximum value of the sensitivity and subsequent decline can be attributed to the limited amount of ammonia adsorption sites on the semiconductor surface and its saturation at room temperature.

To determine the possible range of controlled gas concentrations need to study the dependence of the sensitivity of gas sensors modified by the concentration of toxic gas. Figure 4.10 shows the dependence of the sensitivity values (S) of the sensor modified 6 mM solution of silver ($R_{SE2}$) and an undoped control ($R_{SE1}$) sensor elements of the ammonia concentration in the range from 500 to 5000 ppm.

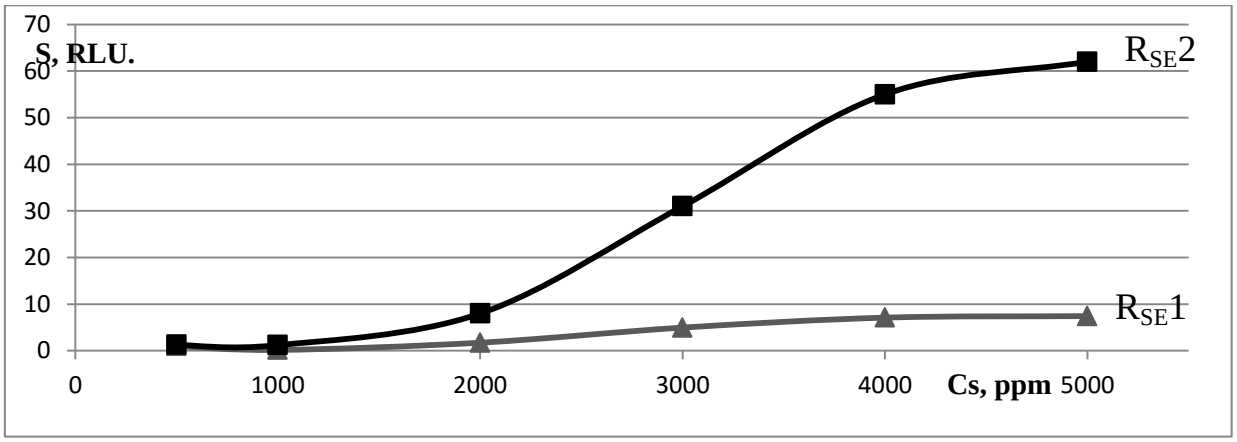


Fig. 4.10. The dependence of gas sensitivity (S) of the concentration of ammonia vapors in air at room temperature for: undoped (control) $R_{SE1}$ sensor; modified sensor 6 mM silver nitrate solution $R_{SE2}$.

Because of the measurements we know (Fig. 4.10) that the sensitivity of the value of the doped element of S2 = 1,29 RLU with ammonia in air concentrations of 500 ppm, while the control element does not exhibit sensitivity in this range. At high concentrations of ammonia (1000 ppm in air) observed time difference of several magnitudes compared with the sensitivity of the two elements. These results allow the development of a new class of sensors with a surface modifying layers sensor operating at room temperature, to control the leakage of ammonia in the areas of its production and storage.

For surface modification of palladium 3mM samples were prepared as 6 mM, 9 mM and 12 mM solutions of $PdCl_2$ + $H_2O$. After the formulation, solutions are placed in a special container, which does not allow the penetration of daylight to avoid photodecomposition solution. 3 mM solution obtained by dissolving 25 mg of palladium chloride in 50 mL of distilled water. The calculation of the required concentration by the formula

$$N = \frac{\vartheta}{V} = \frac{m}{M \cdot V}, \quad (4.1)$$

where m - the mass of salt; M - molar mass; B - amount of $H_2O$.

Для начала рассчитаем молярную массу для вещества $PdCl_2$.

$$M = M(Pd) + 2M(Cl) = 106{,}4 + 71 \left[ {}^{g}/_{mol} \right] \approx 177 \left[ {}^{g}/_{mol} \right] \quad (4.2)$$

Substituting the original data into the formula (4.1), we obtain

$$N = \frac{25\ [mg]}{177 \left[\frac{g}{mol}\right] \cdot 0{,}05\ [l]} = 3 \cdot 10^{-3} \left[\frac{mol}{l}\right] = 3\ mM \quad (4.3)$$

Before applying the impurities on the surface of $SnO_2$ conducted preliminary annealing sensors - on the gas sensor heater voltage was applied to certain crystals to heat up to 450 ° C from the power supply DC Power Supply HY3005. To create favorable conditions for dissolving $PdCl_2$ in a water jar with a solution warmed in a water bath to a temperature of ~ 70 ° C. Topically applying a solution of palladium chloride to the surface of the sensor element under the microscope was carried $SnO_2$ MBS-1 to 56-fold increase. Then, drying was performed in air at room temperature for 30 minutes and then heating the admixture for 1 hour at 380 ° C (= $U_{heat}$ 4V). The second sensor element was left undoped (control) and used for comparative characterization of gas sensitivity. Resistance doped films was measured using multimeters Mastech MY64 series. After brazing impurities in controlling the appearance of a sample under a microscope, it was found that the surface of the sensing

elements covered with a film darkened and palladium salts. In accordance with the appearance of palladium oxide PdO alleged part on the sensor surface:

$$PdCl_2 + H_2O = PdO + 2HCl \quad (4.4)$$

Thus, the method of micro-alloying elements touch sensor of gas impurities and Pd with Ag concentrations of 3 mM - 12 mM has been developed.

Pd salts precipitate solution was analyzed with a scanning electron microscope, and elemental analysis of an area of 500 $mm^2$. On the surface of silicon wafer was coated an aqueous solution of $PdCl_2$ various concentrations and then dried. The precipitate has the form of islands and agglomerates of different sizes - from a few to tens of micrometers. The average density of the islands is 1 micron to 3 concentration of 0.1 mmol, 6 mmol - 0.2 $m^{-2}$, for a concentration of 12 mmol - 2 0.35 microns. Elemental analysis of the surface showed the presence of Pd, Cl and $O_2$ in an amount sufficient to form compounds and $PdCl_2$ PdO, according to the chemical reaction (4.4). Thus, it can be assumed that the precipitate contains the palladium compounds and $PdCl_2$ PdO.

Effect of alloying 3 - 12 mM solution of Pd $SnO_2$ layer on the touch compared to the undoped layer was investigated in the temperature range 25 - 450 ° C to vapors of ethanol with the concentration of Cs = 3000 ppm. Fig. 4.11 shows the results of measurements of gas sensitivity to ethyl alcohol sensor layers $SnO_2$, surface-modified 6 mM Pd.

*(нелег = unalloyed)*

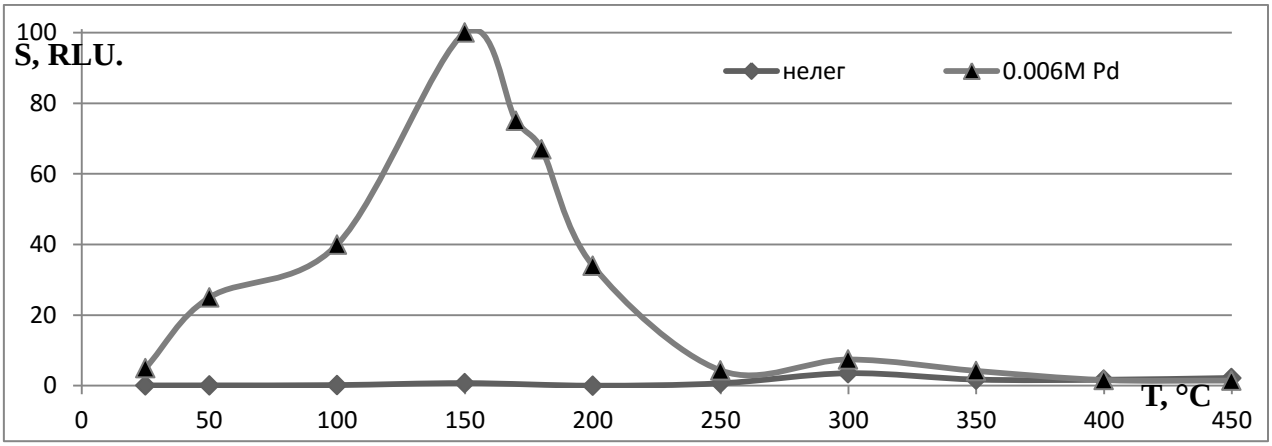


Fig.4.11. Temperature dependence of sensitivity of a gas sensor with a surface modified SE 6 mM palladium and couples to the control sample Cs = ethanol 3000 ppm in the air

We can see in the graph (Fig. 4.11) that samples modified with 6 mM Pd salts have sensitivity to alcohol vapors S = 100 RLU at T = 150 ° C. The concentration of Pd, equal to 6 mmol, as in the case of silver, is optimal for surface modification of films of $SnO_2$. Sensitivity of modified Pd samples to alcohol has increased, as seen in the chart, and, in addition, the operating temperature of the sensor decreased. Unalloyed SE showed the highest sensitivity S = 3,53 RLU to the alcohol at 300 ° C, whereas 6 mM doped, S = 100 RLU at 150 ° C, and S = 8 RLU at 300 ° C. It should be noted that the modified SE sensor begins to react to alcohol vapors already at 100 ° C, while the control at 200 ° C. The table below shows the maximum sensitivity of the values of the corresponding operating temperature for gas sensors for the control samples and modified admixture 6 mM solution of palladium (Table. 4.2).

Table 4.2

The effect of a surface modification by the amount of $SnO_2$ gas sensitivity (S) and the operating temperature ($T_{max}$) pairs alcohol (3000 ppm) in the air.

| | Control | 6 мМ Pd |
|---|---|---|
| S, RLU | 3,53 | 100 / 8 |
| T, °C | 300 | 150 / 300 |

The table 4.2 shows that samples 6 mM which are modified by Pd have a higher gas sensitivity $S_g$, than the control (undoped) sample. It was found that palladium impurity has a significant impact on the increase in sensitivity (30 times) sensor using 6 mM concentration of palladium salt solution for surface modifitsii $SnO_2$.

It is found that as the concentration of palladium maximum temperature sensitivity of the modified gas sensor is continuously decreased from 50 to 300 $^{o}$ C (Fig. 4.12). The magnitude of the maximum sensitivity of the gas changes depending on the concentration of palladium is less clear solution. Initially at 3 mM and 6 mM gas sensitivity compared to the control sample is increased in about 15 - 30 times, respectively, and with 9 mM and 12 mM observed decline in gas sensitivity almost to the original value, which is characteristic for the control sample (Fig. 4.12).

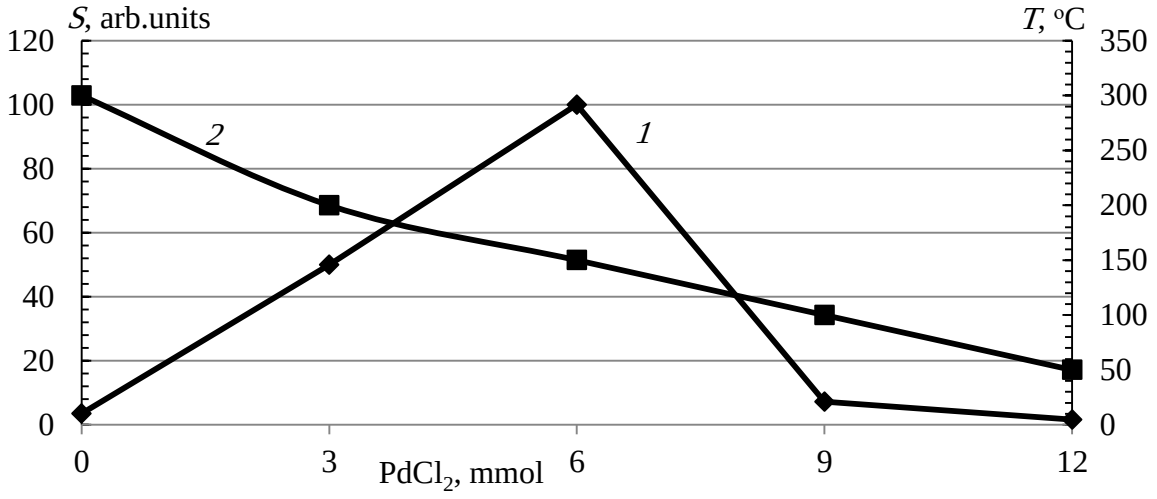


Fig.4.12. The dependence of the valuce (1) of temperature and (2) the maximum sensitivity of the gas sensor to the gas sensitive element pairs ethyl alcohol (3000 ppm) in the air concentrations of palladium in solution

It was also studied the gas sensitivity of gas sensor modified with palladium, to pairs of isopropyl alcohol concentration of 3000 ppm in the air. Results of the study the temperature dependence of the sensitivity of $SnO_2$ film, surface-modified palladium impurity concentration 6 mM to vapors of isopropyl alcohol presented in Figure 4.13. As the figure shows the maximum gas sensitivity control (undoped) sensor is 3 rel. u at 400 ˚C, and surface-modified - 55 RLU at 250 ˚C. Thus, 6 mM solution of palladium impurities on the surface of $SnO_2$ gas reduces the temperature of the maximum sensitivity of more than 100 and increases sensitivity ˚C modified $SnO_2$ film compared to the control sample is almost 20 times (from 3 to 55 RLU).

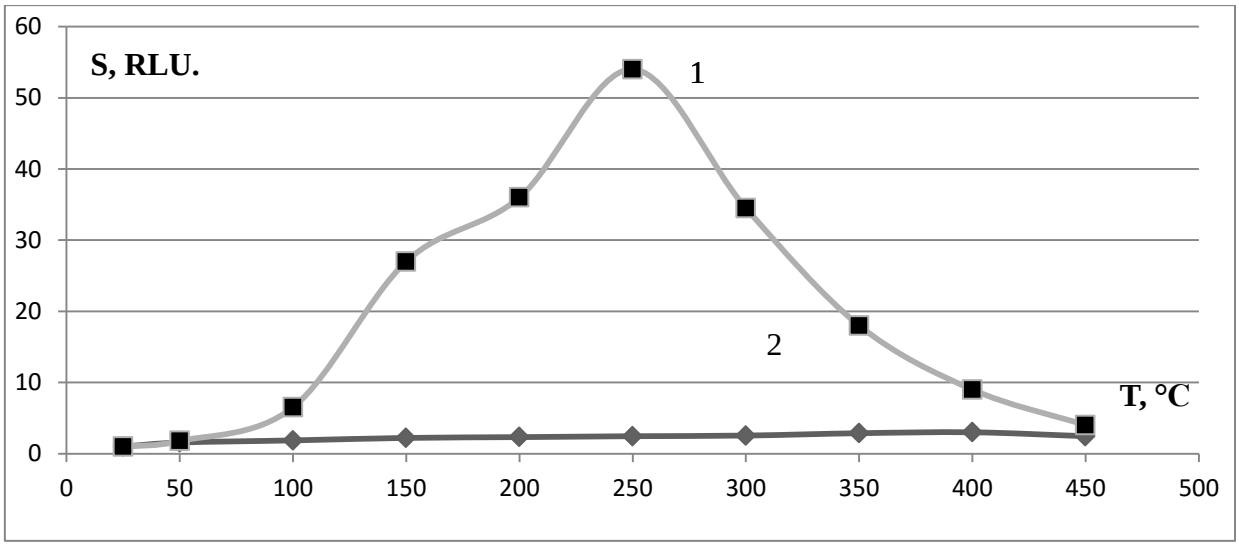


Fig.4.13. The temperature dependence of gas sensitivity of $SnO_2$ film to vapors of isopropyl alcohol 3000 ppm in the air 1 - $SnO_2$, surface modified with palladium impurity concentration 6 mM; 2 - unalloyed film $SnO_2$

We investigated the sensitivity of the gas-gas sensor, a surface-modified 6 mM solution of palladium salt to vapors of acetone concentration of 3000 ppm in air. Fig. 4.14 shows the temperature dependence of gas sensitivity of the gas sensor to the acetone vapors in the air.

It was found that the magnitude of the maximum sensitivity of surface modified element (1) is S = 46 RLU acetone at a concentration equal to the air temperature of 3000 ppm and 250 ˚C. For undoped (control) the sensing element (2) the sensitivity has a value of almost 2 times less: S = 28 RLU at 400 ˚C, 150 ˚C that is greater than in the case of a modified palladium $SnO_2$ sample.

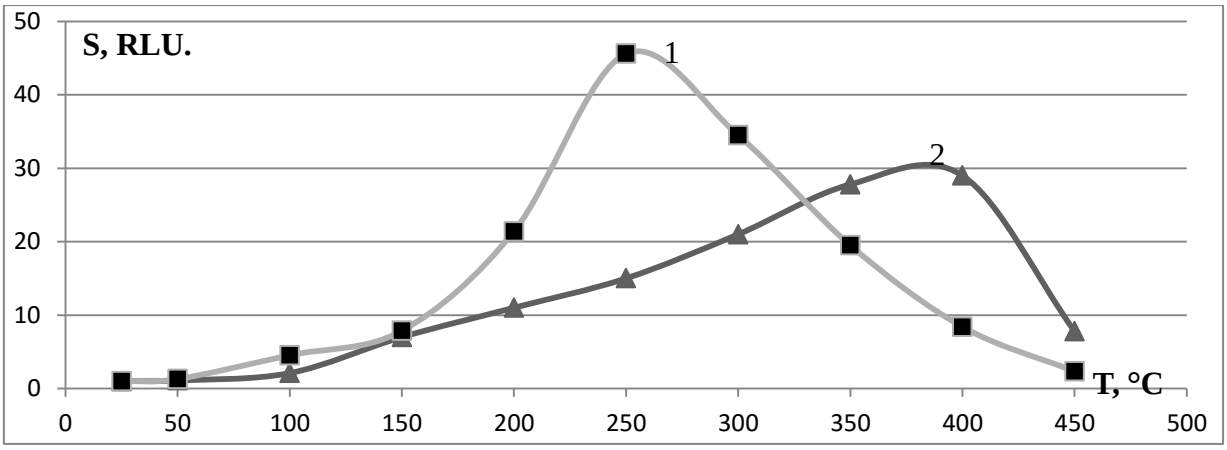


Fig.4.14. The temperature dependence of gas sensitivity of $SnO_2$ film to vapors of acetone Cs = 3000 ppm in air 1 - $SnO_2$ film, surface-modified palladium impurity concentration 6 mM; 2 unalloyed $SnO_2$ film (control).

It was determined by experimental dependence of gas sensitivity on the temperature to 3000 ppm ammonia vapors in air for controlling a gas sensor and 6 mM modified palladium brine sensor. Results of the study are shown in Fig. 4.15. The magnitude of the maximum sensitivity for controlling the gas sensor element (2) is observed at a temperature of 400 ˚C and 34 RLU. The sensitivity of the surface of the modified item (1) is - 45 RLU at 250 ˚C.

Thus, the surface modification of $SnO_2$films of by palladium salt solution with a concentration of 6 mM, resulting in a lower maximum temperature and the sensitivity of the gas to increase the value of the gas response to ammonia vapors in the air.

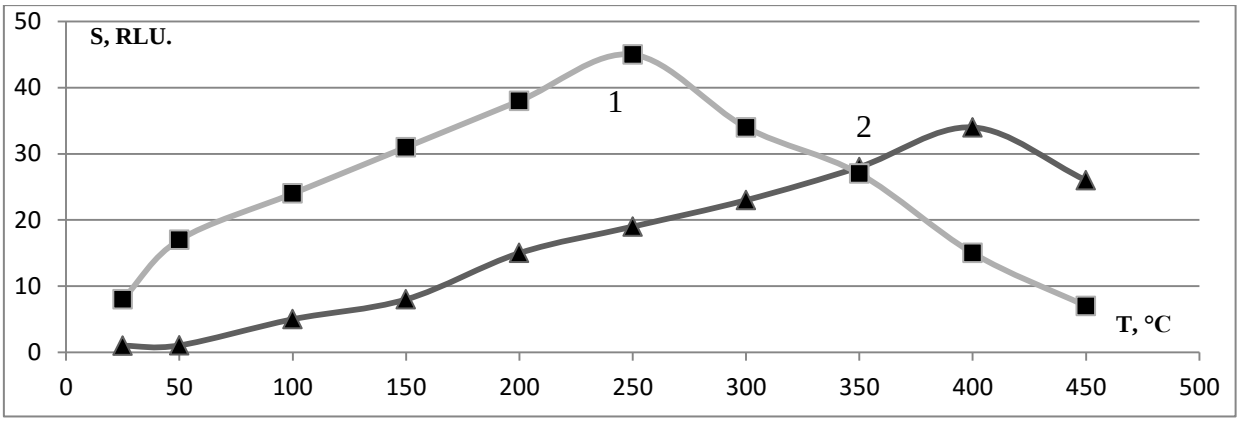


Fig.4.15. The temperature dependence of gas sensitivity of $SnO_2$ film to ammonia vapors Cs = 3000 ppm in the air 1 - $SnO_2$, surface-modified palladium impurity concentration of 6 mM; 2 - unalloyed (control) $SnO_2$ film

As a result of the research the temperature dependence of the sensitivity of the gas sensor $SnO_2$ layers microelectronic gas sensor, surface-modified palladium solution of 6 mM to toxic vapors: ethanol, isopropyl alcohol, acetone and ammonia in the air. It is found that doping of aqueous $PdCl_2$ possible to reduce the operating temperature of 100 - 150 ˚C and improve sensitivity to toxic vapors is approximately 2 timeshas been determined. Below is a summary table of sensitivity to the vapors of various gases and the control of a modified palladium samples.

Table 4.3

The dependence of the maximum gas sensitivity of unalloyed and surface - modified aqueous solution of Pd (6mm) sensing elements of the temperature of gas sensors

| Gas | S, RLU ($S_{unalloyed}/S_{alloyed}$) | $T_{max.work}$ , °C (unalloyed/alloyed) |
|---|---|---|
| Ethanol | 3,5 / 100 | 350 / 150 |
| Isopropanol | 3 / 54 | 400 / 250 |
| Acetone | 29 / 45 | 400 / 250 |
| Ammonia | 34 / 45 | 400 / 250 |

The top of the fractions indicated the sensitivity values (S) of maximum sensitivity and temperature ($T_{max}$) of control samples, and the bottom of the fractions indicated similar surface modified films parameters $SnO_2$.

The catalytic properties of palladium and silver in the bulk and on the surface of metal oxide materials are known and can occur via different mechanisms [84]. In one mechanism of silver and palladium catalysis form a sensor film on the surface of chemisorbed complex with the reducing gas molecules and promote their dissociation. Then the reaction products of the dissociation of the gas molecules react with the oxygen molecules adsorbed on the surface of $SnO_2$, and due to redox reactions and the electron redistribution between the oxygen and gas molecules, the potential barrier height at the surface of the SnO2 is reduced, resulting in increased conductivity sensor. In practice, these processes help to reduce the temperature of oxidation processes on the surface of the $SnO_2$ film and reduce the maximum gas temperature sensitivity. The presence of catalyst on the surface of SnO2 film also contributes to the adsorption of oxygen from air density centers.

Another mechanism for increasing the sensitivity of gas $SnO_2$ films due to the fact that, unlike the n-type $SnO_2$ films oxides PdO $Ag_2O$ and have p-type conductivity [7]. Staying on the surface of $SnO_2$ film in the form of small clusters and agglomerates of the oxides of palladium and silver create clusters around the depletion area due to the fact that the work function of electrons from the oxides of silver and palladium is greater than the work function of $SnO_2$. The presence of the depletion region reduces the "effective" size of the polycrystal grains and $SnO_2$ increases electrical resistance sensor film, which leads to increased sensitivity to its gaseous reductant gases.

As the concentration of the solution increases the proportion of the sensor surface coated catalyst, and the number of adsorption centers induced initially increases and then decreases due to the decrease of the free surface of the film. Therefore, the sensitivity of gas initially increases with increasing concentration of the solution, and then decreases.

### 4.3. The influence of light explosure on a gas response of surface-modified silver-palladium $SnO_2$ films

The resistivity of sensitive elements, surface-modified silver-illuminated LED is not changed, which may be due to the shielding film of semiconductor layer $SnO_2$ $AgNO_3$ salt. Proof of this can serve as a mechanism for the results of the study[76], which shows that the application of an aqueous solution of $AgNO_3$ on the surface of $SnO_2$ lowers the electrical resistance sensing elements and silver salt covers the surface of the sensor with a continuous layer.

When interacting with gas the surface states can be recharge, the same effect can take place with different energy levels. Therefore, the resistance change sensing elements gas sensors was investigated in cooperation with the ammonia vapors (500 - 4000 ppm) in air at room temperature under the action of four kinds of light - violet, blue, green and red light having different photon energies. According to the research it was selected LED with violet radiation as making the most significant contribution to the change in the gas sensitivity (Fig. 4.16).

In the Fig. 4.16 and in the Table. 4.4. dependences of the resistance at room temperature controlling gas sensitivity (S1) the sensor by the concentration of ammonia in the air without the exposure (1) and under the action of purple (2), and blue (3) radiation are given.

Table 4.4

The impact of energy of light quanta of optical radiation of different color LEDs on the gas response of undoped $SnO_2$ films.

| Cs , ppm | $S_1$,RLU | | |
|---|---|---|---|
| | Without light | UV LED | Blue LED |
| 500 | 1 | 1.2 | 1 |
| 1000 | 1.2 | 1.3 | 1 |
| 2000 | 2 | 12 | 2.8 |
| 3000 | 6 | 35 | 3.01 |
| 4000 | 7.4 | 38 | 5.01 |

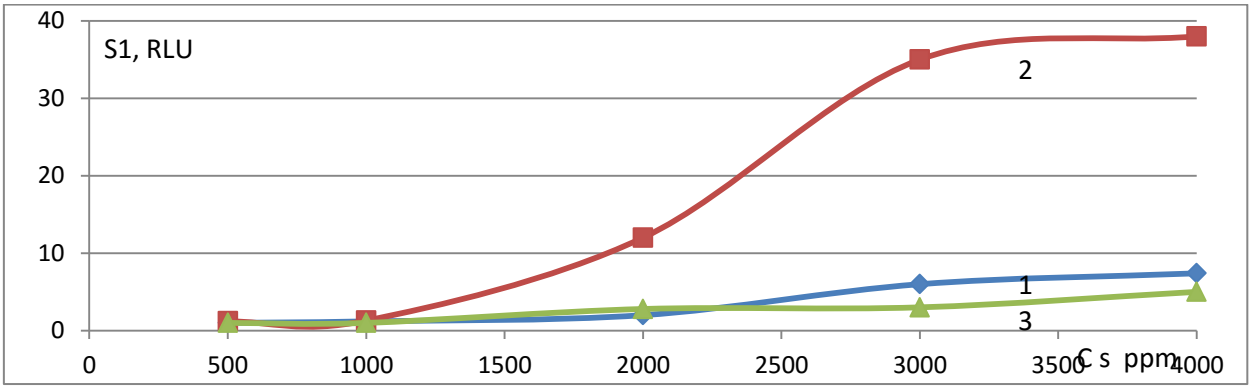


Fig.4.16. The dependence of the gas control response (S1) of the sensor element to various concentrations of ammonia vapor at room temperature without illumination (1) and violet light (2) and blue (3) light.

Exposure to the gas violet LED feedback control samples is noticeable at ammonia concentrations exceeding 2000 ppm in air. In this case the sensitivity of the gas samples illuminated by almost 4 times higher than the control sensitivity of the sensor element without lighting $SnO_2$. When ammonia in air concentrations of 3000 ppm and 4000 ppm response gas sensor element when illuminated with violet light is increased by 5-6 times. This result shows the effectiveness of increasing the sensitivity of the gas to pairs of $SnO_2$ films of ammonia in their light violet LED light quanta energy is comparable with a band gap gazosensornoy $SnO_2$ film (about 3 eV). The energy of light quanta of other used LEDs (green and red) is not greater than the band

gap studied $SnO_2$ films and their impact on surface modified sensors does not have a noticeable effect.

Fig. 4.16 also shows that the influence of the blue LED light on the gas sensor response is within the accuracy of measurements of the gas response (± 10%). The effect of light green and red LEDs on the sensor samples were found.

The Fig 4.17 and the Table. 4.5. shows the dependence of gas sensitivity change of surfactant - modified with silver (S2) sensing element (3) of different concentrations of ammonia in the air, without light exposure for the control sample (1) and under the action of violet light (2) at room temperature.

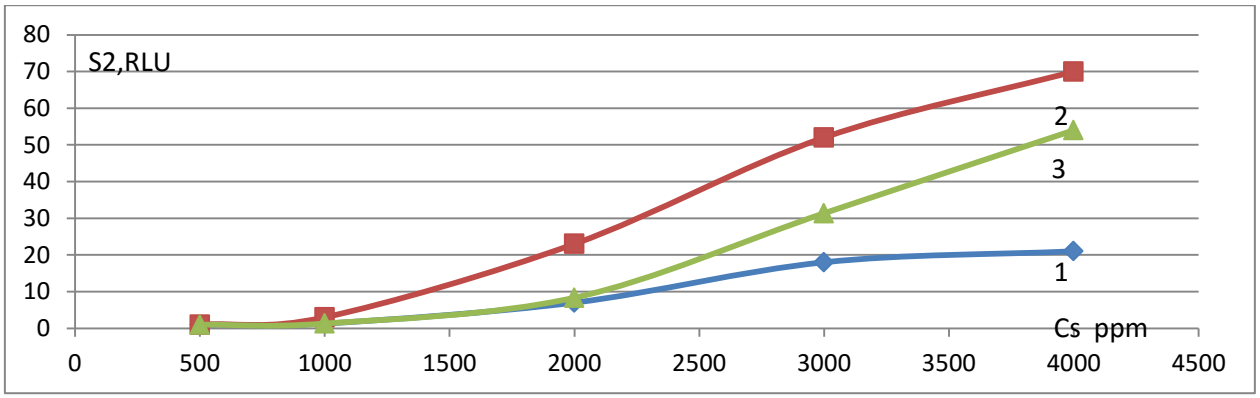


Fig.4.17. The dependence of the sensitivity of the gas sensor element of the concentration of ammonia vapors in air at a temperature of 21 ˚C: (1) - control sample; 2 - under the influence of purple (2) LED radiation surface-modified silver (6 mM); 3 - surface-modified with silver (6 mmol)

Table 4.5

The impact of the energy of light quanta of optical radiation of different color LEDs on the gas response of $SnO_2$ films, surface-modified with a solution of 6 mM $AgNO_3$.

| Cs, ppm | $S_2$,RLU | | |
|---|---|---|---|
| | Control | Alloyed + UV | Alloyed, without any light |
| 1000 | 1,3 | 3 | 1,3 |
| 2000 | 7 | 23 | 8.3 |
| 3000 | 18 | 52 | 31.4 |
| 4000 | 21 | 70 | 54 |

Changing of the resistance of the sensor element, a surface-modified silver ($S_{alloyed}$), ammonia vapor in the air (500 ppm) was 20%, while the resistance of the undoped control sensor ($S_{control}$) does not change. When considering the curves (1), (3) shows the difference in sensitivity between the control sample and doped in the concentration range of ammonia vapor from 1000 to 4000 ppm. For comparison, a control sample reading sensitivity in this range $S_{control}$ = 1.2 (1000 ppm) - 7,4 (4000 ppm) RLU, whereas for the sample doped with Ag, $S_{alloyed}$ = 1.3 (1000 ppm) - 54 (4000 ppm) RLU, indicating a significant contribution modification noble metal surfaces of metal oxides at high concentrations of gas.

By comparing the curves (2), (1) a clear increase is significant and the sensitivity of the sensor element under the influence of the purple LED light. Thus, the value of the control (undoped) Sample sensitivity ammonia concentration in the range of 1000 - 4000 ppm by irradiating violet LED varies $S_{control}$ = 1.3 - 21 RLU (. Figure 4.16), whereas for the sample doped with silver by irradiating violet LED $S_{alloyed}$ = 3 - 70 RLU (Fig. 4.17).

It can be the result of the activation of the optical surface states under the action of light purple in their interaction with the gas, and a blue light almost does not change

the magnitude of the response of the gas and the doped film unalloyed $SnO_2$ gas sensors.

Thus, significant differences of gas sensitivity magnitude values depending on the measurement conditions and the objects observed in the concentration range from 1000 to 4000 ppm. In this case, light can affect not only the surface condition of $SnO_2$ film itself, but also on the adsorbed thereon, and the clusters of silver atoms, as well as ammonia molecules interacting with them. Therefore, we can conclude that the effect of light purple LED increases sensitivity gas sensors of $SnO_2$ film structures, surface-modified silver-ammonia at room temperature and also stimulates sensitivity undoped $SnO_2$ films.

In the section 3.2 it was found that the film surface modified by Ag at room temperature and lighting without water vapor at a concentration of 1000 ppm in the air gas feedback gives S = 1.6 RLU, and at 10,000 ppm S = 6 RLU It was therefore of interest to study the influence of the purple LED light on the response of the gas to water vapor, surface-modified silver $SnO_2$ films.

The results of the influence of the purple LED light at a distance of 2 mm from the sensor response to the gas surface - modified salts $AgNO_3$ $SnO_2$ films to action water vapor in the air are shown in Fig. 4.18 - 4.20.

*(MOM = MOHM)*

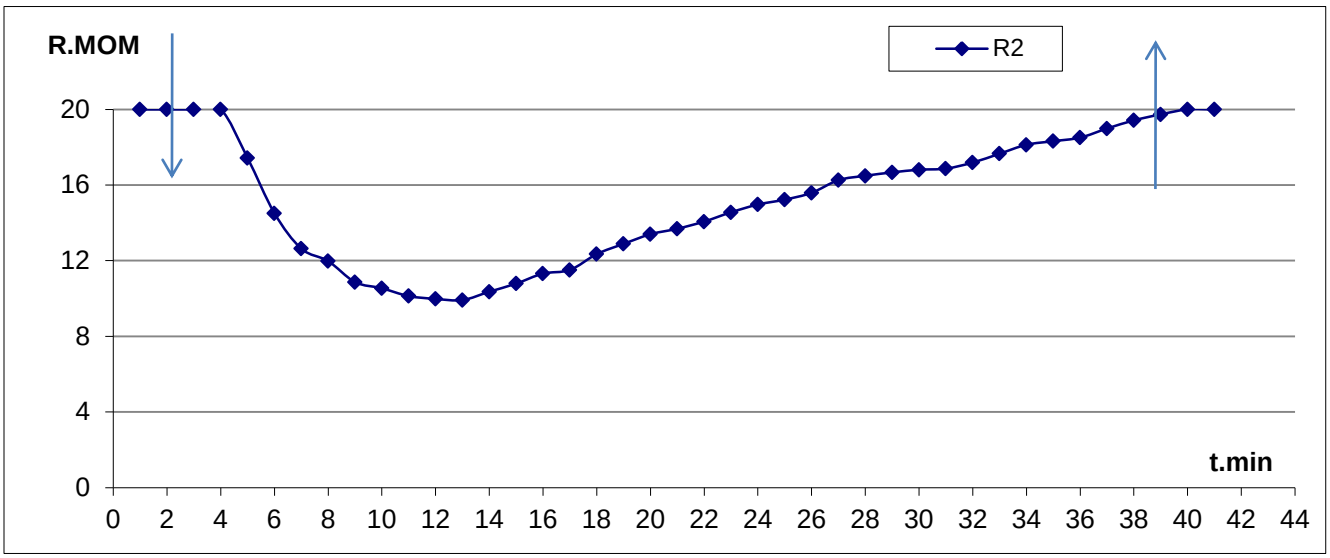


Fig.4.18. Gas response of a surface - modified with silver (12 mM) of $SnO_2$ films to water vapor (3000 ppm) when illuminated purple LED located at a distance of 2 mm from the surface of the film.

*(MOM = MOHM)*

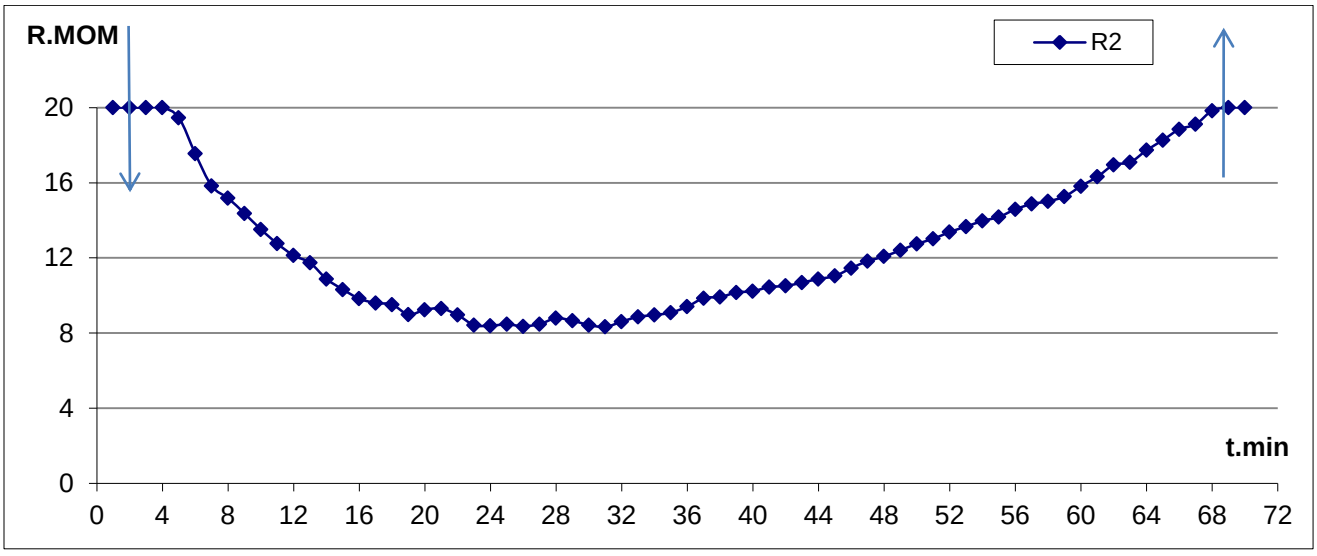


Fig.4.19. Gas response surface - modified with silver (12 mM) of $SnO_2$ films to water vapor (5000 ppm) when illuminated purple LED, located at a distance of 2 mm from the surface of the film.

*(МОм = MOhm)*

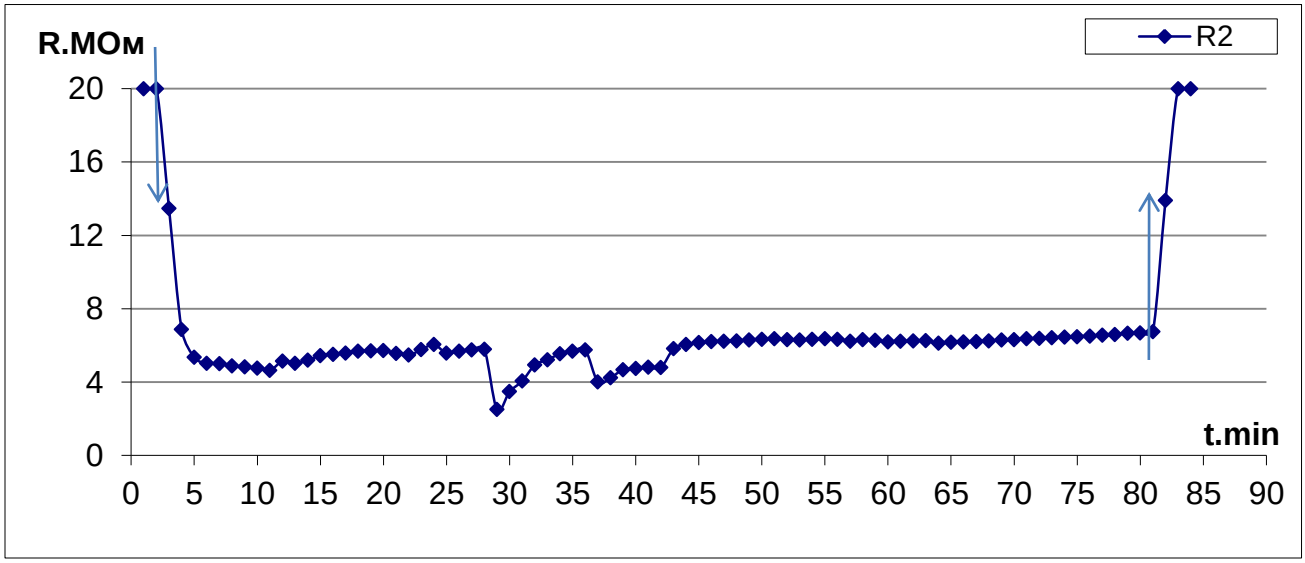


Fig.4.20. Gas response of the surface - modified with silver (12 mM) of $SnO_2$ films to water vapor (10,000 ppm) when illuminated purple LED located at a distance of 2 mm.

Table 4.6

Gas response of the surface-modified silver $SnO_2$ film to water vapor at room temperature and a violet LED illumination

| Cs = ppm | $AgNO_3$ + UV | $AgNO_3$ | Without any light – control |
|---|---|---|---|
| 3000 | 2.0 | 1.7 | 1.7 |
| 5000 | 2.4 | 2.1 | 2.7 |

Experimental results (Table. 4.6) which show that the gas of response silver modified $SnO_2$ film to water vapor at room temperature and a violet LED illumination hardly increases. Thus, the effect violet LED light does not stimulate the processes of interaction of the surface states of $SnO_2$ film with hydroxyl groups OH and does not affect the response of the gas sensor.

We studied the effect of the simultaneous effects of light and surface modification of films $SnO_2$ palladium salts. Figure 4.21 shows the 4.22 Pd salts influence on gas sensitivity of $SnO_2$ films to ethanol vapor. Completed our studying have shown that surface modification of films $SnO_2$ palladium salts leads to an increase in gas sensor response to the gas-reducing agent and a marked reduction in the temperature of maximum sensitivity gas sensors. The same effect causes the impact on the purple LEDs $SnO_2$-sensor gas sensor element is not subjected to surface modification.

*($S_{ЧЭ1} = S_{SE1}$, $S_{ЧЭ2} = S_{SE2}$, $U_H$, $B = U_H$, $V$)*

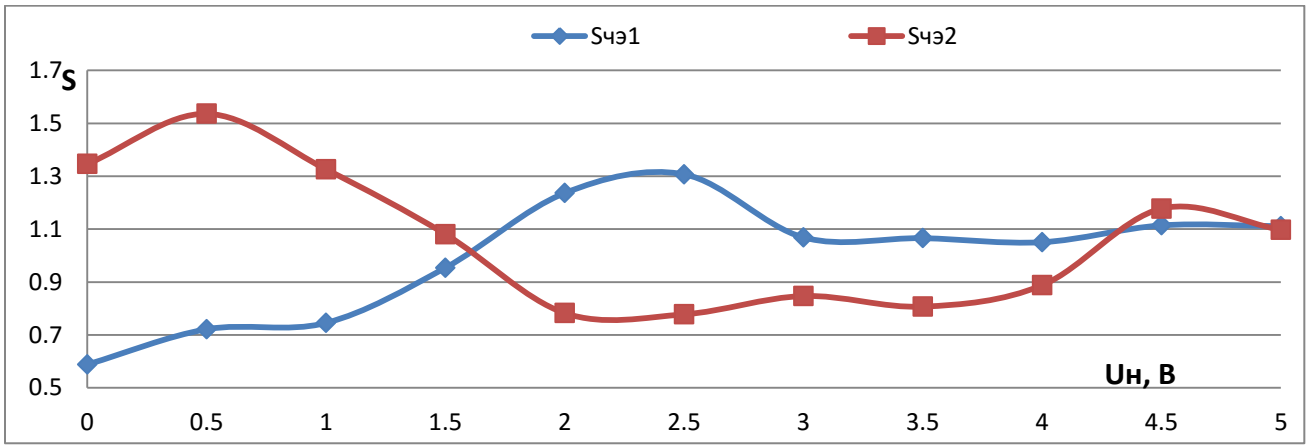


Fig.4.21. The dependence of gas sensitivity of $SnO_2$ film to vapors of ethyl alcohol (2080 ppm) in air of the voltage applied to the heater 1 - unalloyed $SnO_2$; 2 - $SnO_2$, doped palladium 3 mM

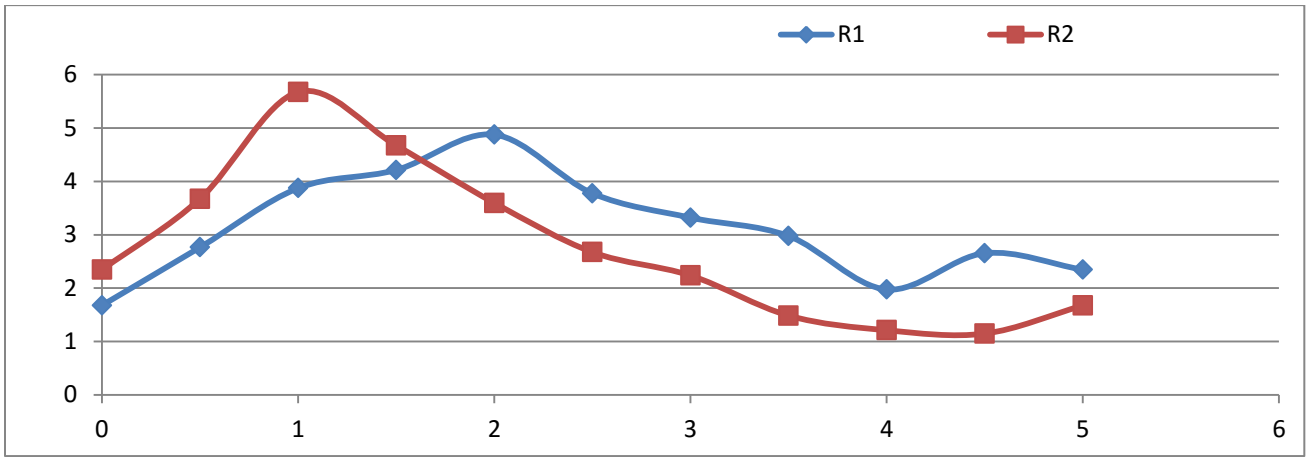


Fig.4.22. The dependence of gas sensitivity of $SnO_2$ film to vapors of ethyl alcohol (2080 ppm) in the air of the voltage applied to the heater 1 - unalloyed $SnO_2$; 2 - $SnO_2$, doped palladium 6 mM

A study of simultaneous effects of the surface modification of $SnO_2$film using salts of palladium and violet LEDs were carried out in a wide temperature range (Fig. 4.23, 4.24).

As it was state earlier, surface modification of $SnO_2$films doped palladium has led to an increase in gas response and to reduce the maximum temperature of the gas sensor sensitivity to a value of about 50 - 100 ° C. The effect of light exposure in the case of palladium impurities manifested significantly less than in the case of silver, and the impurity effect of light on the control samples (2 - 6 times) was significantly stronger than the surface-modified (1.5 - 3 times) structure. The reason for this can be more efficient shielding $SnO_2$film by palladium salts, silver salts than shielding.

($S_{ЧЭ1} = S_{SE1}$, $S_{ЧЭ2} = S_{SE2}$, $U_H$, $B = U_H$, $V$)

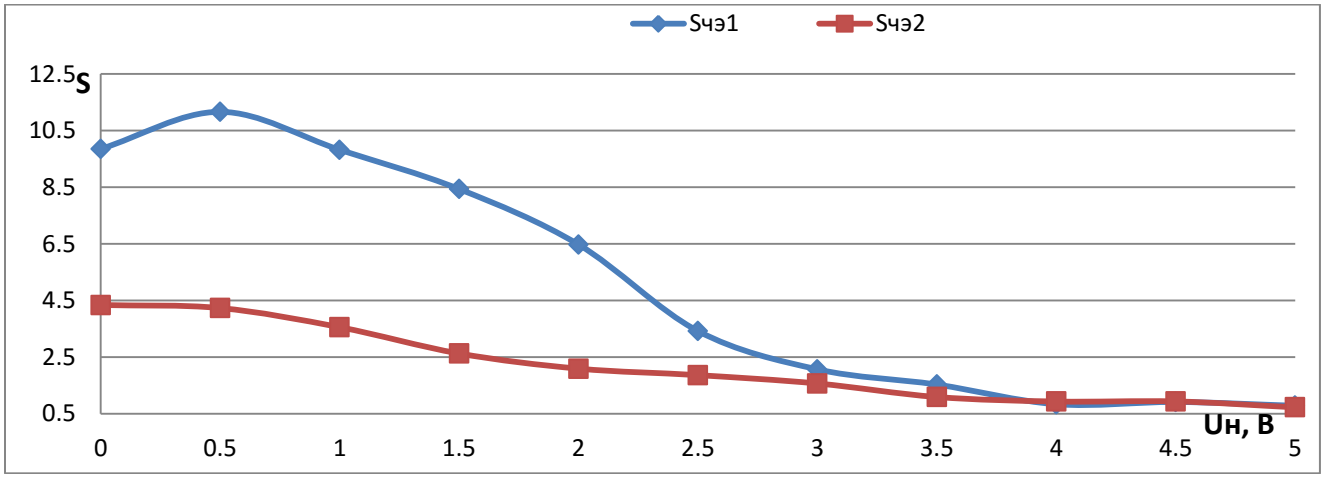


Fig.4.23. The dependence of gas sensitivity of $SnO_2$ film to vapors of ethyl alcohol (2080 ppm) in the air with light from the purple LED voltage applied to the heater 1 - unalloyed $SnO_2$; 2 - $SnO_2$, doped palladium 3 mM

($S_{ЧЭ1} = S_{SE1}$, $S_{ЧЭ2} = S_{SE2}$, $U_H$, $B = U_H$, $V$)

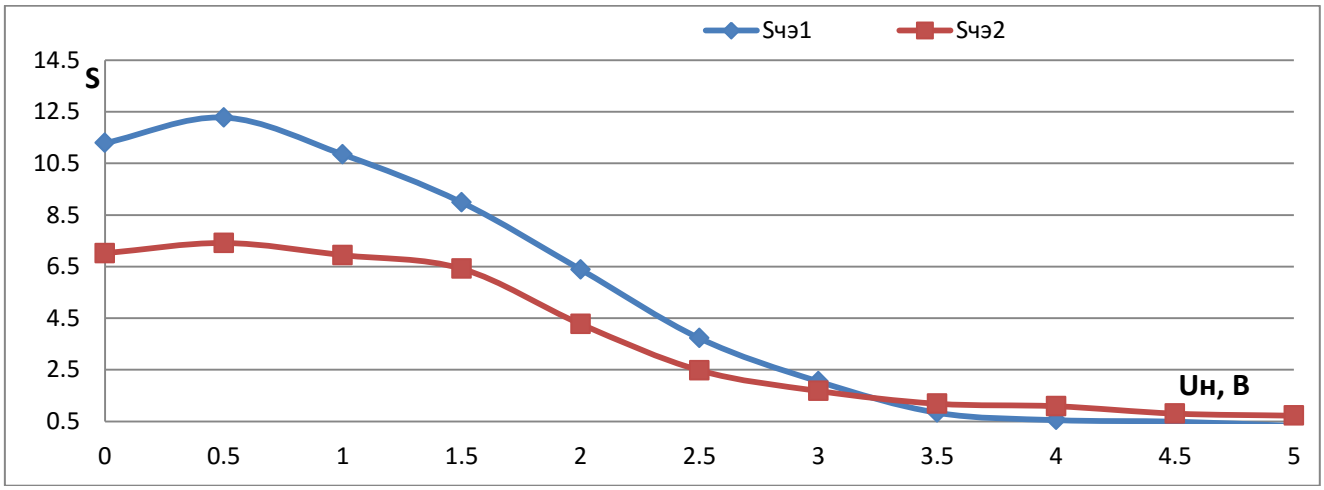


Fig.4.24. The dependence of gas sensitivity of $SnO_2$ film to vapors of ethyl alcohol (2080 ppm) in the air with light from the purple LED voltage applied to the heater 1 - unalloyed $SnO_2$; 2 - $SnO_2$, doped palladium 6 mM

**Conclusions of the 4th chapter.**

1. The optical exposure of purple LED of $SnO_2$ film on the surface during the interaction with the reducing-gases (ethyl alcohol, isopropyl alcohol, acetone) leads to an increase of the gas near the response of the main peak of the gas or its sensitivity to shear alcohols at 10 - 40 ° C to low temperatures. Moreover, a second peak of the response of gas is at 130 - 260 ° C, which can also be used to control the content of this gas in the air.
2. The surface modification of $SnO_2$ films with silver salts (6 - 12 mM) results in a shift of the main peak sensitivity of the gas to alcohols $SnO_2$ film at low temperatures 100 - 300 ° C, and the gas quantity or the response does not change or increases approximately 1, 5 times. In the reaction with ammonia vapors in the air-gas feedback the modified surface of silver salts (12 mM) $SnO_2$ film increased by almost a factor of 2 and a maximum sensitivity of the gas temperature is reduced from 400 to 200 ° C.
3. The use of silver ions (6 mM) for the surface modification of $SnO_2$ films leads to a significant (approximately 7-fold) increase in response to gas vapors of ammonia at room temperature and shear sensitivity threshold from 2000 ppm to 500 ppm.
4. Application of palladium ions (6 mM) for the surface modification of $SnO_2$ film leads to an increase of gas to alcohols response in almost 20 times and reduced sensitivity maximum temperature of 150 - 200 ° C. In the case of acetone and ammonia gas vapors response value is almost unchanged, and the operating temperature of the sensor is reduced to about 150 ° C.
5. At room temperature the influence of to violet light on the surface modified with silver (6 mM) $SnO_2$ film leads to a manifold increase in response to the gas in the ammonia vapors modified and the control samples. Effect of optical feedback to stimulate the gas to water vapor was observed.

6. At elevated temperatures (200 - 400 ° C) the effect of violet light on the surface modified $SnO_2$ film is less pronounced than the surface reference samples (pure $SnO_2$ film). Probably, this is manifested in the shielding effect of the film surface $SnO_2$ layer of silver or palladium salts.

## MAIN RESULTS

1. It is found that as a result of exposure to light of low-power LEDs with energies of 2.36 eV (green) to 3.05 eV (purple) electrical resistance of the sensor element based on $SnO_2$ + 1% Si, at the expense of reduced optical generation of intrinsic and extrinsic non-equilibrium charges carriers. A scheme for the possible optical transitions in the film $SnO_2$ + 1% Si, under the influence of LED light, which occurs as a result of recombination of non-equilibrium charge carriers with deep traps.
2. Optical effects of violet LEDs on $SnO_2$ + 1% of the film surface Si, in interaction with the reducing gases (ethyl alcohol, isopropyl alcohol, acetone) leads to an increase in gas sensitivity near the main sensitivity peak (300 ÷ 400 ° C), by reducing the height grain potential barriers, while there is a second peak of the response of the gas at 130 - 260 ° C, due to the interaction of light with the impurity of surface and bulk states. The impact of green light is characterized by the appearance of only an additional low-temperature peak of the gas sensitivity.
3. Under the influence of water vapor on the electrical sensor layer $SnO_2$ + 1% Si, at room temperature there is a marked decrease in resistance of the sensor at concentrations exceeding 3000 ppm, which corresponds to 74% relative humidity. At room temperature the gas sensitivity films $SnO_2$ + 1% Si, to the vapors of aqueous ammonia ($NH_4OH$), which is distinctly observed at a concentration of 1000 ppm of ammonia and above. This result indicates the possibility of using gases at room temperature sensor for monitoring of high ammonia concentration in the air.
4. The surface modification of $SnO_2$ film + 1% Si, with silver salts (with concentrations of from 6 to 12 mM) results in a shift of the main gas sensitivity of peak film $SnO_2$ + 1% Si, to alcohols in the low temperature region at 100 - 300 ° C, and the quantity of gas response either unchanged or increases by

approximately 1.5 times. In the reaction with the ammonia vapors in the air gas response is surface modified with silver salts (12 mM) $SnO_2$ + 1% Si film increases by almost a factor of 2, and the maximum temperature of the gas decreases the sensitivity is from 400 to 200 ° C.

Application of palladium ions (6 mM) for the surface modification of $SnO_2$ film leads to the increase of gas to alcohols response by almost 20 times and reduced temperature sensitivity maximum at 150 - 200 ° C. The model of the effect of the catalyst on the gas sensitivity of $SnO_2$ films was studied.

5. At room temperature the exposure of violet light on surface modified with silver (6 mM) $SnO_2$ film leads to a manifold increase in response to the gas in the ammonia vapors modified and control samples.

REFERENCES


1. Myasnikov I. A. Semiconductor sensors in the physical and chemical research/ I. A. Myasnikov, V. A. Sukharev, L. Y. Kupriyanov, S. A. Zavyalov. M .: Nauka, 1991. 327 p.
2. Kiselev V. F. Surface phenomena in semiconductors and dielectrics. M .: Nauka, 1970. 399 p.
3. Vigleb G. Sensors: the device and the use of it / G.Vigleb. Moscow: Mir, 1989. 196 p.
4. Samsonov G. V. Physical and chemical properties of the oxides. Handbook / Samsonov G.V., etc. M.:. Metallurgia, 1969. 456 p.
5. Hutson A.R. Semiconductors / .A.R.Hatson. M .: Inostrannaya Literatura, 1962. 497 p.
6. Rekas M., Szklarski Z. Defect chemistry of antimony doped $SnO_2$ thin films // Bull. Polish Academy Sci. Chem.–1996.–Vol.44.–№ 3.–P.155–177.
7. Lazarev V. B. The chemical and physical properties of simple metal oxides / Lazarev, VV Sobolev V.B., Shaplygin I.S. M .: Nauka, 1983. 239 p.
8. Popova L.I., Michailov M.G., Georguiev V.K. Structure and morphology of thin $SnO_2$ films // Thin Solid Films.– 1990.– Vol.186.– P.107 – 112.
9. Onyiat A.I., Okeket C.B. Fabrication and characterisation of tin oxide $SnO_2$ thin films using simple glass spray systems // Appl. Phys.– 1989.– Vol.22.– P.1515 – 1517.
10. Grinevich V.S., Serdyuk V.V., Smyntyna V.A. Filevskaya, L.N. Physico-chemical mechanism of formation of the gas sensor parameters on the base of oxide materials // Journal of Analytical Chemistry.- 1990- Vol 45.-№8.- S.1521 - 1525.
11. Robertson I. Defect levels of $SnO_2$ // Phis. Rev.– 1984.– Vol. B.–№ 30. – P. 3520 - 3522.

12. Barsan N. Conduction model in gas-sensing $SnO_2$ layers: grain-size effects and ambient atmosphere influence // Sensor and Actuators.–1994.– Vol. B.- № 17.-P. 241 - 246.
13. Gutierrez J., Ares L., Robla J.I., Getino J., Horrillo M.C., Sayago I., Agapito J.A. Hall coefficient measurement for $SnO_2$ doped sensor, as function of temperature and atmosphere // Sensor and Actuators.–1993.–Vol. B.- № 15–16.– P.98 – 104
14. Pankratov E.M. / Technology of semiconductor layers of tin dioxide. / Pankratov E.M.,.Ryumin V.P, Shchelkin N.P., M .: Energia. 1969. 56 p.
15. Talanchuk P.M., Kirichek T.Y. Weekend informative parameters of semiconductor sensing elements // Dielectrics and semiconductors.--№35.- 1989. P.93 - 100.
16. Maksimovich N.P., Dyshel D.E., Eremina L.E. Semiconductor sensors for controlling the composition of gaseous media // Journal of Analytical Chemistry - 1990.- T.45.-№7.- S.1312-1316.
17. Gopel W., Schierbaum K.D. $SnO_2$ sensor: current status and future prospects // Sensor and Actuators. – 1995. – Vol. B, 26 -27. – P.1 – 12.
18. Goyat D., Agashe C., Marathe B. et al. Effect of dopant incorporation on structural and electrical properties of sprayed $SnO_2$:Sb films // J. Appl. Phys.– 1993.– Vol.73.–№ 11. – P.7520 – 7523.
19. Beensh-Marchwicka G., Krol-Stepniewska L., Misiuk A. Influence of annealing on the phase composition, transmission and resistivity of $SnO_2$ thin films // Thin Solid Films.–1984.– Vol.113.– P.215 – 224.
20. Ivashchenko A. I., Khoroshun I.V., Kiosse G. A., Maronchuk I. Y., Popushoi V. V. Nature of the changes of the physical properties of polycrystalline thin $SnO_2$films, caused by heat treatment // Kristallografiya.-1997-T.42.- №5.-P.901-905.

21. Voschilova R. M., Dimitrov D. P., Dolotov N. I., Kuzmin A. R., Mahin A. V. Moshnikov V.A. Tairov Y. M. Formation of the structure of gas-sensitive layer of tin dioxide, obtained by magnetron sputtering // Physics and Technology of Semiconductors.-1995-T.29.- №11.-P.1987-1993.
22.. Mayssel. L. Technology of thin films: Handbook: In 2 toms / Ed.. Mayssela L., Glenga R.. M .: Sov. radio, 1977. - T.1. – 390 p.
23. Zemel J.N. Theoretical description of gas - film interaction on $SnO_x$ // Thin Solid Films. – 1988.– Vol.163.– P. 189 – 202
24. Stoev I., Khol D. An integrated gas sensor on silicon substrate with sensitive layer of $SnO_X$ // ISPPME 6th International School on Physical Problems in Microelectronics – 1989.– P.482 – 489.
25. Astafieva L. A., Furriers G. P. An apparatus for manufacturing a tin dioxide films // PTE.-1980.- №5.- P.235 - 237.
26. Kissin V. V., Voroshilov S. A., Sysoev V. V., Simakov V. V. Modelling of the process of low-temperature producing of gas-sensitive film of tin oxide / Journal of Technical Physics, 1999. Vol.69., №4. – P.112-113.
27. Mayssela L. Technology of thin films: Handbook: In 2 toms / Ed.. Mayssela L., Glenga R. M .: Sov. Radio, 1977-V.2. 768 p.
28. Maklakov S. A., Jabotinsky V. A., Ivanovo G. F., Kuzkin V. I., Sleptcov V.V. Getting of silica films by the RF of magnetron sputtering // International electronic engineering, 1982.-№2 (321) .- 100 p.
29. Minaychev V. E. The application of films in vacuum. / Technology of semiconductor devices and microelectronic products. In 10 toms .: Textbook. T.6. M .: "Vysshaya Shkola", 1989.-110 p.
30. Labunov V.A., Danilovich N. I., Vinegar A. S., Minaychev V.E. Modern magnetron spraying devices. / Foreign electronic techniques, 1982. №10 (256) .- -100 p.

31. Korchagin B. V., Orlov V. I. Application of metals and their compounds by magnetron and diode sputtering. // Reviews of electronic engineering, 1986.- Vol. 7. № 15 (1222) .- 42 p.
32. Minaychev V. E., Odinokov V. V. Tyufaeva G.P. Magnetron sputtering devices (magratrons). // Reviews of Electronic Engineering, 1979, 1979. Vol. 7.- № 8 (659)..-56 p.
33. Ivanov R. D. The cathode method of creating of film elements of chips. Ivanov R. D. M .: "Energia", 1972. 112 p.
34. Nikonenko V. A. Mathematical modeling of technological processes: Modeling in MathCAD environment. Workshop / Ed. Kuznetsova G.D. M: MISiS, 2001. 48 p.
35. Serrini P., Briois V., Horillo M.C., Traverse A., Manes L. Chemical composition and crystalline structure of $SnO_2$ thin films used as gas sensors // Thin Solid Films, 1997.-V.304- P.113-122.
36. Wolkenstein F. F. Electronic processes on the surface of the semiconductor during chemisorptions // M .: Nauka, 1987. - 432 p.
37. Wolkenstein F. F. Physics and chemistry of semiconductor surfaces // M .: Nauka, 1973. - 400 p.
38. Gutman E. E. The influence of adsorption of free atoms and radicals on the electrical properties of semi conducting metal oxides // Journal of Physical Chemistry, 1984. - Vol. LVIII. – № 4. - P. 801 - 821.
39. Ihokura H. $SnO_2$ - based inflammable gas sensor // Ph. D. Thesis,1983.–P.52–57.
40. Ayvazov A. A. Modern state and prospects of production of thick-film sensors / Ayvazov A. A., Timoshenko V. I., Kuzin A. S. // International electronic equipment 1991 - № 7. – pp. 36 - 47.
41. Xu C., Tamaki J., Miura N., Yamazoe N. Grain size effects on gas sensitivity of porous $SnO_2$ - based elements // Sensor and Actuators, 1991. -Vol. B.- № 3.- P.147 - 155.

42. Ippommatsu M., Ohnishi H., Saski H., Matsumoto T. Study on the sensing mechanism of tin oxide flammable gas ensor using the Hall effect // J. Appl. Phys., 1991. – Vol. 69 (12). – № 15. – P.8368 – 8374
43. Mitsudo H. Gas sensors // Ceramic., 1980.–№ 15.–P. 339 – 345.
44. Xu C., Tamaki J., Miura N., Yamazoe N. Relationship between gas sensitivity and microstructure of porous $SnO_2$ // J. Electrochem. Soc., 1990.– Vol.58.– № 12.– P
45. Loshkarev V. E. The kinetics of photoconductivity of semiconductors / Lashkarev V. E. // JETP, 1949.- №19. P. 876.
46. Lashkarev V. E. Some features of the photoconductivity of single CdS crystals / Lashkarev V. E., Fedorus G. A. // Math. USSR Academy of Sciences. Ser. of Phys. 1952. №16. P. 81.
47. José V. P. The photoconductivity of copper oxide / José V. P., Rivkin S. M. // DAN SSSR 1949. №68. P. 673.
48. José V. P. The photoconductivity of copper oxide / José V. P., Rivkin S. M. // Math. USSR Academy of Sciences. Ser. of Phys. 1952. №16. P. 93.
49. Rivkin S. M. Photoelectric phenomena in semiconductors / Rivkin S.M. M .: State Publishing House of Physical and mathematical literature, 1963. 496 p.
50. Rivkin S. M. To the question of relaxation of nonequilibrium conductivity in the recombination through traps / Rivkin S. M., Strokan I. B. // DAN SSSR. 1959. №124. P. 1039.
51. Kalashnikov S. G. The recombination of electron and traps in the presence of different types of holes / Kalashnikov S. G. // Journal of Technical Physics. 1956. №26. P. 241.
52. Adirovich E. I. The characteristic time of electron processes in semiconductors / Adirovich E. I., Guro G.M. // DAN SSSR. 1956. № 108 P. 417.

53. Iglitsin M. I. The lifetime of non-equilibrium charge carriers in germanium at arbitrary levels of injection / Iglitsin M. I., Konzevoy Y. A., Sidorov A. I.// Journal of Technical Physics. 1957. № 27. P. 2461.
54. Clarke D. The lifetime in semiconductors as a function of the density of recombination states / D. Clarke // J. Electr. a. Control. 1957. V. 3. P. 375.
55. Pankow J. Optical processes in semiconductors / J. Pankow. M .: Mir, 1973. -456 p.
56. A. Kobayashi, S. Kawaji // Journ. Phys. Soc. 1955. Vol. 10.- P. 270.
57. R.H. Bube // Journ. Chem. Phys., 1957. Vol. 27.- P. 496
58. S.R. Morrison // Journ. Phys. Chem. ,1953.- Vol. 57.-P. 860.
59. Wolkenstein F. F., Karpenko M. V. // Journ. Appl. Phys., 1962. -Vol. 33.- P. 460.
60. G. Brincourt, S. Martinuzzi // Compt. Rend. 1968. Vol. 266. P. 1283.
61. Shapira Y. Relationship between photodesorption and surface conductivity in ZnO / Y. Shapira, R.B. McQuistan, D. Lichtman // Physical Review B., 1977.- Vol. 15.- No. 4.- P. 2163 - 2169.
62. Camagni P. Photosensitivity activation of $SnO_2$ thin film gas sensors at room temperature / P. Camagni, G. Faglia, P. Galinetto, C. Perego, G. Samoggia, G. Sberveglieri // Sensors and Actuators B Chemical., 1996.- Vol. 31.- P. 99 - 103.
63. Comini. E. Light enhanced gas sensing properties of indium oxide and tin oxide sensors / E. Comini, A. Cristalli, G. Faglia, G. Sberveglieri // Sensors and Actuators B Chemical., 2000. Vol. 65. - P. 260 – 263
64. Comini E. UV light activations of tin oxide thin films for $NO_2$ sensing at low temperature / E. Comini, G. Faglia, G. Sberveglieri // Sensors and Actuators B Chemical. 2001. Vol. 78. -P. 73 - 77.
65. Russkih D. V. Relaxation of optically stimulated electrical resistance of thin $SnO_2$ films / Russkih D. V., Rembeza S. I.// Physics and Technology of Semiconductors, 2009 -T. 43.- Vol. 6.- pp 811 - 815.

66. Rembeza S. I. Influence of optical excitation on the electrical properties of the $SnO_2$ films / Rembeza S. I., Sushkov S.A., Koshelev A. M. // Solid-state electronics and microelectronics: Interuniversity Collection of Scientific Papers. Voronezh, VSTU, 2003.- Vol. 3. - P. 47 - 52.
67. Mishra S. Detection mechanism of metal oxide gas sensor under UV radiation / S. Mishra, C. Ghanshyam, N. Ram, R.P. Bajpai, R.K. Bedi // Sensors and Actuators, 2004. - B 91. - P. 387 – 390.
68. Gulyaev A.M. About the impact of optical radiation on the sensitivity of gas sensors based on $SnO_2$ films/ Gulyaev A. M., Le Van Van, Sarach O. B., Mukhina O. B. // Physics and Technology of Semiconductors, 2008 – Vol. 42.-. №6.- pp 742 - 746.
69. Jowett CH.E. The technology of thin and thick films for microelectronics: Translated from English. / Jowett. CH.E. M .: Metallurgia, 1980. 112 p.
70. Figaro: gas sensors. M .: Publishing House "Dodeka - XXI», 2002.64 p.
71. Podlepetsky B. I. Integrated semiconductor sensors: state and prospects of development // News of chips, 1998. - № 5. - pp 38 - 45.
72. Rembeza S. I. Features of design and manufacturing technology of thin-film metal oxide integrated gas sensors / Rembeza S. I., Prosvirin D. B., Vikin O. G., Vikin G. A., Buslov V. A., Kulikov D. Y. // Sensor. №1, 2004. (10). Pp 20 - 26.
73. Rembeza S. I. Technological schemes manufacturing of microelectronic gas sensors / Rembeza S. I., Prosvirin D. B., Vika O. G., Vika G. A., Buslov V. A. // Electronics and Informatics: Proceedings of IV International. scientific and engineering. Conf. M .: MIET, 2002, pp 342 - 343.
74. Rembeza S. I. Thermal stabilization of microelectronic gas sensors / Rembeza S. I., Russkih D. V. // Solid-state electronics and microelectronics: Interuniversity Collection of Scientific Papers.2005. №5. P. 125 - 128.
75. Russkih D. V. High-temperature annealing of test structures of semiconductor of gas sensors / Russkih D. V., Rembeza S. I., Buslov V.A., Kulikov D. Y. // Actual

problems of solid state physics: a collection of Intern reports. scientific. Conf. Minsk, 2007. №2. P. 375 - 377.

76. Bagnyukov K. N., Rembeza S. I., Buslov V. A., Assessorov A. V. Effect of microalloying silver film $SnO_2$ gas sensor's sensitivity to ammonia at room temperature. Journal of Vilnius Gediminas Technical University. 2013. № 9 (2). P. 80-83.
77. Tutov E. A. Solid sensory structures on silicon / Tutov E. A., Ryabtsev S. V., Shaposhnik A. V., Domashevskaya E. P.. - Voronezh: VSU, 2010. - 231 p.
78. Svistova T. V. The physical properties of semiconductor films of tin dioxide for gas sensors: Dis. of Cand. of Sciences: 05.27.01 / Svistova Tamara Vitalevna. Voronezh, 1999. 186 p.
79. Rembeza S. I. Influence of optical radiation of low-power light-emitting diodes on the electrical and gas sensitive properties of SnO2 films / Rembeza S. I., Svistova T. V., Al-Tameemi V. M., Ovsyannikov S. V., Bagnyukov K. N. // UDC 538,975. Voronezh: VSTU, 2013 V.9 № 6.1. P.95 -98.
80. Morrison S. R. Chemical physics of solid body surface.  M .: Mir, 1982.  P. 583.
81. Vaccaro P.O. Photoconductivity in stannicoxide films, prepared by spray pyrolysis / P.O. Vaccaro, J. Saura // J. Mater. Sci. Lett., 1990. – Vol. 9. – P. 389 - 390.
82. Burbulevichus L. I., Weinstein V. M. The study the structural, electrical and optical properties of $In_2O_3$ and $SnO_2$ films. // Proceedings of the USSR Academy of Sciences. Inorganic materials. -1969. -Vol.5 - №3. - P.551-554.
83. Shalimova K.V. Introduction to the physics of semiconductors, M. Energoatomisdat, 1985, 348p.
84. Influence of a surface modification the catalysts on the gas sensitive films $SnO_2$ + 3% SiO (text) / Rembeza S. I., Rembeza E. S., Svistova T. V., Koshelev N. N.,

Al Tameemi V. M. // Physics and engineering of semiconductors, 2015, Volume 49, № 9, P. 1273 - 1277.

85. Influence of optical radiation on the adsorption processes of interaction with the gas-reducing SnO film (text) / Rembeza S. I., Svistova T. V., Koshelev N. N., Ovsyannikov S. V., Al Tameemi V. M. // Technical Physics Letters, 2015, vol. 41, no. 23.P.32-39.
86. Bagnyukov K. N. Influence of micro-alloying silver $SnO_2$ film on the sensitivity to ammonia gas sensor / Rembeza S. I., Bagnyukov K. N., Buslov V. A., Al Tameemi V. M., Svistova T. V. // Proceedings of the International scientific conference "Actual problems of solid state physics." Minsk SSPA "GNPTS NAS on Material", 2013 Volume 3, pp 333-334.
87. Rembeza S. I., Svistova T. V., Rembeza E. S., Borsyakova O. I. Influence of palladium impurities on gas sensing properties of $SnO_2$ films // Material of the III national conference "Physical problems of ecology" .- Moskow.- 2001.- P.247.
88. Watson J. The tin dioxide gas sensor / Watson J., Ihokura K., Colest G.S.V. // Meas. Sci. Technol., 1993. - № 4. - P.717-719.
89. Russkih E. A. Measurements of current-voltage characteristics of test structures based on the thin $SnO_2$ + 1% Si films / Russkih E. A., Rembeza S. I., Rembeza E. S. // Journal of VSTU, 2012. - Vol. 8. - № 10-1. - P. 59 - 62.
90. Rembeza S. I.Stimulated by light gas sensitivity of $SnO_2$ films / Rembeza S. I., Svistova T. V., Al-Tameemi V. M., Bagnyukov K. N. // Journal of VSTU. 2013 Volume 9, №4, P.120-123.
91. Bagnyukov K. N., Al-Tameemi V. M., Rembeza S. I., Svistova T. V. Production and application of semiconductor gas sensors based on thin films $SnO_2$ activated by high-intensity light // Problems of safety in the aftermath of emergencies: Materials of All-Russian Scientific-Practical Conference. Voronezh: Voronezh Institute of the State Fire Service of Russian Emergency Ministry 2012.P.158 - 159.

92. Bagnyukov K. N. Influence of optical radiation on the sensitivity of the gas sensor doped with Pd / Bagnyukov K. N., Rembeza S. I., Svistova T.V., Al Tameemi V. M. // Solid-state electronics and microelectronics: Interuniversity collection of scientific papers - Voronezh: "Voronezh State Technical University", 2013. - №. 12. - P. 166 - 170.
93. Rembeza S. I. The study of current flow mechanism in $SnO_2$ films based on the test structures / Kaygorodova E. K., Rembeza S. I., Svistova T. V., Al-Tameemi V. M. // the 52nd Scientific Conference of the faculty, graduate students, undergraduates and students: Voronezh: VSTU, 2012 , P. 10.
94. Rembeza S. I. Activation of the gas sensitivity of $SnO_2$ films by doping and the effect of light / Rembeza S. I., Svistova T. V., Al Tameemi V. M., Prosvetov R. E., Kaygorodova E. K.// the 54st Scientific Conference of the faculty, graduate students, undergraduates and students: Voronezh: VSTU, 2014, P. 9.